STRATIGRAPHIC AND STRUCTURAL GEOLOGY OF AREA 117, KOOBI FORA REGION, NORTHERN KENYA

by

Michael Joseph Buchanan

A thesis submitted to the faculty of
The University of Utah
in partial fulfillment of the requirements for the degree of

Master of Science

in

Geology

Department of Geology and Geophysics

The University of Utah

May 2010

STATEMENT OF THESIS APPROVAL

The thesis of **Michael Joseph Buchanan**

has been approved by the following supervisory committee members:

Francis H. Brown	, Chair	**March 24, 2010**
Ronald L. Bruhn	, Member	**March 24, 2010**
Thure E. Cerling	, Member	**March 24, 2010**

and by **D. Kip Solomon**, Chair of the Department of **Geology and Geophysics**

and by Charles A. Wight, Dean of The Graduate School.

ABSTRACT

The lowest four members of the Koobi Fora Formation: the Lonyumun Member, the Moiti Member, the Lokochot Member, and the Tulu Bor Member, are exposed in Areas 117, 137 and 116. These deposits include strata that were incorrectly identified as the KBS Tuff and the Surgaei tuff in Findlater's 1976 study. The composite thickness of strata within the study area is approximately 170 m, approximately 100 m of which are deposits of the Lonyumun Member. In addition to these strata, intrusions of Gombe Group basalts are exposed as well as a littoral zone of the lacustrine Galana Boi Formation of Holocene age.

A large lake from 4.2-3.99 Ma, a fluvial deltaic system from 3.99-3.40 and a large fluvial system from 3.40-3.06 Ma deposited strata of the Koobi Fora Formation in this region. This observation is consistent with Brown and Feibel's 1991 study.

Nine tuffs are exposed in the study area. Two of these tuffs, the Naibar and Aberegaiye Tuff, are newly named in this study. The Naibar Tuff was deposited by fluvial action to the shores of the receding Lonyumun Lake. Stratigraphic relationships reveal a date of ~4 Ma. The Gombe Group basalts did not intrude the Naibar tuff. Several tuffs known from elsewhere in the Koobi Fora Region are missing from the section in Area 117, including the Moiti Tuff and the Wargolo Tuff, and the Lokochot Tuff, prominent in other locales in the region is poorly represented in small outcrops. It

is believed that these units were removed by erosion attendant on incision by fluvial channels associated with the Tulu Bor Tuff. Because the Lokochot Tuff is the boundary between the Moiti Member and the Lokochot Member these two units are combined on the geological map. South of the study area proper, and also east of the study area, the upper Burgi Member unconformably overlies strata exposed in Area 117.

The area is affected by a large normal fault west of the Kokoi Highland, which is now named the Kokoi normal fault. Movement along this fault caused footwall deformation in Area 117 which manifests itself as west dipping normal faults. These normal faults bring strata of the Lonyumun Member, the Moiti/Lokochot Member, and the Tulu Bor Member into contact with each other. Movement along this fault must have been initiated after the upper Tulu Bor Member was deposited, but before the upper Burgi Member was deposited.

TABLE OF CONTENTS

LIST OF FIGURES

LIST OF TABLES

ACKNOWLEDGEMENTS

This study received generous support and assistance from many individuals and organizations, without which the study would not have been possible.

I would first like to thank the staff of the Kenya National Museum. The staff members that kept the Koobi Fora Research Station running made the stay in Sibiloi National Park that much more comfortable. Simon Ilar (of Warto) provided warm meals, hot tea and nice friendly conversations after a long day in the field. I would also like to thank Mutua Kiko Nying'ole (of Ileret) for helping me in the field area as a local guide. Mutua provided names of local geographic features, helped point out tuffs and pumices in the field area, and insured that I got back to the car safely. I would like to thank Njoroge Moses (of Nairobi) for tending to the automobile logistics while in the field. During the field season, Orion Rogers was a fabulous colleague to bounce ideas off of. He helped tremendously in measuring stratigraphic sections, and provided good company.

In Nairobi, Dena and Johnny Leakey provided a roof over my head and a comfortable place to sleep. Julius, Clement and Antony cooked fabulous meals. Fredrick Kyalo Manthi of the National Museums of Kenya provided logistical support for transportation of samples out of Kenya.

Matt DeLong and Randy Poulson answered questions and provided support in the Electron Microscopy lab at the University of Utah Department of Physics. Barbara Nash helped a great deal with the Electron Microprobe lab at the University of Utah

Department of Geology and Geophysics. My thesis committee, comprised of T. E. Cerling and R. L. Bruhn, helped answer any questions I had and both had a tremendous open door policy. They provided me with constant support and taught me how to use my imagination in the field of geology.

I would lastly like to thank my thesis advisor, Francis H. Brown. It was a pleasure having him in the field and showing me the many, sometime subtle, intricacies of geological investigations in northern Kenya. His door was always open when I had a problem or needed someone to bounce ideas off of. His immense catalogue of tuffs, and the chemistry that went with them, was of immeasurable help. He constantly encouraged me to strive for excellence.

This study was funded by a generous grant from the National Science Foundation to F. H. Brown, T. E. Cerling, and R. L. Bruhn.

CHAPTER 1

INTRODUCTION

Pliocene and Pleistocene sedimentary deposits of the Turkana Basin have long been known for the thousands of vertebrate fossils, including early hominid fossils, collected from them. Area 117, in the Koobi Fora Region, contains some of the oldest strata of the Koobi Fora Formation and also preserves some of the oldest hominid fossils from that formation.

1.1 Geography and Climate of the Study Area

Three principal rivers feed Lake Turkana, the Omo River to the north, and the Turkwel and Kerio to the south. Other ephemeral streams, called lagas in Oromo, feed Lake Turkana from small drainage basins around the lake. Most large and medium sized ephemeral streams, called Il and Kolom in Dhaasanac respectively, large watering holes, hills and ridges all have local names in Dhaasanac (Brown and Feibel, 1991).

The Koobi Fora region is broken into archeological field areas. Numbered field areas are used as referenced by Brown and Feibel (1986).

Area 117 is located east of Lake Turkana, approximately 40 km south of the Ethiopian border within Sibiloi National Park (Figure 1). It is bounded by Il Naibar to the north, and by Il Abergaiye to the south. The area extends eastward to the edge of

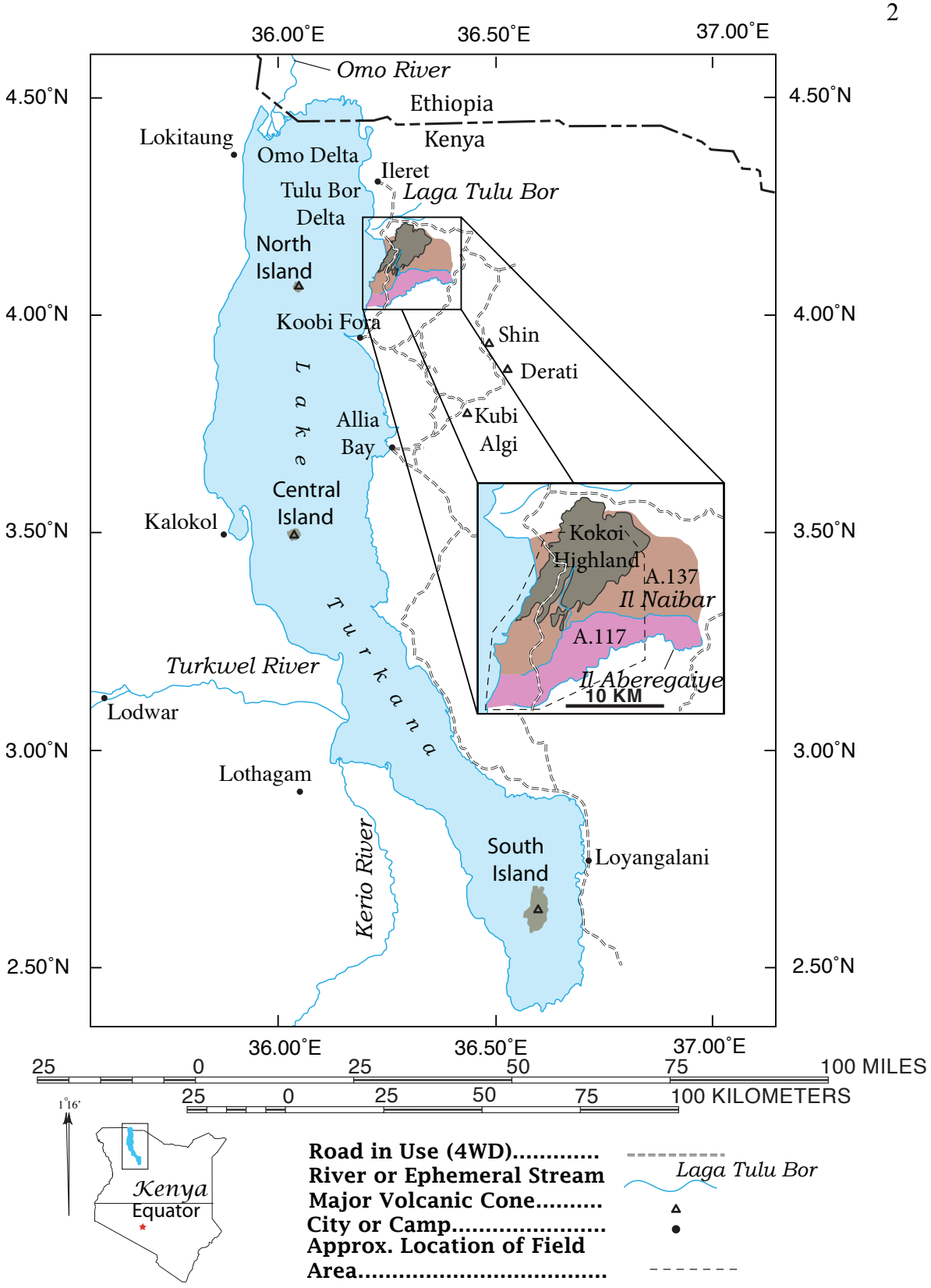

Figure 1. Overview of Lake Turkana with major geographic features of importance to study noted.

exposures, which disappear under a broad flat area between the lowlands of Area 117, and the higher area along the Karari Ridge, where younger strata are exposed. To the west it is bounded by Lake Turkana. The topography of the area is very subdued, with only 100 m of elevation gain from the shore of Lake Turkana to the eastern extent of the area. The areas has cliffs 3 to 15 m high which are capped by erosion resistant volcanic tuffs; in these cliffs mudstones and sandstones are often exposed.

Area 137 is located to the north of Area 117. It is bounded to the north by Il Kimire (Laga Tulu Bor), to the south by Il Naibar, to the west by Lake Turkana, and to the east by Il Kimere. It encompasses the entire area occupied by the Kokoi highland. Topographically, the Kokoi Highland is approximately 180 m higher than Lake Turkana and has a large north-south trending valley occupied by Kolom Nabalware that feeds into Il Naibar. Most of the surface of the Kokoi is covered with rounded basalt clasts (from sand to cobble size), but in canyons there are exposures of north-south trending wavy columnar basalts with some sedimentary packages of siltstone, mudstone and sandstones, and intercalated tuffs.

The field area can be accessed only by rough roads. In inclement weather, the roads become impassable due to the large amounts of clay and mud on the road.

1.2 Previous Work

Before 1968, Teleki and von Höhnel's 1888 report was the only report about the geology and paleontology of the Lake Turkana (Teleki and von Höhnel named the lake the Rudolf Sea after the Crown Prince of Austria) (von Höhnel, 1894; Vondra *et al.*, 1971). In 1968 a 3–month expedition to probe the geology and paleontology of the area

commenced, with a second three-month expedition the next year. This expedition was brought on by an aerial reconnoiter in 1967 that revealed extensive sediments (Leakey, 1970), fossil vertebrates and stone artifacts. The work in the late 1960s was the beginning of primary investigation into the geologic history of the Lake Turkana area. Investigators in his first stage's primary geological investigators included (but were not limited to) A. K. Behrensmeyer, B.E. Bowen, C. F. Vondra, G. D. Johnson, and F. Fitch. During this stage of investigation, an informal stratigraphical nomenclature was proposed (Behrensmeyer, 1970) which used four units (from oldest to youngest): Koobi Fora I (KF-1), Koobi Fora II (KF-2), Koobi Fora III (KF-3) and Galana Boi (Bowen, 1974). In 1973 the stratigraphic nomenclature was formalized. The revised system included three formations: The Kubi Algi Formation, the Koobi Fora Formation, and the Guomde Formation. The Kubi Algi Formation was described as any strata that lay below the Surgaei Tuff complex. The Koobi Fora Formation included strata that lay between the basal contact of the Suregei Tuff Complex and the upper contact of the Chari Tuff. The Guomde Formation was described as strata that lay between the top of the Chari Tuff and the base of sedimentary strata deposited during a late Pleistocene to Holocene highstand of Lake Turkana which were named the Galana Boi Beds (Bowen and Vondra, 1973). This first stratigraphic nomenclature used tuffs as marker beds and correlated sediments petrographically and petrologically. The first geologic map for Miocene to Pliocene deposits east of Lake Turkana was produced as part of B.E. Bowen's 1974 Ph. D. dissertation. This map shows half of the deposits of Area 117 and all of the deposits of Area 137. Bowen (1974) shows all of the sediments south of the Kokoi as being either part of the Lower Member of the Koobi Fora Formation or Quaternary alluvium. As a

note, Il Naibar is named the Kokoi Laga on Bowen's map. In 1975 Lake Rudolf was renamed Lake Turkana after the most populous tribe in the region, the Turkana. In 1976 I.C. Findlater wrote about many of the tuffs in Area 117. Unfortunately, without the aid of compositional analysis, many of these tuff beds were incorrectly identified. Findlater (1976) identified thick beds that he ascribed to the Tulu Bor Tuff and the Surgaei Tuff in the middle of Area 117, and he also ascribed a tuff in the southern part of the Kokoi to the Hasuma Tuff. A tuff in the southern and western portion of Area 117 was suggested to be the KBS Tuff. With the exception of some tuffs ascribed to the Tulu Bor Tuff, all of these units were incorrectly identified due to lack of compositional information.

Brown and Feibel (1986) formally revised the lithostratigraphic nomenclature of the Plio-Pleistocene sediments in the region, because it had been known for some time that the original nomenclature needed updating. The Tulu Bor Tuff was used by Bowen and Vondra as a marker tuff in the lower member of the Koobi Fora Formation. Using X-Ray fluorescence (XRF) analysis on 200 tuff samples collected throughout the region surrounding Koobi Fora Research Station, Brown and Cerling (1982) showed that tuffs that had previously been called the Tulu Bor Tuff were in fact different chemically in many instances. Paleontological work had also shown that the stratigraphy needed revision (Harris and White, 1979; White and Harris, 1977; Feibel *et al.*, 1991). Chemical analysis of tuffaceous beds became the only relatively secure way to correlate from one isolated area of outcrop to another at the member level (see Brown, 1994). The current stratigraphic scheme assembles all Pliocene and early Pleistocene strata of the Koobi Fora region into a single formation, divided into eight members. From oldest to youngest the members of the Koobi Fora Formation are: Lonyumun, Moiti, Tulu Bor, Burgi, KBS,

Okote, and Chari (Figure 2). The members are defined as all strata from the bottom of the basal tuff of each member (which gives the name to the member) to the bottom of the basal tuff of the next highest member. For example, the Tulu Bor Member comprises all strata between the base of the Tulu Bor Tuff and the base of the Burgi Tuff. In many instances, the only way to determine the identity of a tuff is by determining the chemical composition of the glass shards within it. Commonly this is done by using the electron microprobe (EMP) for major elements, and XRF analysis for minor and trace elements. Although early reconnaissance work was done in Area 117, this is the first extensive study of the area, and includes the southern portion of Area 137 and a small location in Area 116.

Key and Watkins (1988) produced a geologic map for the Sabarei area. They mapped an extensive area from just north of the Koobi Fora spit to north of Ileret. To make the map south of Ileret, Key and Watkins (1988) used tonal differences on aerial photographs as well as the map of Vondra and Bowen (1978). This map shows strata of the upper half of Area 117 to be Lower Koobi Fora Formation while the lower half is shown as strata of the Upper Koobi Fora/Guomde Formation. The map also shows a large aeolian sand deposit south of the Kokoi near the lake shore and extensive lake deposits throughout the area. The map depicts all sedimentary strata exposed on the Kokoi Highland as Quaternary colluvium and scree.

Teams from the Iowa State University, the University of California and University of Utah began to correlate and map in detail the strata within the Koobi Fora region and the Turkana Basin in the late 1970s and similar work continues to this day

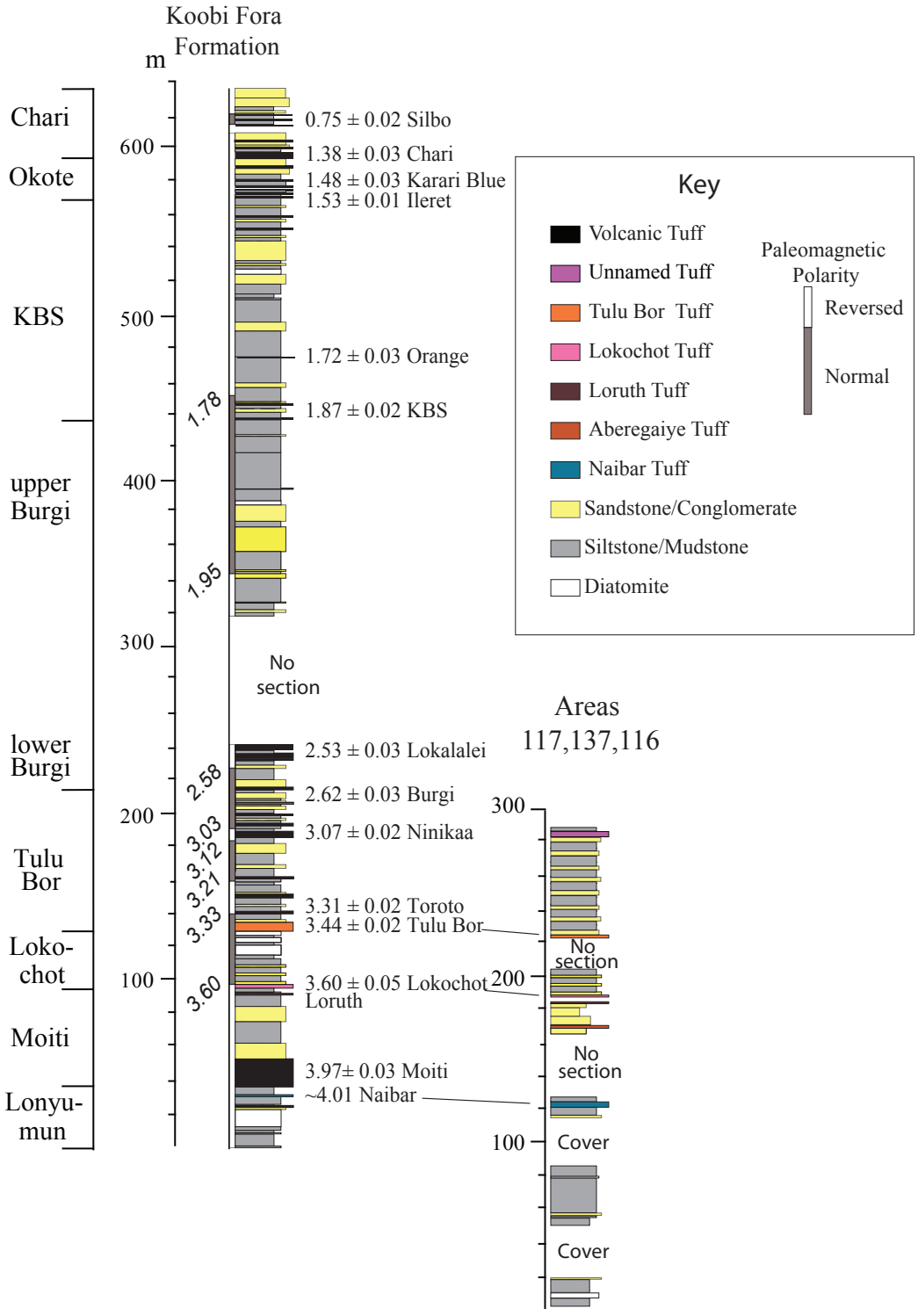

Figure 2. Composite stratigraphic section of the Plio-Pleistocene Koobi Fora Formation. Adapted from Brown and Feibel (1986).

(Bainbridge, 1976; Boschetto, 1988; Burggraf, 1976; Cerling, 1977; Cohen, 1982; Feibel, 1983; Feibel, 1988; Frank, 1976; Gathogo, 2003; Haileab, 1988; Haileab, 1995; Harris, 1978; Levin, 2008; Martz, 1976; Martz and Brown, 1981; Tindall, 1985; White, 1976). Strata in the Koobi Fora region have been correlated to strata west of Lake Turkana (the Nachukui Formation), in the lower Omo Valley in Ethiopia (the Omo Group) (Harris *et al.,* 1988) and deep sea strata in the Gulf of Aden, the Arabian Sea, and the Indian Ocean (Sarna-Wojcicki *et al.*, 1985; Brown *et al.,* 1992; deMenocal and Brown, 1999).

CHAPTER 2

REGIONAL GEOLOGIC SETTING

Africa is comprised of five Archean cratons. Two of these cratons, the Zambian and the Tanzanian Cratons, play an important part in the East African Rift System. These cratons are comprised of paragneisses and orthogneisses, and reach a crustal thickness of 50–60 km (Morley *et al.* 1999a).

The Turkana depression is a vast lowland, occupied by a closed basin, the Omo-Turkana Basin of northern Kenya southern Ethiopia (Haileab *et al.,* 2004). Late Oligocene to Late Pleistocene strata of the Turkana Basin preserve an excellent mammalian fossil record including early primates and hominids (Boschetto *et al.*, 1992, Leakey and Leakey, 1978).

2.1 Structural-Tectonic Setting

The large-scale East African Rift System (EARS) controls all of the major structures in the field area. The EARS is a continental divergent zone that extends 3500 km from the Afar Triple Junction (to the north) to Mozambique (to the south) (Figure 3). The EARS is 50–150 km wide elongate system of normal faults and is broken into two branches: the volcanic poor western branch, which is located west of Lake Victoria, and the volcanic rich eastern branch. The western branch contains a chain of half-graben

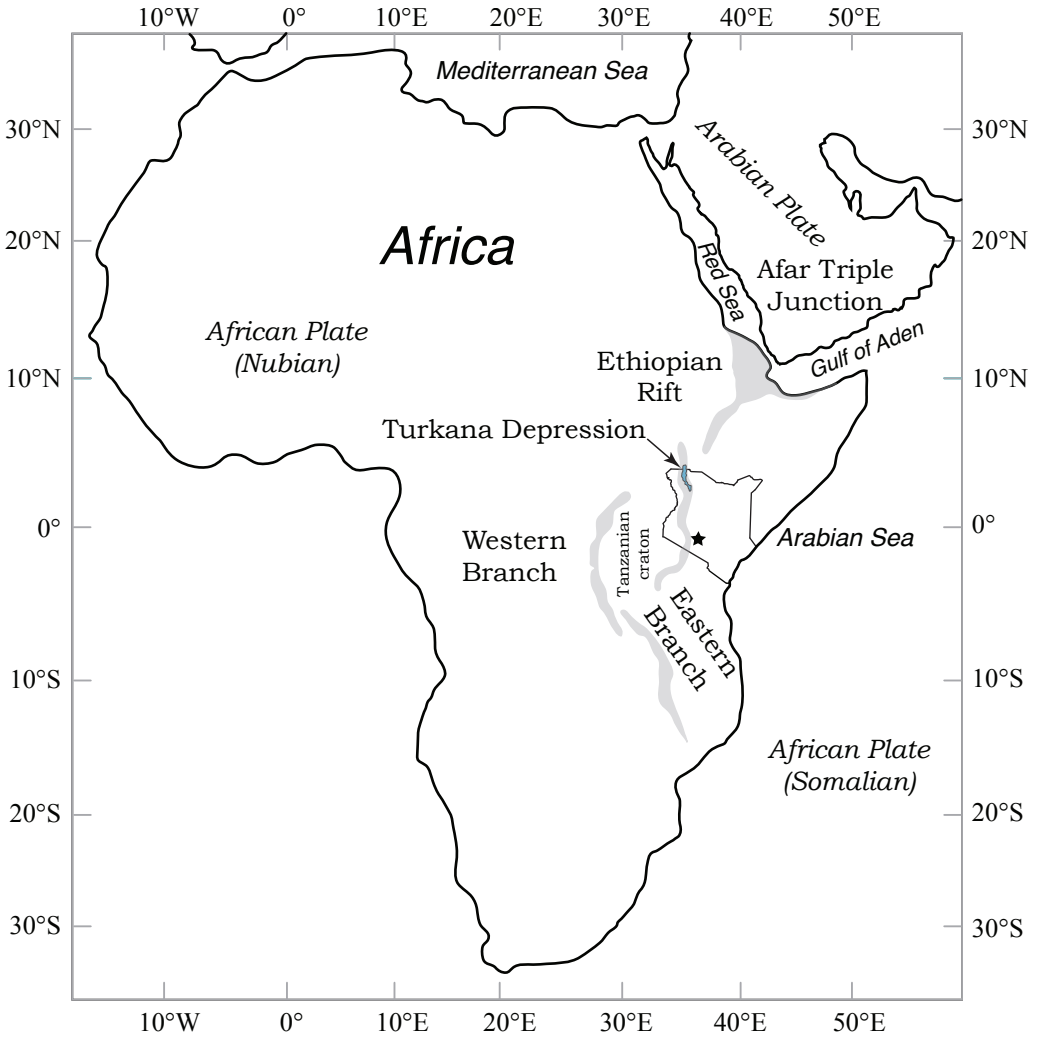

Figure 3. East African Rift System (EARS) showing the eastern and western branches, the Turkana Depression, and the Tanzanian craton.

basins that are covered by deep basinal lakes and may have been initiated later (late Miocene) than those in the eastern branch. The eastern branch's rift basin geometry is less well known, and contains only one large lake, Lake Turkana. The eastern and western branches lie within an orogenic belt that surrounds the Tanzanian craton and large scale rift structures are largely controlled by the presence of this cratonic structure (Morley *et al.*, 1999a).

Two large domes, the Afar (aka the Ethiopian Plateau), and East African (aka Kenyan) Domes, separated by the Turkana depression of northern Kenya, are the largest scale topographic features associated with the EARS. Average elevations are 1,500m for the Afar Dome, 1,200 m for the East African Dome (which contains the highest point in Africa, Mt. Kilimanjaro), and 600m for the Turkana depression. The large lithospheric domes are associated with large negative gravity anomalies and each has a diameter of approximately 1,000 km (Morley *et al.*, 1999b).

Many rift zones are recognized in the eastern branch of the EARS, one of which is the Kenyan Rift. The Omo-Turkana basin lies within the Kenyan Rift, which extends from Lake Baringo in central Kenya to the Omo Rift Valley in northern Kenya/southern Ethiopia (Rosendahl, 1987; Morley *et al.*, 1992). At 150 km the Turkana area is the widest portion of the EARS (not including the Afar Triple Junction). The Kenya Rift contains three or four major half-grabens (Morley *et al.*, 1999b). The major structural features of the Turkana depression are a series of north-south trending normal faults (Haileab, 1995), which must have been active to at least Middle Pleistocene time because faulting has been observed in the Silbo Tuff of the Chari Member 0.74 Ma (Haileab *et al.*, 2004).

The northern Kenyan Rift was initiated during the Late Eocene by the eruption of extensive tholeiitic basalts (Lokitaung and Nabwal basalts). This volcanism may be attributed to adiabatic decompression melting due to lithospheric thinning caused by the initiation of crustal extension coinciding with the formation of the earliest half-grabens in the Turkana region (Morley *et al.*, 1992; Morley *et al.*, 1999b; McDougall and Brown, 2009). During the Miocene, active faulting and volcanism shifted eastward to the eastern side of modern Lake Turkana (Cerling and Powers, 1977; Morley, 1999b).

Early Miocene deposits, which can be correlated to rifting in the Turkana region, thicken to the east. The overlying Late Miocene-Pliocene deposits thicken to the west. This suggests a changing polarity of bounding normal faults of the half grabens, from east to west dipping. By the mid to late Neogene, the bounding faults are almost all east dipping (Morley, 1999a). During the Middle Miocene, rifting and volcanism shifted towards the southern Kenyan rift (Morley *et al.*, 1992; Dunkelman *et al.*, 1988).

During the Pliocene the Paleogene/Miocene system of half-grabens was abandoned in favor of minor fault swarms east of modern day Lake Turkana. This minor fault swarm developed in a narrow trough of high volcanic activity located east of the older half graben system, and has no obvious relationship to the older half grabens. Such swarms are well developed in the Suguta Valley and the Kino Sogo Fault zone (Morley, 1999b). While the fault swarms caused minor extension, geomorphically these areas are spectacular. Between 5 Ma and present, at least 10 km of extension has occurred within the central part of the Turkana basin, which caused a small volume of basaltic material (the Gombe Group basalts) to be erupted (Haileab *et al.*, 2004). The history and style of rifting is unique to the Turkana area. This is suggested by the lack of Late Oligocene or

early Miocene rift basins anywhere else in the EARS (Morley, 1999b). For a complete and thorough discussion of the structural history of the Kenya Rift Zone and the Eastern Rift see Morley *et al.* (1992) and Ebinger *et al.* (2000).

Analysis of faults, dikes, volcanic vent swarms, teleseismicity, and borehole breakouts suggests that the least horizontal stress ($\sigma_{h,min}$) direction of the Kenyan rift has changed direction during the past 12 Ma. During the Middle to Early Pliocene $\sigma_{h,min}$ was oriented ENE-WSW. During the Pliocene $\sigma_{h,min}$ was oriented NE-SW. By the Late Pliocene the $\sigma_{h,min}$ was oriented N-S. The Middle Pleistocene shows a $\sigma_{h,min}$ that is oriented NW-SE, the present orientation. This indicates that during the past 12 Ma the $\sigma_{h,min}$ direction has rotated counter-clockwise at least 30° (Bosworth and Strecker, 1997). Normal faulting and half grabens would reflect this by showing fault trends normal to the $\sigma_{h,min}$ orientation as long as the least horizontal stress is greater than the maximum horizontal stress.

2.2 Stratigraphic Setting

The geology of the Turkana area has four major stratigraphic components: Early Paleozoic crystalline basement comprised of para- and orthogneisses; Cretaceous sandstones which contain dinosaur fossils; Cenozoic volcanics comprised of basalts, rhyolitic tuffs, phonolites; and clastic sediments derived from the erosion and weathering of the crystalline basement. The basement is exposed in uplifted blocks in a few locales but is largely covered by younger Cenozoic volcanic and sedimentary strata.
Rifting created a half graben basin in the Turkana area resulting in the capture of the ancestral Omo River around 4.5 Ma ago. With this, deposition of sediments of the Koobi

Fora Formation began in the Koobi Fora Region. Prior to 4.5 Ma, the Omo River most likely flowed into the Nile drainage basin and ultimately into the Mediterranean Sea (Haileab *et al.*, 2004). Capture of the Omo River created a large lake, three times the size of the present day Lake Turkana (named the Lonyumun Lake). By 4 Ma the large lake had been filled in, and the ancestral Omo River must have passed by the Sibilot region east of Lake Turkana. This meandering river created a large flood plain and a gallery forest. Around 3.5 Ma a small lake again appeared in which diatomites are prominent in its later phases. These diatomites are dominated by *Melosira* (*Aulacosira*). The lake is replaced by a large meandering river at 3.45 Ma, which may have escaped the basin to the southeast and drained into the Indian Ocean. In the axial portions of the basin a significant lake, Lake Lokeridede began to form around 2.06 Ma, and coexisted with a river to the east which lasted on the eastern margin of the basin until around 1.95 Ma. From this time on a lake has been a semi-permanent part of the Turkana Basin. At various times this lake has shrunk to a broad flood plain and at others it has risen to levels around 100 m above the present day lake. A fluvial system probably drained the basin as recently as 750,000 years ago (Harris *et al.*, 2006; Brown and Feibel, 1991; Feibel, *et al.*, 1991), but details of its location have been elusive. The above description is misleading, emphasizing the lacustrine and deltaic phases. This is because the lacustrine phases are well represented in the geologic record. The fluvial phases, however, dominated the Turkana Basin for over 85 percent of the time represented by the Plio-Pleistocene deposits of the Turkana Basin. For a complete discussion see Brown and Feibel (1991). Today Lake Turkana occupies this closed basin at an elevation of 360 m and is the third largest lake in East Africa.

CHAPTER 3

OBJECTIVES

The main objectives for this study includes: 1) mapping all Plio-Pleistocene sediments from the southern limits of the Kokoi, to the unconformity south of Il Aberegaiye (most of Area 117, and parts of Areas 137 and 116); 2) mapping all known and inferred structural elements within the defined field area; 3) assigning all Pliocene and Pleistocene sediments to members of the Koobi Fora Formation as defined by Brown and Feibel (1986); 4) establishing and/or revising correlations of all Plio-Pleistocene strata within the field area with the help of defined tuffaceous markers beds; 5) reconstructing the paleoenvironments using key concepts from stratigraphy, sedimentology, and structural geology, as evidence for depositional environments.

CHAPTER 4

METHODS

4.1 Field Work

Field work for this study was carried out over a 37 day period from June 9th 2008 through July 13th, 2008. The base camp for this study was the Koobi Fora Research Station, approximately 10 km south of the field area. Fieldwork was conducted with the help of F. H. Brown (for the first 10 days), Orion Rogers (MS Geology Student), and Mutua Kiko Nying'ole (a locally hired Dhasaanac field assistant).

4.1.1 Geologic Mapping and Stratigraphic Sections

Geologic mapping of lithological units and structural features was performed using images printed from Google Earth at an approximate scale of 1:12,000. The image dates were August 25th 2005, and were downloaded in April 2008. Latitude and longitude markers were every 0.001 degrees, approximately 110 m.

Google Earth images were used because no topographic maps are available for use and overall; the region has very subdued topography so that very detailed topography would have been required. Satellite images also have the advantage of showing color details that aerial photos do not. Locations of samples previously collected by F. H. Brown and T. E. Cerling were plotted on these images to facilitate reexamining

these tuffs. This was of importance because most of the early samples had been analyzed chemically so that the identity of many tuffs was known at the outset of the work reported here. The final geologic map was produced using United States Geological Survey's geologic map symbolization (Federal Geographic Data Committee, 2006) as a guide. Geologic time is based on the 2009 Geologic Times Scale produced by the Geological Society of America (Walker *et al.*, 2009).

Vertical aerial photographs produced by the Hunting Survey (series HSL KEN 70), flown in 1970 were also used. The area was photographed at a flying height of 12,000 ft, using a camera with a focal length of 6 inches, which produced aerial photographs with an approximate scale of 1:24,000. Changes in the locations of some dry streambeds (lagas) are evident when comparing the earlier aerial photos with the Google Earth images, so that the later imagery is especially advantageous for field location. Additionally, the two sets of images give some sense of how rapidly the topography of the region is changing.

Finding locations on the Google Earth Images was facilitated by a Garmin eTrex Vista global positioning system (GPS) receiver with an accuracy of ~6 m. The GPS was set to use the World Geodetic Survey 1984 (WGS 84) reference ellipsoid with units of decimal degrees. A Brunton Pocket Transit was used to obtain attitudes of bedding and structural features using standard geologic techniques (Compton, 1962; Lahee, 1961).

Stratigraphic sections were measured with a Jacobs Staff with markings at 10 cm intervals. The Jacobs staff was kept perpendicular to the dip with the aid of the Brunton Pocket Transit. Sections were cleaned with a hoe or a machete and measured with the aid of a partner; one would measure and describe the section while the other kept a record.

Each section was numbered according to the area in which it was located and a section number following a period (e.g., section A137.2 is the second stratigraphic section in Area 137).

A local guide was hired to aid in route finding, as well as providing local names for geographic features such as ephemeral streams (lagas) and hills in the area. The guide was crucial for fieldwork.

4.2 Laboratory Analysis

Laboratory analysis was conducted over a 16 month period in the Department of Geology and Geophysics at the University of Utah.

4.2.1 Tephra Preparation

Tuffs were sampled in the field in the following manner: a sample was obtained near one end of contact and samples were taken near the middle of the outcrop and at the end along strike. Tuff samples were also obtained during field investigations and while describing stratigraphic sections. Tuffs were removed from the outcrops with a 60 cm machete and cleaned of surface material (such as lichen, muds and clays). All pumices found that were >1 cm in diameter were also collected. The location of each collected sample was recorded using a GPS. A list of sample localities is given in Appendix B. The sample was sieved, retaining the 0.250–0.125 mm fraction. This fraction was hand carried to the laboratory, whereas the >0.250 mm material was shipped from Nairobi to the University of Utah. Material <0.125 mm was discarded. Permission to send samples was provided by the National Museums of Kenya.

The 0.250-0.125 mm fraction was washed in deionized water to remove surface clays and plant material. The samples were then treated with 10% nitric acid (HNO_3) and placed in an ultrasonic bath to remove any carbonate minerals. The samples were then washed multiple times with deionized water to remove any residual HNO_3, following which they were treated with 5% hydrofluoric acid (HF) in an ultrasonic bath to remove any clay minerals. The spent HF solution was decanted from the sample (Brown and Fuller, 2008), and this process was repeated until the solution contained no suspended clay material. Samples were rinsed a minimum of three times with deionized water and dried in an oven set to 80°C. Magnetic and nonmagnetic separates were obtained using a Frantz Isodynamic Separator. Forward and side tilt, as well as current (hence magnetic field) was adjusted on a sample-by-sample basis. The end result was a glass separate.

The glass separates were placed in methyl methacrylate polymer microprobe mounts (nine samples per mount plus a standard (MM3) and cemented using a two-part epoxy resin. The mounts were ground flat and then polished. The samples were coated with carbon in a Denton Desk II Evaporator so that the samples would be conductive under the electron beam of the microprobe.

Glass shards were prepared for scanning electron microscopy (SEM) analysis by cleaning them in deionized water in an ultrasonic bath for a minimum of 30 minutes three times. The cleaned glass shards were placed on a standard microscope slide affixed with a circular double-sided carbon sticky dot, six samples to a slide. Glass shards are non-conductive and charging effects are a major problem. For this reason, the samples were given a thin (3-5 nm) coat of gold-palladium using a Denton Desk II Evaporator to aid in conduction, and to eliminate charging of the sample.

Diatoms were prepared for scanning electron microscopy by first sieving to <0.250 mm, treating them with 10% nitric acid (HNO_3) in an ultrasonic bath to remove carbonate minerals, and washed multiple times with deionized water to remove any residual HNO_3. Deionized water was added to the material and the beaker was placed in an ultrasonic bath for a minimum of 30 minutes three times to clean them. The samples were placed in a beaker with hot water and then poured into a 500 ml burette containing 300 ml of cold water. Complete diatom frustules, along with minerals and volcanic glass, settled to the bottom of the burette. When most coarse material was out of suspension the stopcock was opened and the heavy material was titrated into a beaker. Frustules were allowed to settle to the bottom of the beaker and the water was decanted.

Dried frustules were mounted on a ½" Zeiss aluminum pin stub with carbon tape. Diatom frustules are nonconductive so they build up surface charges easily under an electron beam. For this reason, the samples were given a thin (5-10 nm) coat of gold-palladium using a Denton Desk II Evaporator to aid in conduction of the electron beam.

Pumices were crushed using a mortar and pestle and sieved. The 0.50–0.25 mm fraction was placed in a large beaker and filled with deionized water. Feldspar and other mineral grains settled out of the water column very rapidly, and the water, along with suspended material from the pumice was decanted into another beaker leaving behind the mineral separates. This was repeated until a large fraction of feldspars were concentrated. Samples were then decanted in a wet sieve (0.250mm) and placed in an oven set to 80°C.

4.2.2 Tephra Compositional and Morphological Analysis

A Cameca SX 50 electron microprobe (EMP) with four wavelength dispersive spectrometers was used for analyses of all samples. The EMP was calibrated for 14 elements using 11 standards. The EMP was set for an accelerating voltage of 15kV, a beam current of 25nA, and a beam diameter of 5 to 20 nm. Analysis time for each element for each sample was the same as for the standards (see Appendices C and D). The relative peak intensities were used to calculate each peak intensity and the Φρz algorithm was used (Pouchou and Pichoir, 1991). Nash (1992) gives a useful and complete discussion of analyzing volcanic glasses using an EMP.

Data from the analyses were converted from element weight percent to oxide weight percent, following which irregular analyses as well as analyses with unacceptably high (>102.5%) or low (<98.5%) totals were removed. The remaining samples were separated into compositional modes and the arithmetic mean and standard deviation were computed. These results were compared to other Turkana Basin tuffs of known composition.

An FEI NovaNano scanning electron microscope was used to determine glass shard morphology and diatom identification. The SEM was typically set to an accelerating voltage of 7 kV, a beam current between 0.13–0.26nA, and a working distance of 6–7 mm. Brightness and contrast were adjusted on a sample-by-sample basis. The images were rastered for 45 nanoseconds per pixel (around 3 minutes per image). Similar settings were used for diatom identification with the exception of the accelerating voltage, which was set between 15 and 20 kv (per Round *et al.*, 1990). For a general discussion of SEM operation see Goldstein *et al.* (2003).

Diatoms were identified by anatomical characteristics of the frustules from the SEM images. These were then compared to the systematic desccriptions given by Müller (1897), Cholnoky (1955), Owen (1981), Gasse (1986) and Round *et al.* (1990) to determine the species of the diatom. Owen (1981) and Gasse (1986) give complete and thorough ecological parameters of modern diatoms which were instrumental in deducing the paleochemistry of the lakes in which these diatoms were formed.

CHAPTER 5

LITHOLOGIC UNITS

Areas 117, 137, and 116 contain deposits of Pliocene and Quaternary age. Pliocene deposits include the lowest four members of the Koobi Fora Formation: the Lonyumun Member (4.3 to 3.97 Ma), Moiti Member (3.97 to 3.60 Ma), the Lokochot Member (3.60 to 3.44 Ma), and the Tulu Bor Member (3.44 to 2.62 Ma; McDougall and Brown, 2008). Unconformably overlying these deposits is the upper Burgi Member, which is located south of Il Aberegaiye in Area 116. The upper Burgi was not studied in detail. Other Pliocene deposits include Gombe Group basalts (Haileab *et al.*, 2004). Quaternary deposits include the Holocene Galana Boi Formation, which overlies the sedimentary strata of the Koobi Fora Formation and in the study area is easily distinguished from the older deposits because of its poorly cemented strata that contain an abundance of white mollusk shells in most outcrops (Owen and Renaut, 1986). Other Quaternary deposits include Holocene to Recent lacustrine deposits of Lake Turkana, active alluvium in dry ephemeral streams, cover (derived from older strata), and alluvial fans associated with the Kokoi Highland and containing material derived from the Gombe Group Basalts. Outcrops of the Koobi Fora Formation, the Gombe Group basalts, the Galana Boi Formation, and other Quaternary deposits are shown in Appendix A.

Geologic terms are used as defined by Jackson in the Glossary of Geology (1997). Lithologic units are described as defined by Lahee (1961) and Compton (1962). The Koobi Fora Formation is used as defined by Brown and Feibel (1986), the Gombe Group Basalts by Haileab *et al.*, (2004), and the Galana Boi Formation by Owen (1981) and Owen and Renaut (1986). Identification of the morphology of volcanic glasses follows Cerling (1977). Diatom frustule structural, symmetry and morphology is as defined by Round, Crawford and Mann (1990).

The composite thickness of the four exposed members of the Koobi Fora Formation in the study area is approximately 285 m (Figure 2). Correlated stratigraphic sections of the four representative members of the Koobi Fora Formation are provided (Figure 4) as well as a location map for the measured stratigraphic sections (Figure 5). A key to lithologic symbols used on measured stratigraphic sections is given in Figure 6.

The importance of volcanic tuffs within the sections cannot be overstated. Without these it would be very difficult to precisely identify members of the Koobi Fora Formation within the field area. Many past workers in the field area (including Bowen, 1974; and Findlater, 1976) tried doing just this, but were only partly successful. The procedure used here was to map each continuous outcrop of tuff in the field, and then to determine the chemical composition of the glass fraction separated from samples in each of the outcrops. Volcanic glass from each volcanic event has a unique chemical composition (Figure 7). The chemistry of the volcanic glasses was then compared with the composition of previously analyzed tuffs from the region to identify the tuff (see Table 1). Combining the compositional information with mapping and field observations, the lithologic units of Areas 117, 137, and 116 were identified. Volcanic

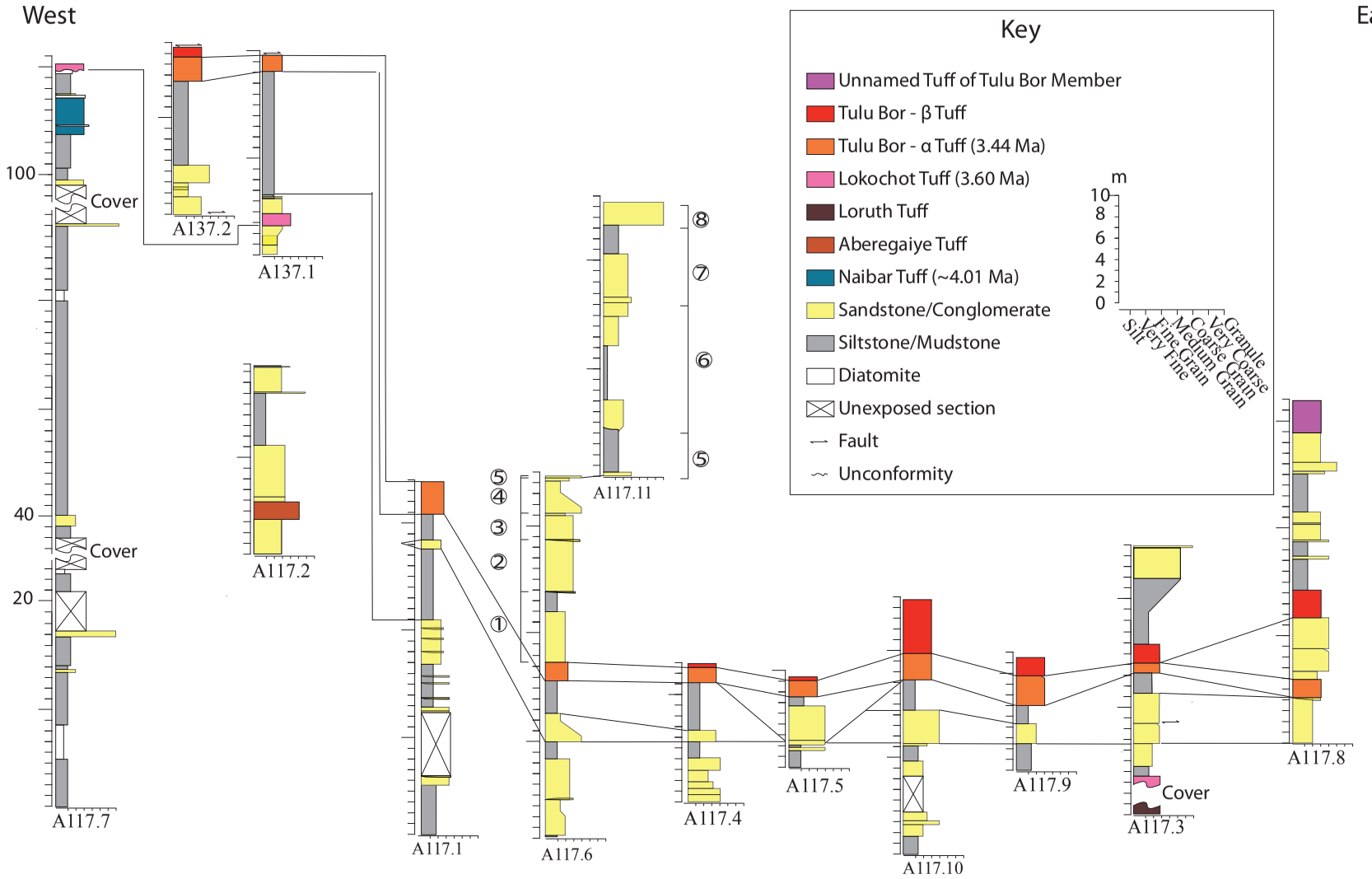

Figure 4. Correlated stratigraphic sections of the Koobi Fora Formation in Areas 117 and 137.

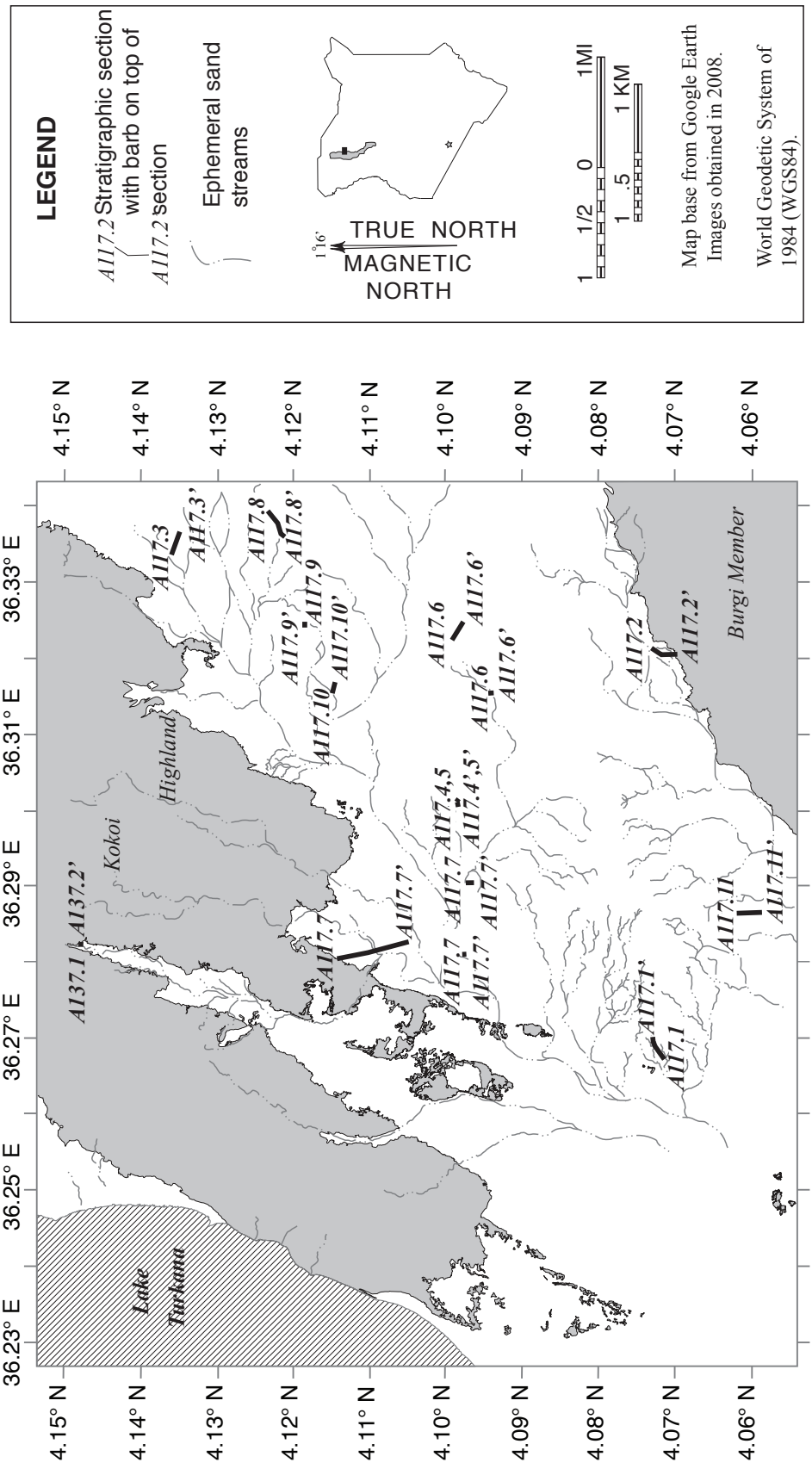

Figure 5. Locations of stratigraphic columns of the Koobi Fora Formation in Areas 117 and 137.

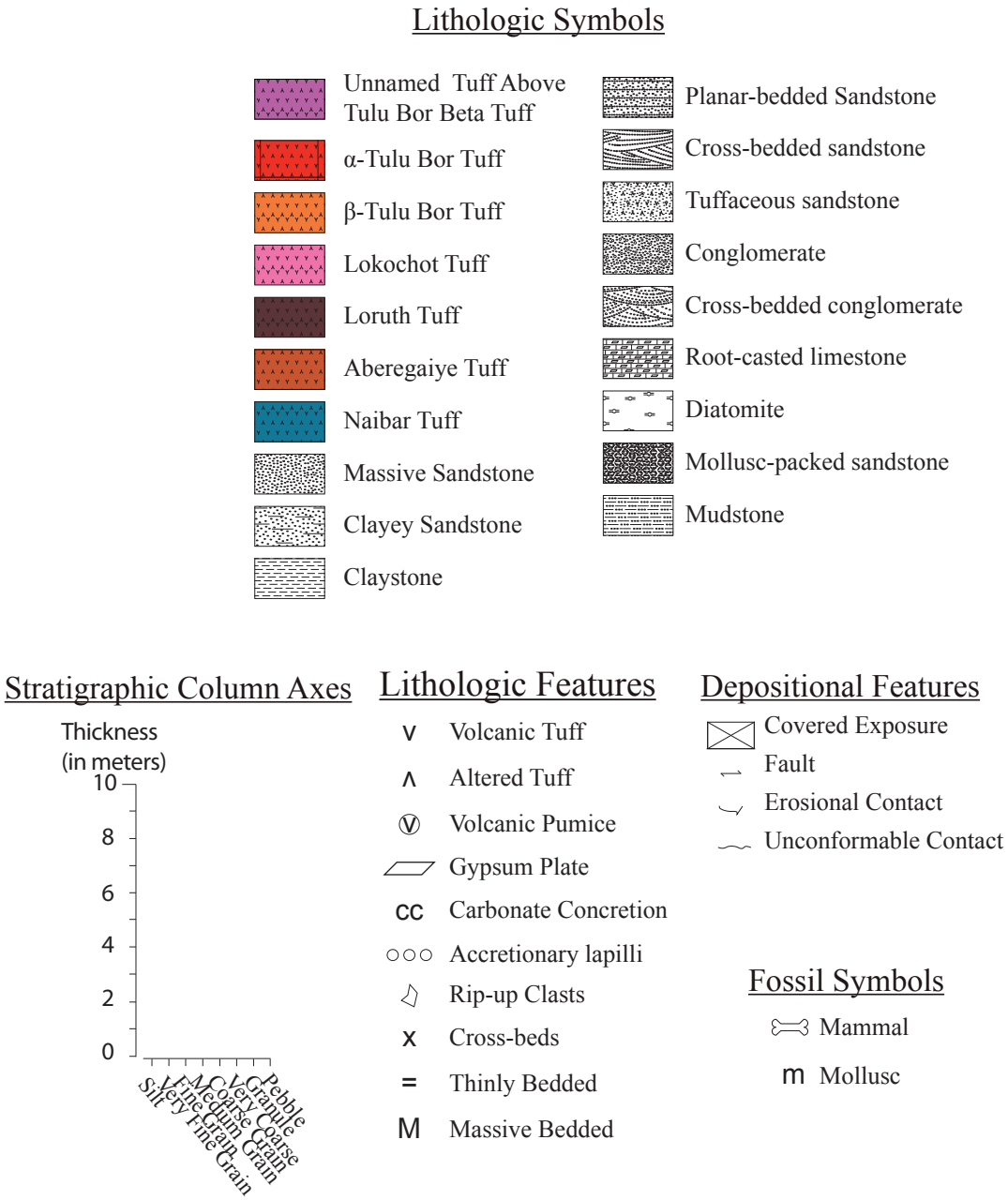

Figure 6. Key to lithologic symbols used in the stratigraphic sections of the Koobi Fora Formation in Areas 117 and 137 (Adapted from Brown and Feibel, 1986).

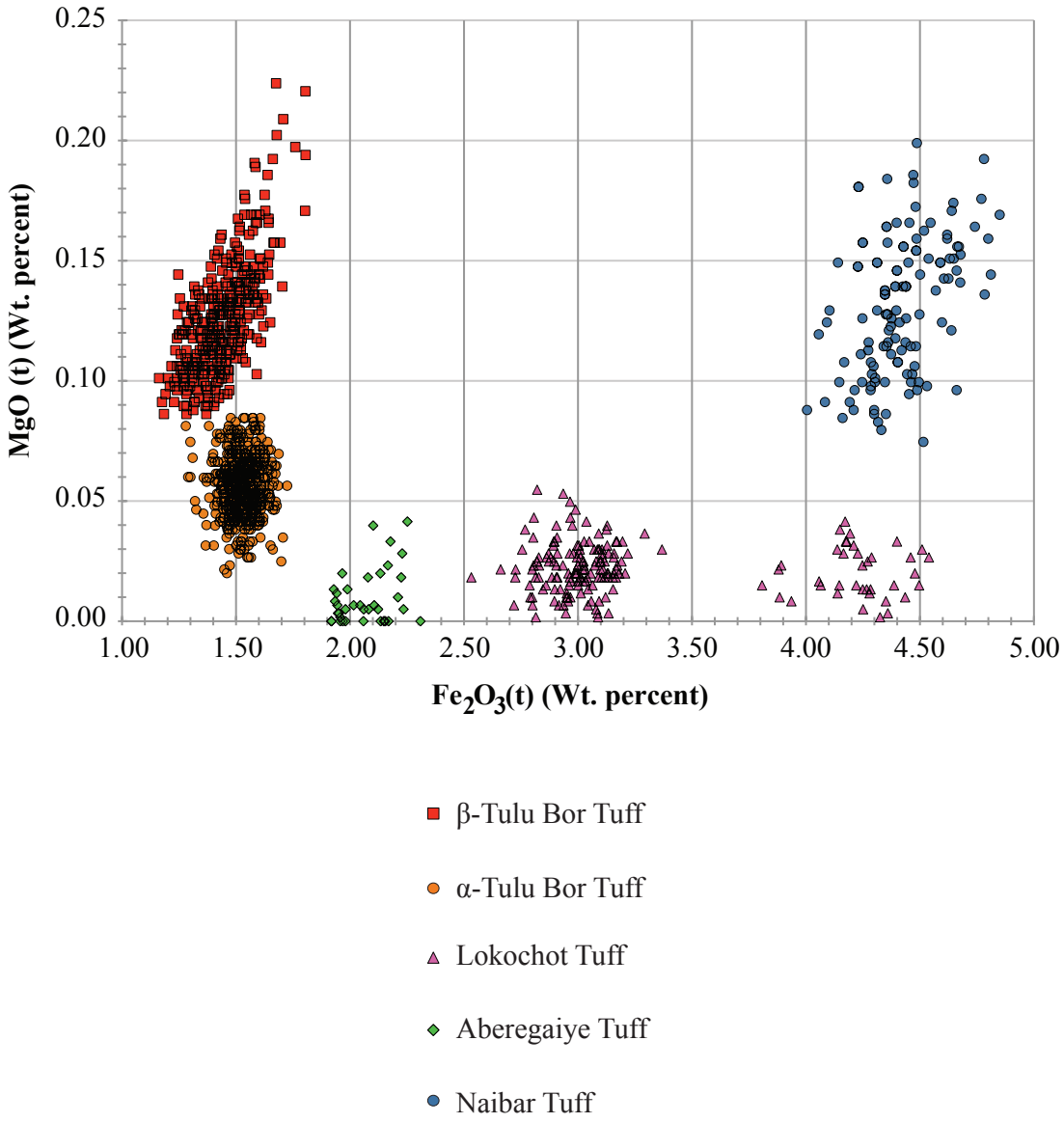

Figure 7. Bivariate (Fe_2O_3 (T) vs. MgO) plot of electron microprobe analyses of glass shards from rhyolitic tuffs from the study area. Note the two distinct modes within the Lokochot Tuff.

Table 1. Electron microprobe analyses of glasses from tuffs collected in Areas 117, 137, and 116.

Sample #	N	SiO_2	TiO_2	Al_2O_3	Fe_2O_3[a]	MnO	MgO	CaO	Na_2O	K_2O	F	Cl	Less Cl, F for O	H_2O[b]	Total
Unnamed Tuff above Tulu Bor (mode 1)															
K80-213		72.76	0.12	10.86	2.46	0.07	0.02	0.19	3.52	4.31	0.16	0.12	0.09	6.73	101.33
1 σ	3	0.46	0.03	0.06	0.19	0.00	0.02	0.01	0.81	0.14	0.02	0.01	0.01	1.71	0.40
MB08-28		73.03	0.13	11.01	2.84	0.04	0.00	0.18	3.85	4.01	0.12	0.16	0.09	5.90	101.30
1 σ	2	0.56	0.04	0.27	0.49	0.02	0.00	0.01	0.44	1.22	0.01	0.00	0.01	1.42	0.00
Unnamed Tuff above Tulu Bor (mode 2)															
K80-187		71.58	0.37	11.42	2.80	0.20	0.17	0.17	2.27	2.84	-0.07	0.17	0.04	7.43	99.53
1 σ	7	0.58	0.07	0.14	0.10	0.04	0.01	0.02	0.38	0.37	0.00	0.02	0.00	0.74	0.64
K80-213		70.26	0.35	11.63	2.81	0.19	0.18	0.17	3.60	4.44	0.15	0.15	0.13	6.26	100.26
1 σ	4	0.16	0.07	0.01	0.07	0.01	0.01	0.02	0.71	0.17	0.02	0.01	0.01	0.89	0.22
MB08-28		71.16	0.41	11.20	3.19	0.17	0.17	0.15	3.00	2.72	0.19	0.13	0.12	8.37	100.88
1 σ	5	0.99	0.02	0.25	0.18	0.01	0.01	0.01	0.52	0.24	0.04	0.01	0.03	1.14	0.48
β-Tulu Bor Tuff															
MB08-01		72.47	0.14	12.22	1.54	0.07	0.06	0.30	3.20	2.51	0.02	0.10	0.05	6.71	99.38
1 σ	19	0.81	0.03	0.38	0.05	0.02	0.01	0.01	0.20	0.31	0.04	0.01	0.02	0.75	0.44
MB08-02		72.11	0.15	11.85	1.52	0.05	0.06	0.29	3.13	2.45	0.06	0.09	0.06	7.34	99.14
1 σ	19	0.60	0.03	0.31	0.04	0.02	0.01	0.01	0.59	0.22	0.05	0.01	0.02	0.47	0.39
MB08-09		72.41	0.14	11.97	1.53	0.05	0.05	0.29	3.46	3.33	0.11	0.09	0.08	6.73	100.19
1 σ	13	0.34	0.04	0.50	0.08	0.01	0.01	0.02	0.21	0.36	0.05	0.01	0.02	0.75	0.34
MB08-10A		73.78	0.14	11.97	1.47	0.05	0.05	0.29	3.63	3.51	0.07	0.10	0.07	5.21	100.33
1 σ	12	0.46	0.03	0.08	0.05	0.03	0.01	0.01	0.11	0.15	0.05	0.01	0.02	0.41	0.46
MB08-11		72.56	0.15	12.05	1.51	0.05	0.06	0.29	3.59	3.71	0.17	0.10	0.11	6.31	100.54
1 σ	15	0.39	0.03	0.28	0.05	0.02	0.01	0.01	0.25	0.30	0.03	0.01	0.01	0.52	0.24

Table 1. cont.

Sample #	N	SiO_2	TiO_2	Al_2O_3	Fe_2O_3[a]	MnO	MgO	CaO	Na_2O	K_2O	F	Cl	Less Cl, F for O	H_2O[b]	Total
MB08-18		72.15	0.15	11.81	1.57	0.06	0.05	0.29	4.21	3.59	0.11	0.09	0.08	5.87	99.98
1 σ	19	0.55	0.03	0.13	0.05	0.02	0.01	0.02	0.26	0.75	0.04	0.01	0.02	1.00	0.38
MB08-19		72.04	0.11	11.24	1.47	0.05	0.04	0.25	3.87	3.05	0.23	0.16	0.15	6.98	99.46
1 σ	2	0.29	0.00	0.01	0.03	0.01	0.02	0.01	0.03	0.02	0.01	0.02	0.01	0.26	0.18
MB08-20		73.09	0.16	11.73	1.53	0.06	0.06	0.29	3.88	3.09	0.18	0.10	0.11	6.25	100.39
1 σ	13	0.46	0.02	0.29	0.05	0.02	0.02	0.01	1.08	0.36	0.04	0.01	0.02	0.93	0.37
MB08-21		73.75	0.15	12.81	1.51	0.07	0.06	0.30	4.54	2.97	0.09	0.09	0.07	4.10	100.50
1 σ	19	0.33	0.03	0.41	0.07	0.02	0.01	0.04	0.16	0.54	0.06	0.01	0.03	0.61	0.36
MB08-22		72.24	0.18	11.74	1.61	0.05	0.08	0.36	4.43	3.60	0.12	0.10	0.07	5.08	99.59
1 σ	13	0.64	0.05	0.31	0.05	0.02	0.04	0.13	0.21	0.41	0.02	0.01	0.01	0.58	0.36
MB08-27		73.99	0.15	12.36	1.60	0.05	0.06	0.29	4.24	3.28	0.18	0.09	0.11	4.68	100.97
1 σ	15	0.26	0.03	0.28	0.04	0.02	0.01	0.01	0.22	0.27	0.03	0.01	0.01	0.49	0.31
MB08-29		73.71	0.15	12.40	1.58	0.05	0.06	0.28	4.18	3.90	0.19	0.10	0.12	4.30	100.92
1 σ	14	0.44	0.04	0.25	0.04	0.02	0.01	0.02	0.14	0.13	0.03	0.01	0.01	0.42	0.32
MB08-32		72.56	0.14	11.70	1.53	0.05	0.06	0.29	4.43	3.50	0.16	0.09	0.10	6.24	100.72
1 σ	20	1.02	0.04	0.12	0.05	0.02	0.01	0.01	0.22	0.26	0.05	0.01	0.02	0.66	0.39
MB08-33		71.96	0.15	11.68	1.52	0.05	0.06	0.29	4.42	3.67	0.17	0.09	0.11	6.33	100.39
1 σ	20	0.95	0.04	0.11	0.04	0.01	0.01	0.01	0.15	0.19	0.03	0.01	0.01	0.66	0.41
MB08-34		72.10	0.15	11.71	1.53	0.06	0.05	0.29	4.52	3.65	0.16	0.09	0.10	6.27	100.59
1 σ	19	0.73	0.03	0.14	0.04	0.02	0.01	0.01	0.17	0.31	0.05	0.01	0.02	0.63	0.29
MB08-35		73.12	0.17	12.05	1.55	0.05	0.05	0.29	4.11	3.56	0.19	0.09	0.12	5.68	100.90
1 σ	15	0.59	0.02	0.22	0.08	0.02	0.01	0.01	0.22	0.34	0.03	0.01	0.01	0.76	0.41

Table 1. cont.

Sample #	N	SiO_2	TiO_2	Al_2O_3	Fe_2O_3[a]	MnO	MgO	CaO	Na_2O	K_2O	F	Cl	Less Cl, F for O	H_2O[b]	Total
MB08-38		73.17	0.14	12.00	1.55	0.05	0.06	0.30	3.98	3.50	0.16	0.09	0.10	5.72	100.70
1 σ	15	0.37	0.04	0.14	0.04	0.02	0.01	0.02	0.31	0.40	0.03	0.01	0.01	0.71	0.27
MB08-39		73.51	0.15	12.55	1.49	0.05	0.06	0.30	4.41	3.41	0.16	0.10	0.10	5.99	102.16
1 σ	8	0.49	0.02	0.09	0.04	0.03	0.01	0.02	0.13	0.14	0.03	0.01	0.01	0.47	0.31
MB08-42		73.68	0.14	12.05	1.54	0.04	0.05	0.30	3.84	3.40	0.16	0.09	0.10	5.37	100.68
1 σ	15	0.32	0.04	0.23	0.04	0.02	0.02	0.01	0.66	0.28	0.03	0.01	0.01	0.63	0.40
MB08-43		70.26	0.29	13.58	2.79	0.10	0.13	0.59	2.28	2.73	0.11	0.07	0.09	6.80	99.92
1 σ	17	2.77	0.12	0.43	1.28	0.06	0.05	0.15	1.69	1.12	0.03	0.02	0.01	2.23	1.04
MB08-46		71.88	0.16	11.65	1.50	0.06	0.06	0.30	4.42	3.54	0.17	0.09	0.11	6.61	100.42
1 σ	18	0.27	0.02	0.18	0.04	0.02	0.01	0.01	0.16	0.41	0.03	0.01	0.01	0.54	0.19
MB08-49		73.40	0.14	11.73	1.55	0.06	0.06	0.30	4.10	3.51	0.17	0.09	0.11	5.47	100.59
1 σ	15	0.48	0.03	0.24	0.06	0.02	0.02	0.01	0.35	0.47	0.03	0.01	0.01	0.87	0.50
MB08-50		73.74	0.15	12.07	1.57	0.05	0.06	0.30	3.99	3.65	0.17	0.09	0.11	4.98	100.82
1 σ	15	0.35	0.02	0.25	0.06	0.02	0.01	0.01	0.66	0.25	0.03	0.01	0.01	0.54	0.25
MB08-51		73.70	0.16	11.89	1.61	0.06	0.06	0.30	3.93	3.36	0.15	0.09	0.10	5.15	100.47
1 σ	15	0.54	0.04	0.42	0.20	0.02	0.01	0.04	0.26	0.33	0.03	0.01	0.01	0.84	0.45
MB08-52		73.51	0.15	12.08	1.57	0.05	0.06	0.30	4.30	3.32	0.09	0.09	0.07	4.83	100.39
1 σ	10	0.19	0.03	0.15	0.05	0.01	0.01	0.01	0.18	0.22	0.06	0.01	0.03	0.38	0.19
MB08-55		73.19	0.15	12.02	1.57	0.05	0.05	0.30	4.09	3.45	0.17	0.09	0.11	5.49	100.66
1 σ	11	0.35	0.02	0.17	0.02	0.03	0.01	0.02	0.42	0.42	0.02	0.01	0.01	1.10	0.23
MB08-60		73.37	0.17	11.68	1.62	0.05	0.06	0.32	3.81	3.58	0.16	0.09	0.09	5.81	100.68
1 σ	9	0.35	0.03	0.10	0.04	0.02	0.01	0.02	0.21	0.42	0.04	0.01	0.02	0.73	0.35

Table 1. cont.

Sample #	N	SiO_2	TiO_2	Al_2O_3	Fe_2O_3[a]	MnO	MgO	CaO	Na_2O	K_2O	F	Cl	Less Cl, F for O	H_2O[b]	Total
MB08-61		72.20	0.12	11.74	1.53	0.05	0.06	0.29	4.33	3.59	0.13	0.10	0.09	5.72	99.88
1 σ	19	0.39	0.03	0.08	0.05	0.02	0.01	0.01	0.14	0.45	0.04	0.01	0.02	0.54	0.22
MB08-65		73.50	0.14	12.55	1.48	0.05	0.06	0.29	3.91	3.58	0.10	0.10	0.08	5.77	101.58
1 σ	12	0.51	0.04	0.29	0.07	0.02	0.01	0.02	0.26	0.35	0.05	0.01	0.02	0.61	0.50
MB08-66		73.49	0.14	12.53	1.52	0.05	0.06	0.30	4.02	3.42	0.16	0.09	0.10	4.61	100.40
1 σ	20	0.34	0.04	0.28	0.09	0.02	0.02	0.06	0.34	0.49	0.03	0.01	0.01	0.68	0.34
MB08-67		73.06	0.18	11.95	1.95	0.07	0.05	0.29	4.24	3.37	0.21	0.08	0.13	4.71	100.16
1 σ	14	0.36	0.04	0.32	0.12	0.03	0.01	0.02	0.36	0.34	0.03	0.01	0.01	0.49	0.32
MB08-71		72.37	0.14	11.62	1.53	0.04	0.05	0.30	4.74	3.28	0.18	0.09	0.11	6.30	100.65
1 σ	15	0.41	0.03	0.13	0.04	0.02	0.01	0.01	0.17	0.24	0.04	0.01	0.02	0.42	0.25
MB08-74		72.79	0.19	12.72	1.28	0.04	0.10	0.47	4.24	3.60	0.16	0.09	0.10	4.67	100.36
1 σ	14	0.30	0.04	0.20	0.04	0.02	0.01	0.02	0.17	0.38	0.03	0.01	0.01	0.54	0.31
MB08-82		72.44	0.14	12.04	1.46	0.05	0.06	0.29	4.06	3.69	0.18	0.09	0.11	6.24	100.75
1 σ	11	0.36	0.02	0.37	0.06	0.02	0.01	0.01	0.20	0.40	0.04	0.01	0.02	0.82	0.32
MB08-83		73.09	0.16	12.52	1.48	0.05	0.06	0.32	3.78	3.42	0.19	0.10	0.12	5.92	101.10
1 σ	13	0.75	0.02	0.45	0.04	0.02	0.02	0.06	1.05	0.45	0.04	0.01	0.02	1.23	0.47
MB08-84		72.90	0.14	12.37	1.43	0.05	0.06	0.28	4.04	3.42	0.18	0.09	0.11	5.76	100.72
1 σ	12	0.30	0.02	0.25	0.05	0.02	0.01	0.02	0.24	0.42	0.02	0.01	0.01	0.69	0.27
MB08-87		73.66	0.14	12.25	1.52	0.06	0.06	0.29	4.35	3.38	0.13	0.10	0.09	5.76	101.68
1 σ	13	0.68	0.03	0.23	0.05	0.02	0.02	0.01	0.27	0.25	0.05	0.01	0.02	0.63	0.76
MB08-93		73.72	0.15	12.29	1.49	0.05	0.05	0.29	4.04	3.49	0.16	0.10	0.10	6.25	102.08
1 σ	20	0.38	0.02	0.12	0.03	0.02	0.01	0.01	0.20	0.25	0.04	0.01	0.02	0.46	0.42

Table 1. cont.

Sample #	N	SiO_2	TiO_2	Al_2O_3	Fe_2O_3[a]	MnO	MgO	CaO	Na_2O	K_2O	F	Cl	Less Cl, F for O	H_2O[b]	Total
α-Tulu Bor Tuff															
K77-27		71.21	0.23	12.68	1.55	0.05	0.14	0.58	2.77	3.46	0.03	0.09	0.05	6.36	99.25
1 σ	30	0.76	0.04	0.22	0.11	0.01	0.03	0.08	0.58	0.37	0.05	0.01	0.02	1.37	1.03
MB08-14		72.17	0.22	12.32	1.39	0.04	0.11	0.48	3.67	3.15	0.03	0.09	0.05	6.46	100.18
1 σ	17	0.69	0.04	0.17	0.09	0.01	0.02	0.05	0.23	0.57	0.05	0.01	0.02	0.96	0.34
MB08-15		71.07	0.26	12.67	1.45	0.04	0.14	0.56	3.23	2.87	0.14	0.09	0.09	7.42	99.96
1 σ	19	0.69	0.04	0.28	0.12	0.02	0.03	0.07	0.31	0.38	0.04	0.01	0.02	0.76	0.35
MB08-16		71.35	0.23	12.57	1.44	0.04	0.13	0.54	3.21	3.40	0.14	0.09	0.09	7.39	100.56
1 σ	19	0.76	0.04	0.27	0.11	0.02	0.02	0.06	0.48	0.40	0.04	0.01	0.01	1.34	0.36
MB08-17		71.56	0.24	12.72	1.44	0.04	0.13	0.55	3.30	3.01	0.15	0.09	0.10	7.24	100.49
1 σ	20	0.59	0.04	0.22	0.07	0.02	0.02	0.06	0.24	0.37	0.04	0.01	0.02	0.75	0.35
MB08-36		70.90	0.22	12.24	1.42	0.04	0.12	0.54	4.32	3.16	0.16	0.09	0.10	7.06	100.29
1 σ	20	0.59	0.04	0.13	0.08	0.02	0.02	0.05	0.20	0.78	0.03	0.01	0.01	0.86	0.34
MB08-37		69.82	0.23	12.63	1.39	0.04	0.13	0.55	3.76	2.99	0.11	0.08	0.08	8.61	100.38
1 σ	15	0.50	0.05	0.30	0.09	0.02	0.02	0.06	0.28	0.31	0.04	0.01	0.02	0.56	0.29
MB08-44		72.37	0.25	13.69	1.50	0.05	0.14	0.56	3.95	2.78	0.11	0.09	0.08	4.75	100.27
1 σ	20	0.51	0.05	0.32	0.08	0.02	0.02	0.05	0.23	0.43	0.02	0.01	0.01	0.80	0.28
MB08-47		72.72	0.21	12.84	1.38	0.04	0.11	0.49	4.24	3.48	0.09	0.09	0.07	4.44	100.16
1 σ	12	0.42	0.04	0.29	0.10	0.01	0.02	0.06	0.22	0.43	0.04	0.01	0.02	0.86	0.30
MB08-48		72.15	0.23	12.64	1.41	0.04	0.12	0.52	4.16	3.08	0.14	0.09	0.09	5.46	100.10
1 σ	17	0.55	0.04	0.27	0.13	0.02	0.03	0.06	0.18	0.42	0.03	0.01	0.01	0.71	0.16
MB08-53		72.35	0.21	12.55	1.32	0.04	0.10	0.47	4.14	3.58	0.15	0.09	0.10	5.27	100.27
1 σ	10	0.28	0.04	0.16	0.03	0.02	0.01	0.01	0.12	0.48	0.02	0.01	0.01	0.68	0.23

Table 1. cont.

Sample #	N	SiO_2	TiO_2	Al_2O_3	Fe_2O_3[a]	MnO	MgO	CaO	Na_2O	K_2O	F	Cl	Less Cl, F for O	H_2O[b]	Total
MB08-54		70.69	0.23	12.18	1.46	0.05	0.12	0.52	3.99	2.87	0.11	0.09	0.08	7.19	99.51
1 σ	17	0.47	0.04	0.11	0.09	0.02	0.02	0.06	0.29	0.56	0.04	0.01	0.02	0.81	0.36
MB08-56		71.78	0.23	12.55	1.48	0.05	0.12	0.55	3.18	2.80	0.10	0.09	0.08	6.81	99.79
1 σ	10	0.34	0.03	0.11	0.08	0.01	0.02	0.03	0.18	0.27	0.05	0.01	0.02	0.46	0.30
MB08-62		70.30	0.24	11.52	2.91	0.12	0.10	0.25	3.66	2.91	0.15	0.12	0.12	7.10	99.49
1 σ	18	0.80	0.08	0.61	0.53	0.03	0.03	0.15	0.51	0.57	0.04	0.05	0.01	0.90	0.36
MB08-70		70.86	0.24	12.23	1.43	0.05	0.12	0.53	4.39	2.90	0.15	0.09	0.10	7.47	100.46
1 σ	18	0.48	0.04	0.11	0.08	0.02	0.02	0.04	0.22	0.77	0.03	0.01	0.01	0.98	0.26
MB08-71		72.37	0.14	11.62	1.53	0.04	0.05	0.30	4.74	3.28	0.18	0.09	0.11	6.30	100.65
1 σ	15	0.41	0.03	0.13	0.04	0.02	0.01	0.01	0.17	0.24	0.04	0.01	0.02	0.42	0.25
MB08-73		71.25	0.21	12.65	1.30	0.05	0.11	0.49	4.02	3.62	0.19	0.09	0.11	6.75	100.75
1 σ	10	0.54	0.05	0.20	0.13	0.02	0.03	0.05	0.17	0.43	0.03	0.01	0.01	0.78	0.43
MB08-75		71.66	0.27	12.72	1.61	0.06	0.16	0.65	3.79	3.03	0.16	0.09	0.10	6.47	100.68
1 σ	9	0.53	0.05	0.27	0.11	0.02	0.04	0.09	0.18	0.48	0.03	0.01	0.01	0.93	0.13
MB08-85		71.45	0.24	13.03	1.42	0.04	0.14	0.57	3.75	3.23	0.17	0.09	0.11	6.61	100.73
1 σ	20	0.68	0.05	0.40	0.13	0.01	0.04	0.10	0.27	0.46	0.03	0.01	0.01	0.98	0.35
MB08-86		72.56	0.20	12.49	1.30	0.04	0.11	0.46	4.44	3.56	0.15	0.09	0.10	5.06	100.48
1 σ	20	0.31	0.03	0.13	0.05	0.02	0.01	0.01	0.14	0.25	0.03	0.01	0.01	0.45	0.25
MB08-88		73.37	0.17	13.09	1.41	0.04	0.08	0.35	4.30	3.79	0.14	0.09	0.09	4.42	101.26
1 σ	12	0.44	0.05	0.41	0.12	0.02	0.03	0.10	0.24	0.53	0.02	0.01	0.01	0.77	0.27
MB08-89		71.01	0.21	12.10	1.36	0.04	0.12	0.49	4.16	3.88	0.16	0.08	0.10	6.82	100.43
1 σ	15	0.54	0.04	0.11	0.10	0.02	0.02	0.05	0.21	0.49	0.04	0.01	0.02	0.67	0.22

Table 1. cont.

Sample #	N	SiO_2	TiO_2	Al_2O_3	Fe_2O_3[a]	MnO	MgO	CaO	Na_2O	K_2O	F	Cl	Less Cl, F for O	H_2O[b]	Total
Kaado tuff															
K83-1584		71.43	0.35	12.14	2.43	0.15	0.17	0.19	4.14	1.84	0.14	0.09	0.10	7.12	100.27
1 σ	17	0.43	0.04	0.14	0.09	0.03	0.02	0.02	0.37	0.26	0.04	0.01	0.02	0.74	0.36
Lokochot Tuff (mode 1)															
MB08-08		74.08	0.19	10.93	3.08	0.09	0.02	0.17	3.56	3.90	0.19	0.14	0.14	4.08	100.50
1 σ	10	0.50	0.02	0.29	0.07	0.02	0.01	0.02	0.67	0.58	0.04	0.01	0.02	1.21	0.44
MB08-12		73.79	0.18	10.68	3.15	0.09	0.02	0.18	2.84	3.14	0.22	0.14	0.16	5.64	100.17
1 σ	12	0.35	0.02	0.26	0.09	0.03	0.01	0.02	0.19	0.21	0.05	0.01	0.02	0.46	0.23
MB08-13		73.77	0.18	10.27	3.11	0.08	0.02	0.18	2.96	3.44	0.22	0.14	0.16	5.33	99.81
1 σ	11	0.42	0.03	0.30	0.06	0.03	0.00	0.02	0.23	0.13	0.06	0.01	0.03	0.39	0.26
MB08-26		71.95	0.19	10.27	3.05	0.09	0.02	0.17	4.18	3.43	0.22	0.13	0.15	5.90	99.69
1 σ	19	0.42	0.03	0.11	0.07	0.02	0.01	0.02	0.92	0.36	0.03	0.01	0.02	0.71	0.41
MB08-30		73.61	0.19	10.58	3.00	0.08	0.02	0.18	3.54	3.26	0.22	0.13	0.15	5.96	100.87
1 σ	12	0.44	0.04	0.38	0.06	0.03	0.01	0.02	0.42	0.26	0.05	0.01	0.02	0.76	0.41
MB08-59		71.85	0.22	10.06	3.91	0.13	0.01	0.17	2.86	2.33	0.37	0.16	0.23	7.97	100.17
1 σ	12	0.54	0.03	0.07	0.04	0.01	0.01	0.01	0.02	0.11	0.06	0.00	0.02	0.56	0.04
MB08-63		73.58	0.17	10.39	3.10	0.08	0.02	0.17	3.54	3.45	0.25	0.13	0.17	5.39	100.35
1 σ	9	0.21	0.03	0.07	0.05	0.01	0.01	0.01	0.42	0.20	0.06	0.01	0.02	0.35	0.35
MB08-68		71.65	0.17	10.57	2.83	0.08	0.03	0.16	4.24	3.28	0.25	0.13	0.16	7.15	100.61
1 σ	14	0.34	0.03	0.11	0.05	0.02	0.01	0.01	0.28	0.24	0.05	0.01	0.02	0.57	0.27
MB08-69		74.07	0.18	11.12	2.83	0.09	0.01	0.17	4.71	4.07	0.17	0.13	0.13	3.85	101.55
1 σ	11	0.79	0.04	0.77	0.24	0.02	0.01	0.02	0.26	0.29	0.03	0.02	0.02	0.31	0.70

Table 1. cont.

Sample #	N	SiO_2	TiO_2	Al_2O_3	Fe_2O_3[a]	MnO	MgO	CaO	Na_2O	K_2O	F	Cl	Less Cl, F for O	H_2O[b]	Total
MB08-80		73.97	0.23	10.42	3.04	0.09	0.03	0.18	4.03	4.23	0.22	0.13	0.15	3.89	100.59
1 σ	4	0.45	0.07	0.10	0.04	0.02	0.01	0.02	0.55	0.64	0.04	0.01	0.02	1.66	0.19
MB08-81		72.35	0.19	10.23	2.93	0.09	0.02	0.17	4.08	4.07	0.18	0.13	0.13	5.53	100.08
1 σ	14	0.72	0.04	0.09	0.07	0.02	0.01	0.01	0.42	0.65	0.08	0.01	0.03	1.27	0.47
MB08-91		74.00	0.17	10.87	2.96	0.09	0.03	0.17	4.11	3.60	0.20	0.13	0.14	5.56	101.98
1 σ	9	0.50	0.04	0.10	0.06	0.01	0.02	0.02	0.49	0.56	0.04	0.01	0.02	1.22	0.34
Lokochot Tuff (mode 2)															
MB08-08		72.92	0.25	10.18	4.45	0.12	0.01	0.19	2.29	2.64	0.18	0.18	0.16	6.42	100.04
1 σ	4	0.42	0.02	0.31	0.09	0.01	0.01	0.01	0.23	0.29	0.08	0.01	0.04	0.71	0.22
MB08-12		72.90	0.24	10.02	4.35	0.13	0.03	0.18	2.06	2.54	0.14	0.17	0.14	6.85	99.77
1 σ	3	0.54	0.03	0.19	0.16	0.01	0.01	0.01	0.37	0.11	0.08	0.01	0.03	0.81	0.51
MB08-13		73.19	0.21	9.64	4.29	0.14	0.03	0.18	1.87	2.48	0.10	0.18	0.13	6.50	99.01
1 σ	3	0.05	0.07	0.34	0.10	0.03	0.02	0.01	0.29	0.13	0.11	0.01	0.04	0.21	0.54
MB08-26		71.62	0.23	9.49	4.21	0.13	0.03	0.17	3.43	2.55	0.27	0.17	0.19	6.92	99.32
1 σ	1														
MB08-30		73.56	0.21	10.08	4.35	0.14	0.01	0.18	2.65	2.73	0.23	0.18	0.18	6.43	100.95
1 σ	3	0.33	0.04	0.13	0.08	0.03	0.01	0.01	0.05	0.10	0.07	0.01	0.03	0.30	0.26
MB08-59		72.68	0.17	10.56	2.79	0.08	0.02	0.17	3.63	3.13	0.28	0.13	0.17	6.73	100.43
1 σ	2	0.49	0.03	0.41	0.12	0.02	0.01	0.02	0.38	0.35	0.05	0.01	0.02	0.68	0.38
MB08-63		72.74	0.21	9.61	4.34	0.14	0.00	0.18	2.62	2.60	0.15	0.18	0.15	6.56	99.60
1 σ	2	0.23	0.09	0.07	0.07	0.02	0.00	0.01	0.25	0.10	0.12	0.01	0.05	0.07	0.75
MB08-80		73.04	0.23	9.68	4.28	0.13	0.01	0.19	3.48	3.45	0.30	0.17	0.21	5.26	100.37
1 σ	5	0.28	0.01	0.12	0.05	0.04	0.01	0.01	0.97	0.85	0.13	0.01	0.05	1.81	0.37

Table 1. cont.

Sample #	N	SiO_2	TiO_2	Al_2O_3	Fe_2O_3[a]	MnO	MgO	CaO	Na_2O	K_2O	F	Cl	Less Cl, F for O	H_2O[b]	Total
MB08-81		71.76	0.23	9.47	4.16	0.14	0.02	0.19	3.85	3.60	0.22	0.17	0.17	5.96	99.95
1 σ	4	0.64	0.03	0.13	0.09	0.02	0.01	0.01	0.74	0.97	0.05	0.01	0.02	2.02	0.39
MB08-91		73.34	0.22	10.12	4.22	0.13	0.02	0.18	3.59	3.18	0.25	0.18	0.19	6.18	101.78
1 σ	7	0.26	0.02	0.25	0.08	0.03	0.01	0.01	0.79	0.99	0.09	0.01	0.04	1.91	0.36
Loruth Tuff															
K82-746		71.44	0.17	11.73	2.96	0.09	0.00	0.32	3.49	4.25	0.14	0.15	0.12	5.37	100.16
1 σ	12	0.41	0.03	0.08	0.10	0.03	0.00	0.04	0.30	0.36	0.04	0.01	0.02	0.95	0.50
MB08-25		70.77	0.18	12.07	2.98	0.09	0.00	0.36	4.10	3.23	0.25	0.16	0.17	6.66	100.89
1 σ	20	0.37	0.03	0.25	0.07	0.02	0.01	0.01	0.40	0.40	0.04	0.01	0.02	0.48	0.32
Aberegaiye Tuff															
K81-586		74.31	0.12	11.67	1.92	0.05	0.01	0.23	1.07	2.64	0.22	0.18	0.15	7.79	100.22
1 σ		0.35	0.05	0.30	0.08	0.01	0.01	0.02	0.40	0.38	0.04	0.05	0.03	0.29	1.13
MB08-45		74.89	0.13	11.87	2.16	0.07	0.01	0.28	4.10	2.62	0.21	0.14	0.14	4.33	100.82
1 σ		0.61	0.04	0.31	0.07	0.01	0.01	0.01	0.86	0.78	0.05	0.01	0.02	1.70	0.51
MB08-77		73.57	0.13	11.73	1.96	0.07	0.01	0.26	4.09	2.24	0.22	0.14	0.14	6.13	100.55
1 σ		0.41	0.03	0.32	0.03	0.02	0.01	0.01	0.34	0.32	0.04	0.01	0.02	0.68	0.57
Moiti Tuff, pumice															
ANU 83-1		70.93	0.32	10.57	4.41	0.16	0.00	0.29	4.61	4.09					
1 σ	19	0.63	0.05	0.15	0.10	0.02	0.02	0.01	0.27	0.14					

Table 1. cont.

Sample #	N	SiO_2	TiO_2	Al_2O_3	Fe_2O_3[a]	MnO	MgO	CaO	Na_2O	K_2O	F	Cl	Less Cl, F for O	H_2O[b]	Total
ANU 83-2		71.67	0.31	10.56	4.43	0.17	0.01	0.29	4.63	4.22					
1 σ	16	0.51	0.05	0.20	0.10	0.03	0.01	0.02	0.22	0.09					
Naibar Tuff, pumice															
MB08-06A		74.47	0.32	10.56	4.49	0.19	0.12	0.17	0.87	2.77	0.09	0.16	0.07	5.76	100.08
1 σ	13	0.79	0.03	0.28	0.10	0.02	0.02	0.01	0.18	0.33	0.03	0.02	0.01	0.52	0.86
MB08-06B		73.28	0.34	11.30	4.70	0.24	0.15	0.22	0.83	2.71	0.04	0.13	0.05	6.24	100.31
1 σ	11	0.48	0.04	0.09	0.08	0.08	0.02	0.02	0.09	0.05	0.03	0.01	0.01	0.29	0.36
Naibar Tuff															
K75-117a		71.76	0.36	11.15	4.49	0.22	0.14	0.21	2.28	3.57	0.06	0.13	0.05	5.63	100.09
1 σ	15	1.57	0.07	0.78	0.16	0.03	0.04	0.06	0.68	0.56	0.06	0.02	0.02	1.34	0.67
K82-870	1,1	71.48	0.29	10.78	4.42	0.21	0.12	0.20	2.14	2.90		0.13	0.07	6.84	99.69
1 σ	9	2.05	0.05	0.59	0.18	0.03	0.04	0.04	0.52	0.57	0.06	0.01	0.02	1.64	2.10
K82-870	1,2	70.77	0.34	11.32	4.41	0.22	0.16	0.25	2.13	2.88		0.12	0.06	7.17	99.92
1 σ	11	2.42	0.10	1.30	0.16	0.03	0.09	0.12	0.47	0.52	0.05	0.03	0.02	1.68	2.01
K82-876		71.10	0.23	11.09	3.62	0.16	0.11	0.18	1.92	2.48	0.00	0.13	0.07	9.28	100.43
1 σ	12	1.24	0.05	0.61	0.48	0.03	0.01	0.03	0.32	0.22	0.06	0.01	0.03	1.41	1.31
MB08-03		71.11	0.23	11.81	3.08	0.13	0.11	0.20	3.22	3.56	0.14	0.12	0.12	6.26	100.11
1 σ	3	0.67	0.02	0.36	0.23	0.01	0.02	0.01	0.56	0.87	0.08	0.01	0.03	1.16	0.21
MB08-05		72.28	0.30	10.66	4.42	0.18	0.12	0.16	3.12	3.55	0.12	0.14	0.13	5.03	100.18
1 σ	18	0.61	0.05	0.54	0.11	0.02	0.02	0.03	0.79	0.70	0.07	0.02	0.03	1.24	0.56

Table 1. cont.

Sample #	N	SiO_2	TiO_2	Al_2O_3	Fe_2O_3[a]	MnO	MgO	CaO	Na_2O	K_2O	F	Cl	Less Cl, F for O	H_2O[b]	Total
MB08-07		72.50	0.30	10.81	4.47	0.19	0.12	0.16	3.26	3.72	0.12	0.15	0.13	4.40	100.30
1 σ	17	0.72	0.04	0.42	0.14	0.02	0.02	0.03	0.52	0.40	0.07	0.01	0.03	0.79	0.39
MB08-58		74.06	0.19	10.93	2.91	0.10	0.02	0.17	4.06	3.24	0.23	0.13	0.16	4.05	100.18
1 σ	19	0.23	0.03	0.32	0.07	0.03	0.01	0.01	0.31	0.39	0.05	0.01	0.02	0.46	0.43
MB08-78		72.13	0.30	10.88	3.58	0.16	0.12	0.17	3.82	3.48	0.18	0.14	0.14	5.49	100.50
1 σ		0.15	0.01	0.19	0.12	0.02	0.01	0.01	1.31	0.96	0.06	0.01	0.03	1.63	0.86
MB08-79		71.45	0.31	10.17	4.14	0.18	0.10	0.15	3.31	3.23	0.01	0.16	0.08	5.99	99.39
1 σ	4	0.32	0.05	0.18	0.06	0.02	0.02	0.01	0.36	0.49	0.04	0.01	0.02	0.97	0.28
MB08-90		71.55	0.30	10.49	4.30	0.21	0.12	0.18	2.34	2.28	0.10	0.14	0.12	7.90	100.09
1 σ	5	1.15	0.05	0.52	0.09	0.02	0.04	0.05	0.08	0.05	0.05	0.01	0.02	0.02	0.31
Kanyeris Tuff															
IL03-008		71.70	0.42	12.51	2.17	0.12	0.21	0.72	2.88	2.47	0.23	0.04	0.13	7.01	100.53
1 σ	14	1.12	0.03	0.20	0.19	0.03	0.03	0.10	0.53	0.65	0.04	0.01	0.02	1.28	0.64
IL03-012		71.65	0.45	12.52	2.24	0.13	0.22	0.76	1.88	1.61	0.16	0.04	0.10	8.34	100.06
1 σ	11	0.62	0.04	0.10	0.12	0.02	0.02	0.06	0.32	0.16	0.05	0.01	0.02	0.83	0.41
MB08-05		71.57	0.47	12.10	2.06	0.11	0.20	0.59	2.90	3.11	0.18	0.03	0.10	6.83	100.22
1 σ	2	1.05	0.09	0.43	0.46	0.02	0.09	0.20	0.62	0.63	0.05	0.00	0.02	1.18	0.37
MB08-07		71.40	0.47	12.53	2.29	0.13	0.21	0.69	3.17	3.29	0.16	0.05	0.10	5.56	100.01
1 σ	3	0.26	0.07	0.18	0.05	0.01	0.01	0.05	0.16	0.10	0.00	0.01	0.00	0.23	0.27
MB08-79		70.07	0.39	10.91	4.36	0.22	0.17	0.22	3.25	3.18	0.03	0.12	0.08	6.54	99.57
1 σ	2	0.56	0.01	0.04	0.00	0.03	0.02	0.03	0.43	0.91	0.01	0.00	0.01	1.67	0.20

a) All iron expressed as Fe_2O_3 b) Water calculations as explained in Nash (1992)

glass obtained from pumices found within some tuff units can be similarly identified. The chemical composition of the glasses within the pumices should be similar to those found within the volcanic tuff; if the tuff and pumice derive from the same volcanic event.

Age determinations are based on feldspars separated from the pumices found within volcanic tuffs using the Ar/Ar method. Through correlation of tuffs on a compositional basis, numerical ages determined in one section can be carried to other sections. For a more detailed discussion see McDougall and Brown (2008) and Brown (1994).

5.1 Lonyumun Member

The Lonyumun member is named after Il Lonyumun, an ephemeral stream in the southern part of the Koobi Fora region that is located east of Sibilot and is tributary to Il Lokochot. The type section is in Area 260 with a type thickness of 36.8 m (Brown and Feibel, 1986) and is defined as all sedimentary strata that lie below the base of the Moiti Tuff. The Lonyumun Member is comprised of claystones with montmorillonite "popcorn" surfaces, mudstones, diatomites, and sandstones. This member is distinguished in the field by its prominent laminated claystones, laminated diatomites, and massive mudstones. The claystones are pale olive to pale brown and commonly have large plates of gypsum scattered on the surface and fish fossils replaced with a mixture of an iron oxide/hydroxide mineral and a dark green mineral, probably mitridatite (Rogers and Brown, 1979). The diatomites are normally very pale yellow to white, well lithified, and sometimes altered. Mudstones (in the upper part of the member) are pale brown to

medium brown, and commonly have bright orange coprolites on the surface of the exposures.

The Lonyumun Member is principally exposed north of Il Naibar, and there are also a few scattered outcrops within the Kokoi Highland. The composite thickness of the Lonyumun Member in Area 117 is 106.25 m, making it the thickest member in the area. The Lonyumun Member was included as part of the Lower Member of the Koobi Fora Formation by Bowen (1974), and said to be younger than the Gombe Group Basalts.

5.1.1 Lithologic Description

The following description of the Lonyumun Member is based on exposures near Kolom Nabalware and near Il Naibar (section A117.7, Figure 4, Figure 5, Figure 8). Nowhere in the study area is the Lonyumun Member seen to rest on older rocks, so the thickness here is simply the maximum observed. Brown and Feibel (1986) also faced this difficulty in their original definition of the member. Some of the lower lithologic units are intruded by basalts of the Gombe Group and where this is the case, the sedimentary strata are highly altered by contact metamorphism. In the study area, the Moiti Tuff is not exposed, so the top of the Lonyumun member is locally taken to be the top of a pale green tuff with small (millimeter-scale) pumices which is named the Naibar Tuff in this study (see below). For a complete lithologic description of the Lonyumun Member see Appendix E.

The stratigraphy is broken into two major intervals. The lower interval, 66.25 m thick, contains repeating layers of compacted light brown or grey, massive, highly compacted claystones or mudstones. In some beds large gypsum plates were noted,

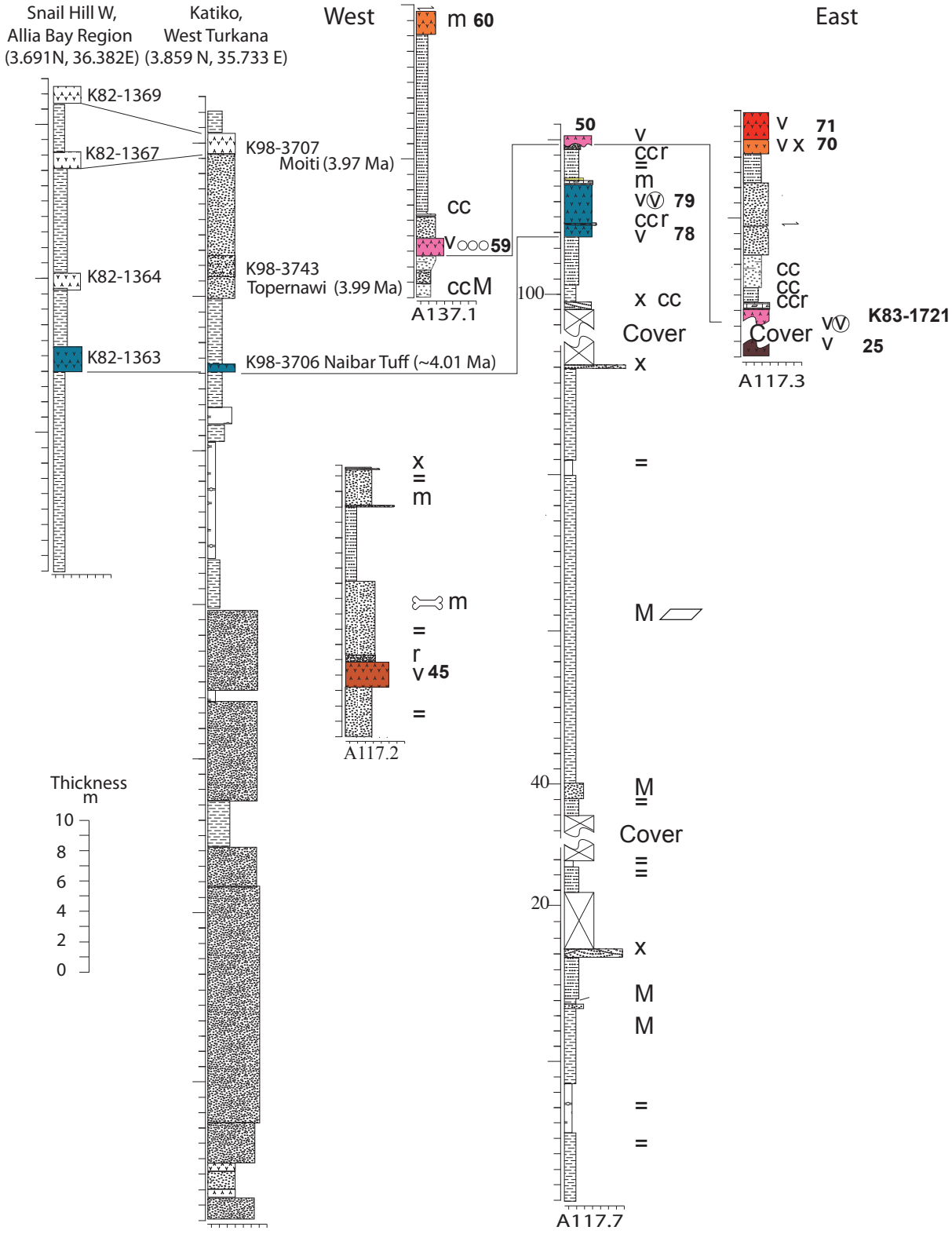

Figure 8. Stratigraphic sections of the Lonyumun Member up to the undifferentiated Moiti/Lokochot Member. See Figure 7 for the key to symbols. The last two digits of each sample number of the form MB08-XX

mainly on the exposed surface. Large green clasts, interpreted as replaced fishbone are present in the upper part of this interval. Thinly laminated beds of highly compacted yellow or white diatomite are a prominent feature of this interval and are over- or underlain by claystones wherever relations were clear. Two fine-grained cross-bedded quartz sandstones are also present in this section dominated by claystones. These sandstones are 0.25 and 1.00 m thick, and occur 12.5 and 38.15 m above the base of this section. Two polymictic pebble conglomerates occur within this part of the member about 15.85 and 66.05 m above the base. Both of these show faint cross-bedding and have a fine-grained sandstone matrix. Outcrops of the lower part of the member are separated from those of the upper part by Quaternary alluvium and Il Naibar stream deposits. The thickness of the covered strata is estimated to be 29 m.

Above this covered interval is the upper 11 m of section. The lowest unit is a 50 cm thick cross-bedded sandstone capped by a 5 cm limonitized, calcite-cemented, sandstone with internal molds of *Cleopatra* rich in manganese oxide. Atop this is a 1.05 m thick claystone. A highly compacted, mudstone containing numerous ferruginized coprolites lies above the claystone.

Overlying the mudstone just described is a 3.55 m thick tuff (for sample numbers see Table 1). Here, this tuff is named the Naibar Tuff due to its proximity to Il Naibar, the most prominent stream in the region. Its type locality is defined here as the exposure south of Il Naibar with geographic coordinates near 4.0966N, 36.2795E. Haileab (1995) provided analyses of this tuff (samples K82-870 and K82-876), but described it as either unknown, or associated with the informally named Nabwal Tuff. The name "Nabwal,"

however, is not available, because it has been used by Watkins (1986) for a sequence of basalts exposed on the Surgaei highlands which form the northeastern boundary of the sedimentary deposits of the Koobi Fora Formation. Directly atop the Naibar Tuff is another thin (~2-10 cm) layer with prominent rhizoliths preserved in calcite.

The Naibar Tuff has two distinct layers separated by a thin (~2 cm) concreted calcite layer with rhizoliths (Figure 9). The lower layer (sample MB08-78; 1.05 m) is a pale green medium-grained vitric tuff with minor feldspar and quartz grains. The upper layer (sample MB08-79; 2.50 m) is a thick, grey tuff with many mineral grains (either cognate or detrital) including quartz, feldspar, and iron-oxides. The glass shards have bubble junction, pumiceous (called "froth" in Cerling, 1977) and platy morphologies with very little alteration due to weathering and minor pitting due to impacts of other tephra from the volcanic eruption (Figure 10). A 10 cm calcite-concreted, ostracod-rich sandstone lies above the Naibar Tuff. It is followed by a very fine-grained parallel laminated mudstone that is 2.1 m thick with a thin layer of rhizoliths preserved in calcite at the top. The Lokochot Tuff lies unconformably above the Lonymun Member near Il Naibar (see Appendix A).

From the above description, it will be noted the only strata that can be assigned to the Moiti Member are those in the 2.2 m of section just described. In the Allia Bay region, some 40 km to the south of Il Naibar, the Naibar Tuff lies ~13 m below the Moiti Tuff, and therefore belongs technically within the Lonyumun Member, the base of which is defined as the base of the Moiti Tuff. Therefore the thin section that lies between the Naibar Tuff and the Lokochot Tuff may well belong to the upper part of the Lonyumun Member. Neither the Moiti Tuff, nor other tuff known to lie near it in the sections in

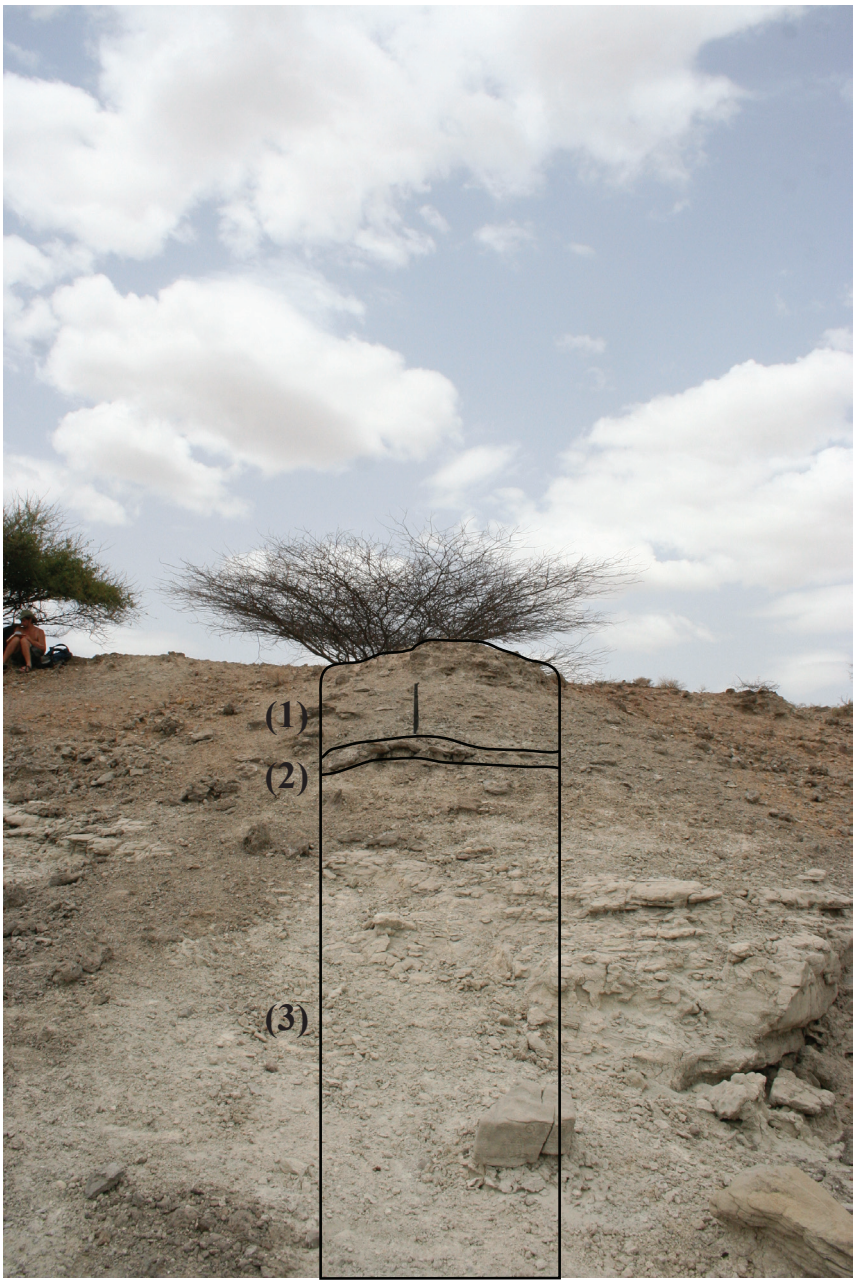

Figure 9. The Naibar Tuff at the top of the Lonyumun Member. Note three distinct layers: 1) Dark grey tuff having only glass shards of Naibar Tuff composition. 2) Calcite concreted unit showing rhizoliths. 3) Pale green tuff with glass shards of Naibar Tuff and Kanyeris Tuff compositions. Machete is 60 cm long. Figure location: 4.0979 N 36.2817 E, looking south.

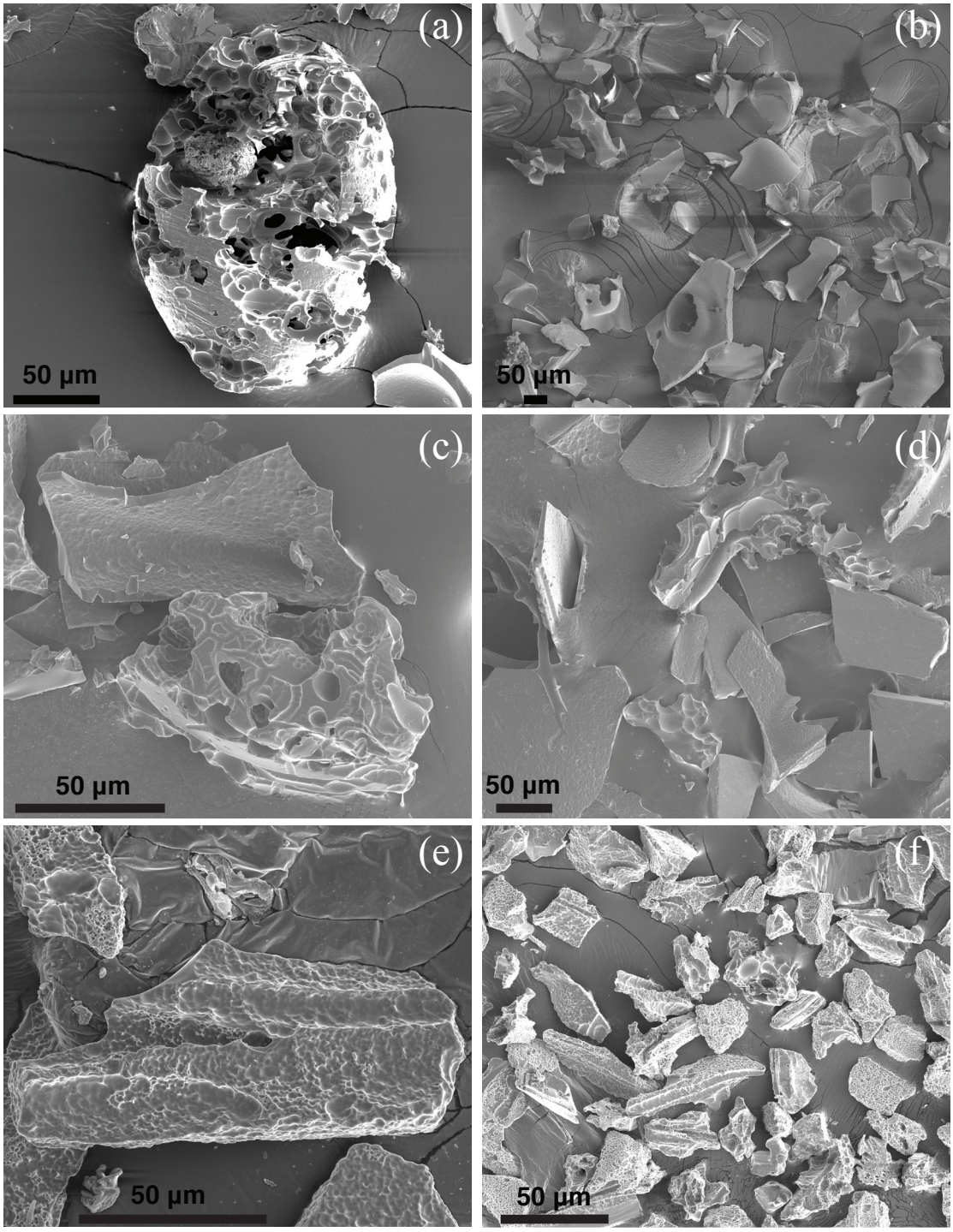

Figure 10. Electron micrographs of volcanic glass shards from rhyolitic tuffs of the Koobi Fora Formation: a) and b) Naibar Tuff; c) and d) Lokochot Tuff; e) and f) Unnamed tuff of Moiti Member. Scale bars are 50 µm.

Allia Bay has been identified in Area 117. For this reason, the Moiti Member is treated as absent in Area 117, and the Lokochot Tuff is regarded as resting disconformably on the Lonyumun Member. Similar difficulties were found with this part of the section in the Ileret region (Gathogo and Brown, 2007). In order to depict where the evidence for lack of the Moiti Member is clearest, the base and top of the Naibar Tuff is mapped (Appendix A), which gives the approximate location of the top of the Lonyumun Member.

Brown and Feibel (1986) commented that glass shards from pumices found in the Moiti Tuff (see Table 1) are similar to glass shards of the Naibar Tuff (sample 75-117A in Brown and Feibel, 1986) (see Table 1), but compositionally different from glass shards of the Moiti Tuff itself. Many well-rounded calcite concreted cobble-sized (10–13cm) pumices were found on the surface of the Naibar Tuff. The chemical composition of glass separated from two of these pumice clasts is compositionally indistinguishable from that of glass shards from the Naibar Tuff, but it is compositionally distinct from glass shards in the Moiti Tuff, and also from glass in pumice collected from the Moiti Tuff in the Allia Bay Region.

The basal part of the Naibar Tuff contains a secondary compositional mode (Table 1) that corresponds to the composition of glass shards in the Kanyeris Tuff (Gathogo and Brown, 2007). Thus the Kanyeris Tuff is most likely older than the Naibar, making it one of the oldest tuffs of the Koobi Fora Formation.

The relationship between the Naibar Tuff and other dated tuffs of the Koobi Fora and Nachukui Formations can be illustrated by sections from Snail Hill in the Allia Bay region and from Katiko west of Lake Turkana. At Snail Hill, the Naibar Tuff lies below the 3.97 Ma Moiti Tuff. At Katiko, the Naibar Tuff lies below the 3.99 Ma Topernawi

Tuff (McDougall and Brown, 2008). As no disconformities has been noted in either of the sections, and because the Naibar Tuff lies approximately the same distance below the Topernawi Tuff as the Topernawi Tuff lies below the Moiti Tuff, it is a reasonable assumption that the Naibar is near 4 Ma in age or just slightly older. This is consistent with the Naibar Tuff's reversed magnetic polarity (Table 2).

The Gombe Group Basalt, which intruded the sediments of the basal Lonyumun Member, yields K/Ar dates between 4.20 and 3.95 Ma (Haileab *et al.*, 2004), although most values lie between 4.2 and 4.0 Ma. Additionally, Gombe Basalts have been seen to intrude strata of the Lonyumun Member at many localities (e.g., Allia Bay, Nasechebun, Namoritunga (Haileab *et al.*, 2004)), but have never been observed to intrude strata immediately above or below the Moiti (3.97 Ma), or Topernawi Tuffs (3.99 Ma), so it is likely that the Gombe Basalts are older than 4 Ma. On this basis, all of the Lonyumun Member must be older than 4 Ma, but the only secure maximum age for strata ascribed to the Lonyumun Member derives from Lothagam southwest of Lake Turkana , where pumice clasts which have been dated at 4.22 Ma lie below the Muruongori Formation which has been correlated with the Lonyumun Member of the Nachukui Formation (Feibel, 2003).

5.1.2 Discussion

A large lake, the Lonyumun Lake, covered a large part of Areas 137 and 117 for most of the time of the Lonyumun Member. This is also the case for areas to the north (Gathogo, 2003) and to the south (Brown and Feibel, 1986; Brown and Feibel, 1991; Feibel *et al.,* 1991).

Table 2. Paleomagnetic data for Naibar Tuff.

Demag Field (mT)	Declination	Inclination	M, emu	X(N), emu	Y(E), emu	Z(down)
0	357.6	-20.6	5.29E-05	4.95E-05	-2.05E-06	-1.86E-05
10	281.5	-56.7	8.89E-06	9.70E-07	-4.78E-06	-7.43E-06
18	198	-14.3	1.15E-05	-1.06E-05	-3.46E-06	-2.84E-06
25	182.3	-20	1.57E-05	-1.48E-05	-5.85E-07	-5.37E-06
35	195.4	8.3	1.84E-05	-1.75E-05	-4.81E-06	2.65E-06
45	186.8	6.8	1.60E-05	-1.58E-05	-1.90E-06	1.91E-06
55	162.9	-23.4	1.63E-05	-1.43E-05	4.40E-06	-6.47E-06
65	160.7	-16.5	1.38E-05	-1.25E-05	4.38E-06	-3.93E-06
77	195.7	-22.2	8.48E-06	-7.56E-06	-2.13E-06	-3.21E-06
89	178.9	-11	2.05E-05	-2.01E-05	3.94E-07	-3.90E-06
100	184.1	-7	6.35E-06	-6.28E-06	-4.48E-07	-7.77E-07
100	180.7	1.9	1.19E-05	-1.19E-05	-1.47E-07	4.06E-07

Location: 4.0966 N, 36.2796 E

The basal Lonyumun Member is made up of siltstones and diatomites with localized fossilized fish, which would indicate a pelagic lacustrine environment. Above this, thin sandstone beds with rip-up clasts of mudstones are present, and these sandstones also contain lenses of pebble conglomerates. These localized coarser grained sand units may result from lower lake level so that streams could extend farther into the Lonyumun Lake. As noted above, coarser beds are present at 12, 16, 38, 66 m above the base of the Lonyumun Member. If these are present because of changes in lake level, and if lake level changes correspond to precessionally modulated rainfall, then deposition of the Lonyumun Member should encompass at least five wet cycles, corresponding to a duration of at least 100 ka. Thus if the top of the Lonyumun Member is 4 Ma, the base may be only ~4.1 Ma old in this region, comfortably within the maximum age gleaned from correlation with strata at Lothagam.

Gypsum crystals within the claystones of the Lonyumun Member have been interpreted by Cerling (1977) as the result of oxidation of sulfides originally present in the laminated claystones.

The upper section of the Loyumun Member starts with a cross-bedded sandstone. Above this lies a coarsening upward sequence going from claystone to mudstone. The mudstone contains abundant coprolites, probably from crocodiles. This would indicate a marginal lacustrine environment with localized fluvial channel deposits. This is in sharp contrast to the situation in Allia Bay, where the air fall Moiti Tuff lies within the uppermost part of the lacustrine strata of the Lonyumun Member, and fluvial conditions do not obtain in that region until somewhat later.

Above this is the fluvial Naibar Tuff. The Naibar Tuff is broken into two units: the lower unit which contains glass shards of Kanyeris Tuff composition, and the upper member which contains only glass shards of Naibar Tuff composition. These units are separated by a thin calcite concreted layer with numerous rhizoliths. Eruptive products that form the Naibar Tuff were almost certainly brought into the the basin by fluvial processes (see arguments in Brown, 1972). The lower unit was deposited first, and the river that brought the Naibar Tuff into the basin must have passed over exposures of the Kanyeris Tuff, incorporating some shards from that unit. A short depositional hiatus ensued, but it was long enough for plants to take root above the lower part of the Naibar Tuff. Deposition continued to bring additional ash to the region, and this forms the upper unit of the Naibar Tuff. In some locations a thin, well-cemented mollusc packed sandstone lies immediately above the Naibar Tuff, and in others an ostracod-rich sandstone is present. These units are interpreted as having been deposited in a littoral lacustrine environment, meaning that a lake existed not too far to the south.

5.2 Gombe Group Basalts

The Gombe Group basalts are named after the Gombe Plateau, which lies east of Northern Lake Turkana (Haileab *et al.*, 2004). They are exposed north of Il Naibar in the Kokoi Highlands (the majority of Area 137), make up a prominent hill named Kulau in the southeast, and other small hills surrounded by alluvium within Area 117. The basalts are medium grained and mainly aphanitic, but can contain small phenocrysts. The Gombe Group basalts are at most 200 m thick (Haileab *et al.*, 2004) and show little or no dip.

5.2.1 Lithologic Description

The Gombe basalts are composed of ~ 50% plagioclase, ~ 20% clinopyroxene, ~ 20% glass and minor Fe-Ti oxides (Tables 3 and 4) (Haileab *et al.*, 2004). In the Kolom Nyasaga Uġuo Gaġwea valley of the Kokoi, many outcrops as thick as 9 m consisting of wavy columnar basalts with 2-4 cm glassy selvages are well exposed (Figure 11). These glass selvages contain expansion cracks from water saturation (Figure 12). A cursory reconnoiter of the Kokoi Highland of Area 137 revealed at least five basaltic dikes, but more are thought to be present.

The Gombe Basalts are in intrusive contact with strata of the Lonyumun Member along the southern portion of the Kokoi highland and within Kolom Nabalware. This contact is characterized by large pillow structures approximate 10-70 cm in diameter with 1-2 cm thick glassy selvages (Figure 13). Behind these "pillow structures," wavy columnar basalts can be seen in small valleys within the Kokoi. These basalt columns are hexagonal in cross section but do not appear to be preferentially oriented. No hyaloclastic ashes has been noted in the study area. The geochronology of the Gombe Group basalts is presented in Haileab *et al.* (2004), where a temporal range of 3.95–4.20 Ma is suggested (see discussion above).

5.2.2 Discussion

The Gombe Group basalts, which make up the majority of the Kokoi Highland, intruded strata of the Lonyumun Member. The intruding Gombe basalts are in the form of dike structures and lava flows. The outer walls of the dikes are pillow basalts with

Table 3. Major element analysis of Gombe Group Basalts.

Sample No.	SiO_2	Al2O3	Fe_2O_3[a]	MnO	MgO	CaO	Na_2O	K_2O	TiO_2	P_2O_5	LOI	Total
SE of Jarigole												
K84-1815[b]	49.26	13.02	15.26	0.22	4.54	8.7	3.15	0.85	3.67	0.51	0.65	99.82
Kokoi Highland												
K09-573	49.76	13.44	14.1	0.22	3.72	8.78	3.19	0.84	3.42	0.58	2.18	100.2

a) Total iron as Fe_2O_3
b) from Haileab *et al.* 2004

Table 4. Trace element analysis of Gombe Group basalt.

Sample	K84-1815[a]	K09-573
Trace Elements (ppm)		
V	412	385
Cr	<20	< 20
Co	40	43
Ni	90	20
Cu	47	50
Zn	156	160
Ga	23	22
Ge	2	1.9
Rb	19	21
Sr	358	385
Y	42	46.1
Zr	242	299
Nb	27	37.9
Ba	276	330
La	29.7	36.9
Ce	65.1	76.5
Pr	8.5	9.73
Nd	37.4	41.9
Sm	8.9	9.77
Eu	3.0	2.99
Gd	8.9	9.83
Tb	1.5	1.6
Dy	8.6	8.84
Ho	1.7	1.75
Er	4.5	4.6
Tm	0.6	0.659
Yb	3.7	4.1
Lu	0.5	0.554
Hf	6.5	7
Ta	2.0	2.64
W	6.0	168
Th	2.8	3.02
U	0.73	0.86

a) From Haileab *et al.* 2004

Figure 11. Basalt dikes. a) wavy columnar basalts that make up the center of basaltic dike on the east side of the valley of Kolom Nyasaga Uġuo Gaġwea. Orion Rogers for scale (1.93 m). Figure location: 4.0984 N 36.2633 E looking east b) bulbous structures at the top of a dike on the Kulua Hill. Brunton compass for scale (7 cm. wide). Figure location: 4.0483 N 36.2668 E

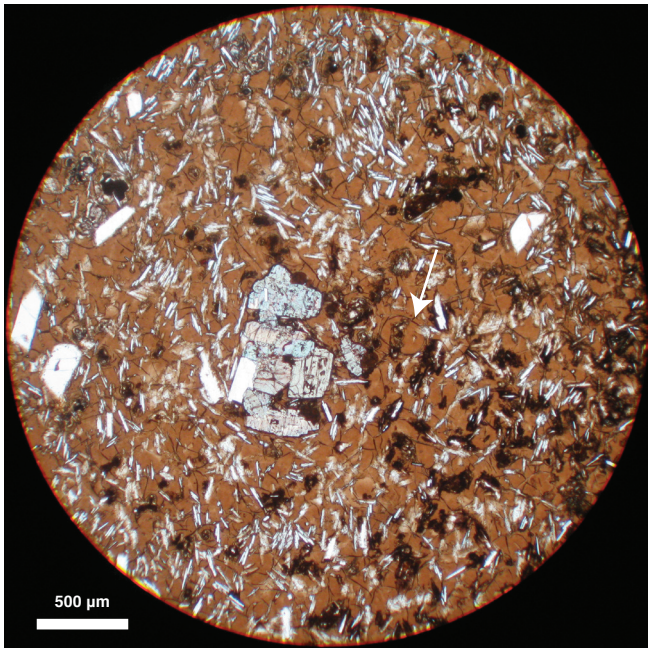

Figure 12. Photo micrograph of Gombe Group Basalt chilled margin (sample MB08-64). Minerals present are clinopyroxene, plagioclase, ilmenite, and volcanic glass. Hydrated volcanic glass (brown) is expanded and has formed spherical cracks (arrow).

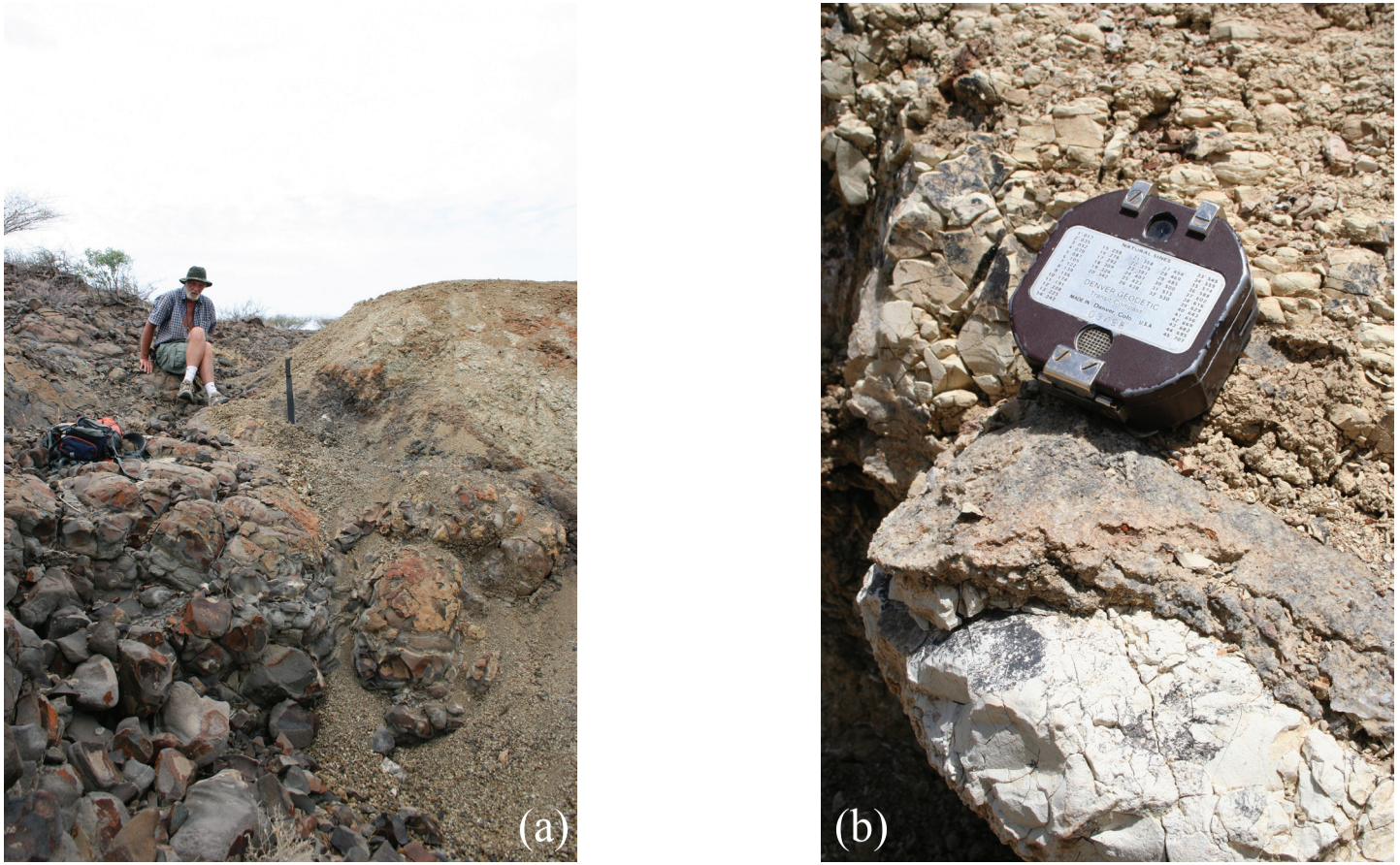

Figure 13. Pillow structures caused by the intrusion the Gombe Basalts into the Lonyumun Member. a) Near a large dike on the southern margin of the Kokoi Highland, machete is 60 cm long. Figure location: 4.1156 N 36.2813 E looking north b) Glassy selvages found on the contact between the Gombe basalt and the Lonyumun member near Kolom Nyasaga Uġuo Gaġwea. Brunton compass for scale (7 cm. wide). Figure location: 4.1053 N 36.2581 E.

glassy selvages; which formed when the hot lava of the Gombe Basalts intruded into the relatively cold, water-saturated sediments of the Lonyumun Member. Wavy columnar basalts form the cores of these dikes. The top of these dikes have pillow structures in many locations and can be easily followed in the field (Figure 11).

The intrusion of the Gombe Basalts into the beds of the Lonyumun Member caused the dip of the beds to change drastically. The dip of the Lonyumun Member strata is measured at 2-3°. Along the baked margin contact, the beds are tilted to a maximum dip of 30°. Bowen (1974) and Findlater (1976) shows the Gombe Group basalts as older than the sediments with which they are in contact. With this assumption, and with the drastic dip change of the strata near the basalts contact, the contact was interpreted as a normal fault. Taking the ages of the Gombe Group basalts and the Lonyumun Member, plus the pillow structures of the basalt at the contact indicates that the contact is a baked margin and not a fault. However folding of Lonyumun Member strata by Gombe Group basalts did cause minor faulting of at least 8 m as seen in Kolom Nabalware (Figure 14).

5.3 Lokochot and Moiti Members

The Moiti Member is named after Il Moiti, an ephemeral stream in the Allia Bay region. The type section is located in Area 260; the member has a type thickness of 59.9 m, and it is defined as all sedimentary strata between the base of the Moiti Tuff and the Lokochot Tuff (Brown and Feibel, 1986).

The Lokochot Member is named after Il Lokochot, which forms the northern boundary of Area 250. The type section is in Area 261, near Jarigole, where the

Figure 14. Minor normal fault caused by the intrusion of the Gombe Group basalts into the Lonyumun strata. Intrusion of the Gombe basalt is to the left (west). Arrow indicates approximate location of fault. Orion Rogers for scale (1.93 m). Image location: 4.1049 N 36.2590 E looking south.

thickness is 34.4 m. The member is defined as all sedimentary strata between the base of the Lokochot Tuff and the Tulu Bor Tuff (Brown and Feibel, 1986).

The treatments of these two members is somewhat difficult within Areas 117 and 137 for three reasons: 1) members of the Koobi Fora Formation are defined on the basis of basal ash layers 2) The Moiti Tuff has not been identified within the field area and the Lokochot Tuff is in scattered outcrops, usually near fault zones 3) The overlying Tulu Bor Member is marked by large basal fluvial channels that undoubtedly eroded an unknown amount into underlying sedimentary strata of the Moiti and Lokochot Members. For these reasons it is prudent to combine these members into a single member.

The combined Moiti/Lokochot Members are identifiable in the field by their location below the erosion-resistant Tulu Bor Tuff. The Lokochot Tuff can be identified by the presence of accretionary lapilli near its base; it is also darker gray than the Tulu Bor Tuff. The accretionary lapilli are a useful, but not infallible guide to identification of the tuff in the field. The combined Moiti/Lokochot Members crop out in various locations scattered throughout Areas 117, 137, and 116, mainly between Il Naibar and Il Aberegaiye in Area 117 and along Il Nabalware in Area 137 and south of Il Aberegaiye in Area 116.

5.3.1 Lithologic Description

The following description of the combined Moiti and Lokochot members is based on exposures in Area 137 near Kolom Nabalware (section A137.1, A137.2) and various outcrops between Il Naibar and Il Abergaiye (sections A117.1, A117.3, A117.4, A117.5, A117.6, A117.8, A117.9, A117.10) and a single outcrop south of Il Aberegaiye. The top

of the combined Moiti/Lokochot Member is taken as the base of the α-Tulu Bor tuff, while the base is taken as the top of the Naibar Tuff.

In only four locations can the Moiti and Lokochot Members be recognized with confidence: within the Kokoi along Kolom Nabalware, along section A117.3, northeast Area 117 and near Il Aberagaiye in Area 116 (section A117.2)

The first confirmed Moiti Member outcrop consists of two lithologic units below the Lokochot Tuff (sample MB08-59) in Area 137 (A137.1). The first unit is a mudstone and the second unit is a coarsening upward sequence from mudstone to sandstone. This section is 2.70 m thick.

In section A117.3 the Moiti Member was identified by the occurrence of the Loruth Tuff (sample MB08-25), which lies an unknown distance below the Lokochot Tuff in section A117.3 and has a thickness of about 0.50 m (Harris *et al.*, 1988). The Loruth Tuff contains around 50% glass shards with quartz, pyroxene, feldspar and iron-oxides accessory minerals. The glass shards have bubble junction, flat, stretched and pumiceous morphologies.

Section A117.2 of the Moiti Member contains an unnamed tuff, that lies stratigraphically below the Lokochot Tuff elsewhere (F. H. Brown, personal communication). Here, this tuff is named the Aberegaiye Tuff due to its proximity to Il Aberegaiye. This tuff has interstitial feldspars and quartz, shows flat pumiceous and stretched shards which are highly weathered (Figure 10). A medium-grained quartz sandstone (3.25 m thick) lies below this tuff. Overlying this tuff is a fining upward sequence of sandstone to mudstone, followed by another fining upward sequence from

conglomerate to sandstone. Lying uncomformably above this section is the Burgi Member.

The only complete section of the Lokochot Member is in Area 137, near Kolom Nabalware (sample MB08-59, section A137.1). The Lokochot Tuff is 110 cm thick, bluish-grey, medium-grained, and has a thinly bedded three centimeter thick accretionary lapilli layer 24 cm above the base. The tuff is composed of >80% glass shards but also contains quartz, pyroxene, feldspars and iron-titanium oxides. Morphologically, the glass component is made principally of flat, bubble junction, and frothy shards (Figure 10). This is the most complete section of the Lokochot Tuff but many other smaller, outcrops are situated near Il Naibar in the southwestern part of Area 117 (samples MB08-12 MB08-13), resting uncomformably above the Naibar Tuff (samples MB08-06, MB08-08, section A117.7) and/or the sediments of the Lonyumun Member (samples MB08-63). Above the basal tuff sits a sandstone, followed by a claystone that contain clasts of volcanic tuff. Above this lies the β-Tulu Bor Tuff (sample MB08-61).

The Kaado Tuff (sample K80-1584), which lies stratigraphically below the Tulu Bor Tuff on the west side of Lake Turkana (Harris *et al.*, 1988), is found near Il Aberegaiye in Area 117 (section A117.3). It has bubble junction, flat and stretched glass shards. The tuff is made up of approximately 70% glass shards with quartz, feldspar and biotite. It is ~1 m thick and overlies a brown sandstone with calcite concretions.

Section A117.1 exposes the maximum thickness of the combined Moiti/Lokochot Member, and is the westernmost exposure of this interval. This section contains 4.5 fining-upward sequences of sandstone to mudstone. The first unit is a mudstone and is the upper part of a fining-upward sequence. This unit is highly fossiliferous, containing

fish vertebrae, fragments of turtle shells, and crocodile scutes. Many of the sandstones contain gastropod shells or rip-up clasts of mudstone.

Sections farther east contain thicker units of well-compacted, cross-bedded sandstones that are not present in the previously described section, and thinner sections of siltstones

The upper interval of sections A117.4 and A117.5 are incised by the basal Tulu Bor Member and the channels are filled with coarse-grained sandstone with well formed cross-beds that contain ~50% glass shards of α-Tulu Bor Tuff composition (Figures 15 and 16). These sections, combined with the character of the basal Tulu Bor Member, form the basis for combining the Moiti and Lokochot Member.

Alkali feldspars separated from pumices collected from the Lokochot Tuff in the Kibish region ~150 km north of Area 117, yield an arithmetic mean Ar^{40}/Ar^{39} date of 3.596 ± 0.045 Ma (McDougall and Brown, 2008). The Lokochot Tuff in Kenya and Ethiopia lies precisely on the Gilbert-Gauss geomagnetic boundary, with the lower Lokochot Tuff being reversed and the upper Lokochot Tuff being normal (Brown *et al.*, 1978), which agrees with the Ar^{40}/Ar^{39} date.

In all samples analyzed, the Lokochot Tuff has two principal modes, one with about 3% Fe_2O_3, and the other with about 4% Fe_2O_3 (Figure 7). This feature of this tuff was first noted by Cerling (1977) in his doctoral dissertation, although at that time the tuff had not been named.

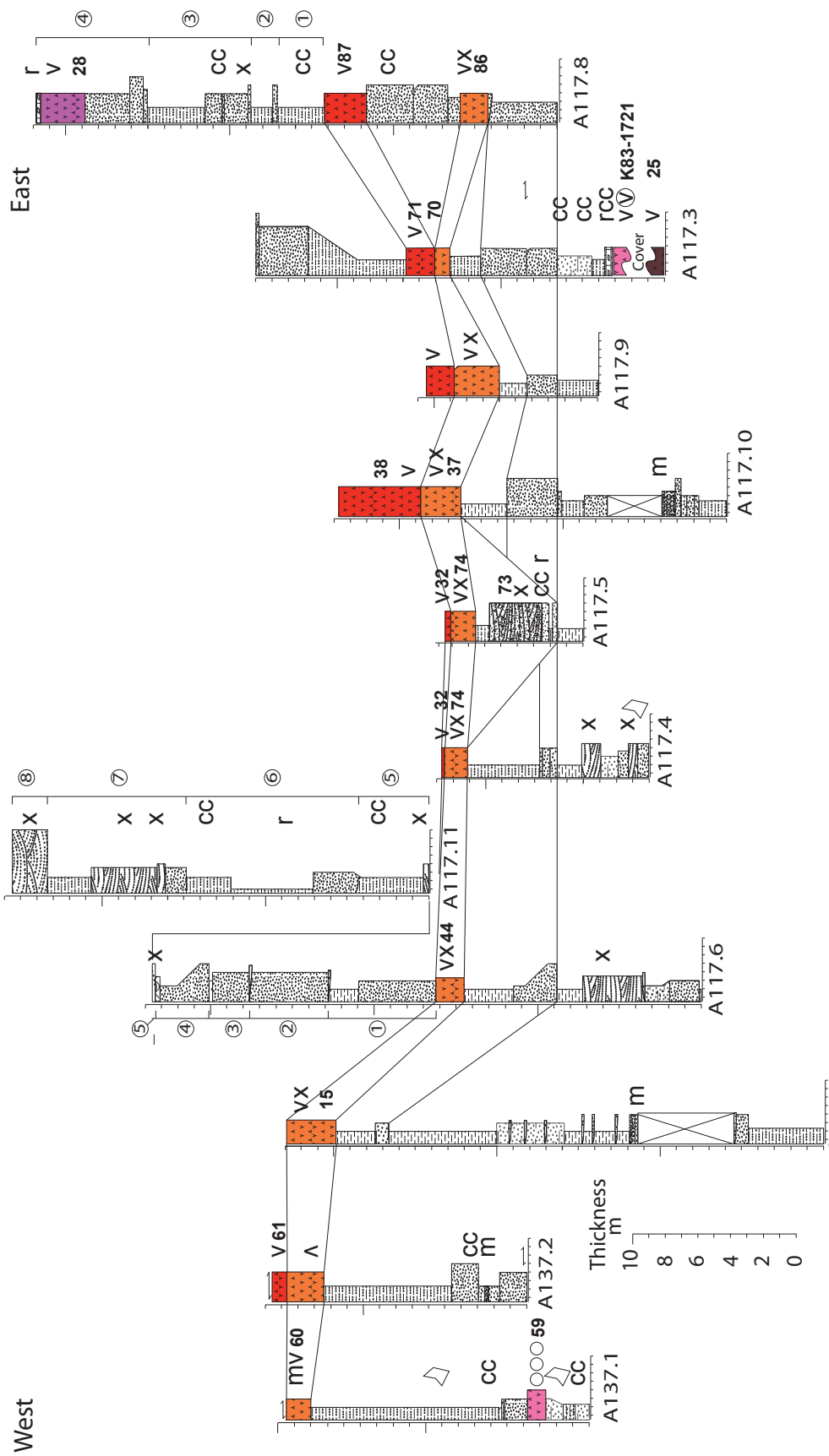

Figure 15. Stratigraphic sections of the undifferentiated Moiti/Lokochot member and the Tulu Bor Member in Area 117 and Area 137. See figure 7 for key to symbols. The last two digits of each sample number of the form MB08-xx are given on the section.

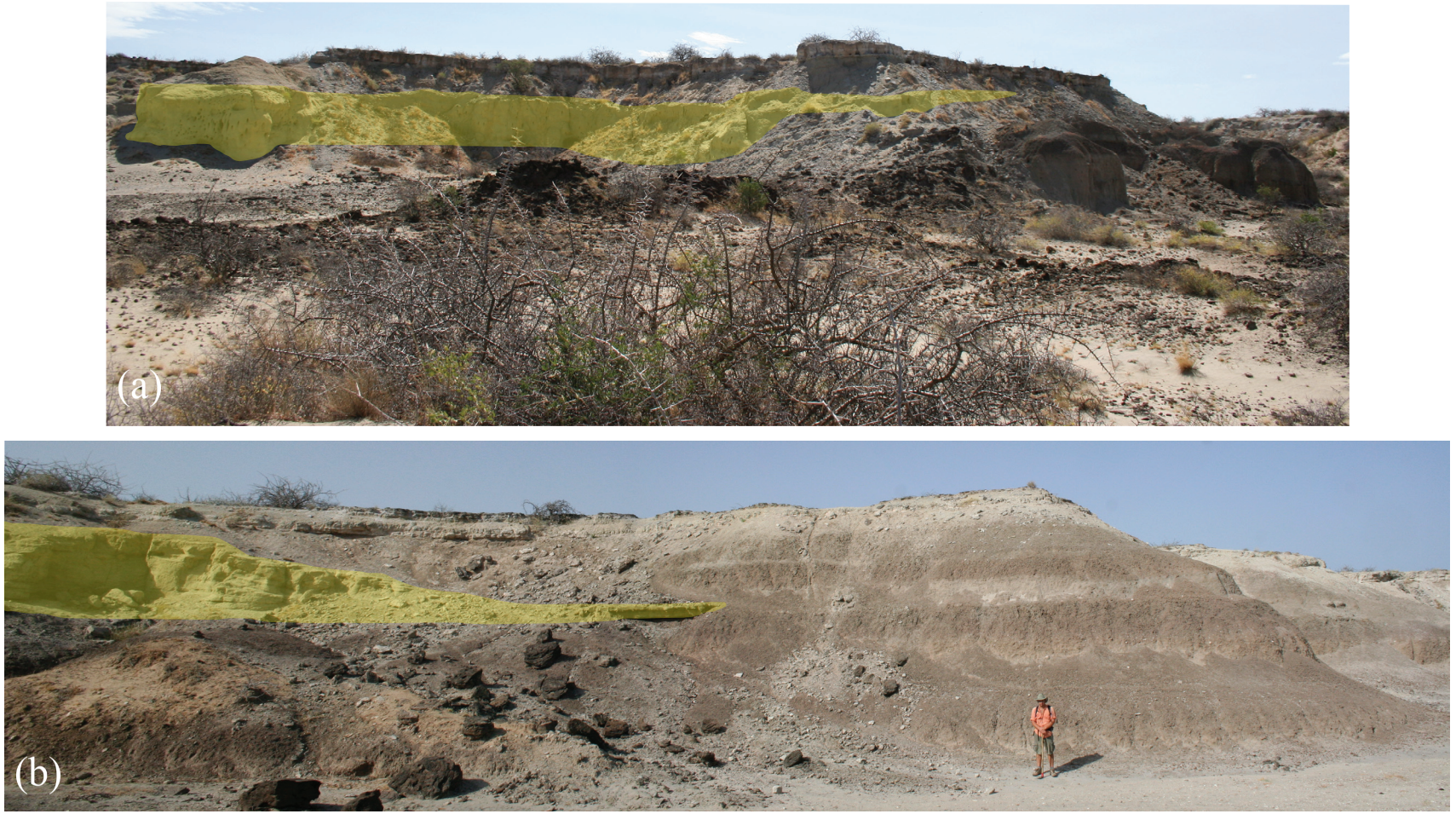

Figure 16. Fluvial channels (yellow overlay) at the base of the Tulu Bor Member incising the Moiti/Lokochot Member. α-Tulu Bor is the prominent tuff at the top of the cuesta in both images. Figure location: 4.1005 N 36. 3007 E looking N50E a) Near section A117.5; b) same area looking north. Orion Rogers (1.93 m) is standing where section A117.4 was measured. Section A117.5 was measured through the thickest part of the channel to the left. Figure location 4.0991 N 36.3016 E.

5.3.2 Discussion

The Moiti and Lokochot members are combined and treated as single mapping unit. This is done because the overlying unit, the Tulu Bor Member, has incised an unknown amount into underlying strata. The Moiti Tuff has not been found in the study area, but this does not mean that the Moiti Member is missing. The Moiti Member is seen in Area 137 and tuffs of the Moiti Member are present in Area 117. Although the Moiti Tuff is not present in the study area, it does crop out in the northern part of Area 40 (Gathogo, 2003). The Moiti Tuff has been interpreted as a fluvially deposited tuff and may not have been deposited in many areas around Koobi Fora. The Loruth Tuff has been identified in Area 117, and also at Loruth Kaado west of Lake Turkana (Harris *et al.,* 1988). The Lokochot Tuff crops out locally in Areas 117 and 137, the presence of accretionary lapilli indicates that the tuff was deposited from the air.

The coarsening upward sequences of silts and cross bedded sands are part of a deltaic system that must have drained into a lake that was present during this temporal range, from 3.969 Ma (age of Moiti Tuff) to 3.438 (age of Tulu Bor Tuff). Other indications of a lacustrine environment are mollusc packed sandstones that may represent a littoral environment, and fish vertebrae in the same rock unit as crocodile scutes and turtle shells. These findings are consistent with what was reported by Brown and Feibel (1991) and Feibel *et al.* (1991). In the absence of defining tuffaceous marker beds, it is not possible to distinguish between the Moiti and Lokochot Members in this area.

5.4 Tulu Bor Member

The Tulu Bor Member is named for the Tulu Bor Tuff, which takes its name from from Laga Tulu Bor (locally called Il Kimire) located north of the Kokoi Highland. The type section of the member is located in Areas 202 and 204, where it has a thickness of 86.2 m and is defined as all sedimentary strata between the base of the Tulu Bor Tuff and the base of the Burgi Tuff.

In the study area the Tulu Bor Member is comprised of a basal tuff, the α-Tulu Bor, and in some localities another tuffaceous layer is present above this (β-Tulu Bor). Above the Tulu Bor Tuff is a series of fining upward sequences starting with coarse-grained pebble conglomerate fining to mudstones. This member outcrops in various locations scattered throughout Areas 117 and 137, mainly between Il Naibar and Il Aberegaiye in Area 117 and along Il Nabalware in Area 137. The composite thickness of the Tulu Bor Member is 42.75 m (section A117.6 and A117.11) in Area 117.

5.4.1 Lithologic Description

The base of the Tulu Bor Member is defined as the base of the α-Tulu Bor Tuff, which is unconformably in contact with the underlying combined Moiti/Lokochot Member. The Tulu Bor Member is the youngest member within the Koobi Fora Formation found within the study area. Its upper boundary in this area is simply the highest exposed bed within the member.

The Tulu Bor Tuff is divided into two units, the α-Tulu Bor and the β-Tulu Bor (Brown and Cerling, 1982); for samples see Table 1) which differ slightly in composition. In Area 117, the α-Tulu Bor Tuff ranges in thickness from 0.90 m to 2.85

m, ranges in color from white to pale yellow, has medium grained glass shards, typically shows current cross beds, and locally has coarse-grained pumice lenses. The morphology of the glass shards are flat, stretched and bubble junction (Figure 17).

The glass shards are pitted by impact with other tephra during the volcanic eruption, and the pits are possibly accentuated by weathering. In the area near sections A117.4 and A117.5, a large coarse-grained sandstone channel incises into the underlying sedimentary strata of the combined Lokochot/Moiti Members and biotite is a very visible component of the sand. This channel lies 0.85 m below the base of the main bed that makes up the α-Tulu Bor Tuff (Figure 16), and contains a 1 cm thick coarse-grained sandy pink layer that contains ~80% glass shards of α-Tulu Bor composition in the 0.250-0.125mm fraction.

The β-Tulu Bor Tuff ranges in thickness from 1.45 m to 4.90 m, is blue-gray or white in color, and can be described as "clean", having a composition of >90% glass shards with most of the other minerals being quartz and feldspar. The β-Tulu Bor Tuff has the same glass shard morphologies as those described for the α-Tulu Bor Tuff (Figure 17). In at least two localities (samples MB08-35 and MB08-83), the β-Tulu Bor Tuff has accretionary lapilli (Figure 18). The α-Tulu Bor and the β-Tulu Bor locally occur in tandem, separated by compacted fine-grained sandstone, but in other locations either unit may be missing. Atop the Tulu Bor Tuff is a thin (~2-10cm) white calcite layer with rhizoliths. The Tulu Bor Tuff is the most widespread lithologic unit in the field area and often forms distinct cuestas that control much of the exposure that is present. Above the Tulu Bor Tuff are a series of 8 upward fining cycles as seen in A117.6 and A117.11

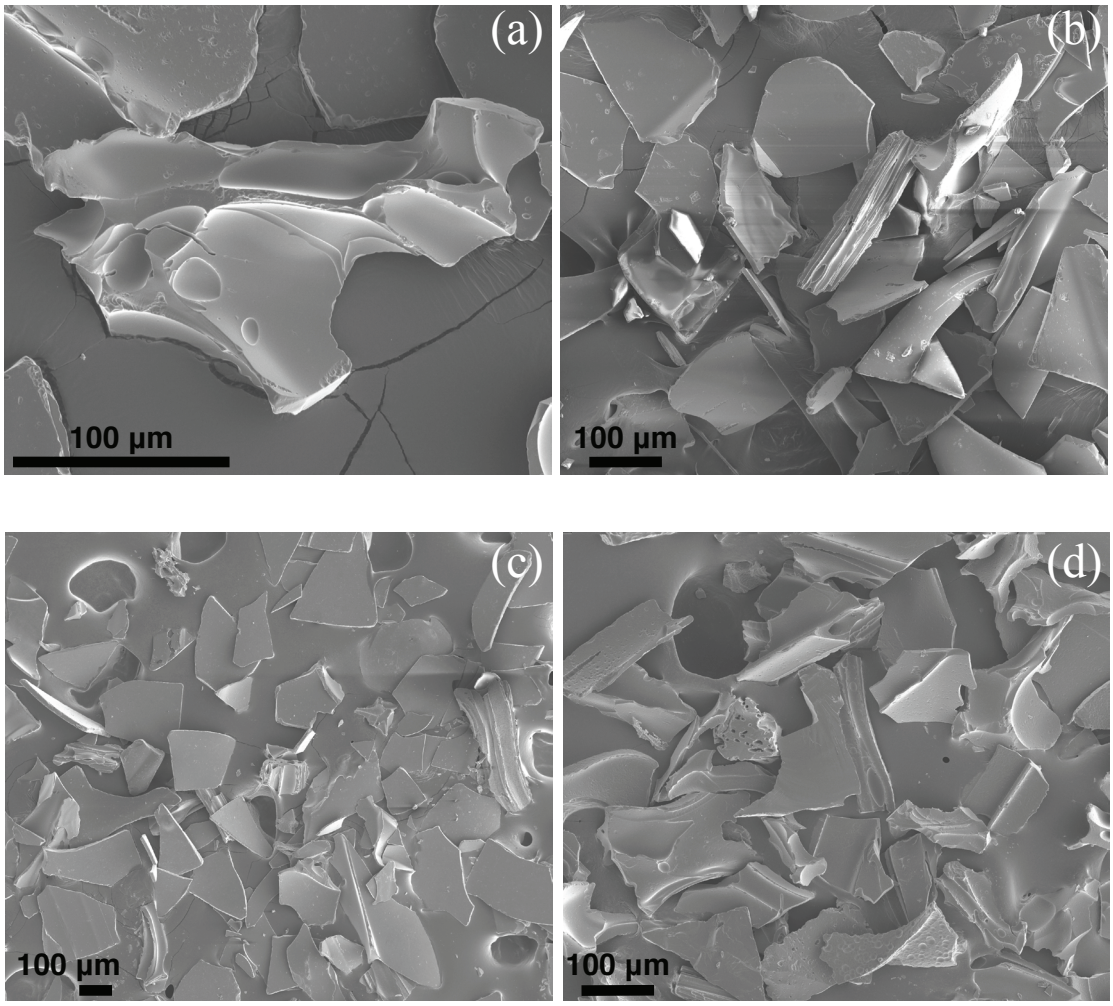

Figure 17. Electron micrographs of volcanic glass shards from rhyolitic tuffs of the Koobi Fora Formation. a) and b) α-Tulu Bor Tuff; c) β-Tulu Bor Tuff; d) Unnamed Tuff of the Tulu Bor Member. Each scale bar is 100 micrometers.

Figure 18. Accretionary lapilli within the β-Tulu Bor Tuff.
Figure location: 4.1067 N 36.30609E

(Figure 15). These fining upward cycles begin with a coarse grained well-cemented, cross-bedded sandstone; followed by a fining-upward compacted sandstone and end with a mudstone or siltstone. Some cycles feature layers of well-cemented sandstone. Occasionally, a later cycle has eroded into the preceding cycle marked by an erosional surface or missing section (usually the top mudstone). To the east of this cyclic sequence, a pumice clast (K80-176) was found within a fluvial channel (Feibel *et al.,* 1989). The glass within this pumice has been altered to chabazite, but alkali feldspar crystals are very fresh and abundant (see Appendix F).

Two tuffs were found within the upper Tulu Bor Member. The bottom tuff (sample MB08-40) is 0.10 m thick and is separated from the top 0.60 m thick tuff (MB08-41) by a 0.60 m thick mudstone. These tuffs are white and are highly altered. Three attempts to separate glass from these tuffs were unsuccessful.

The easternmost exposure of the Tulu Bor Member shows four fining upward sequences (section A117.8). Within the top of the last sequence is a light blue, parallel laminated rhyolitic volcanic tuff with a thin layer with prominent root-casts above it (sample MB08-28). This tuff contains glass shards compositionally indistinguishable from those of two other tuffs from the Koobi Fora Formation, samples K80-187 and K80-213II (Table 1). Sample K80-213 is located in Area 130 and can be correlated to a sequence of tuffs in Area 116 the lowest of which is K80-187. The next tuff above is K80-186 followed by K80-185, which is the Ninikaa Tuff of the Tulu Bor Member. These fining upward cycles contain the richest fossil assemblage within the field area. Vertebrate fossils observed include *Hydrocynus*, *Sindacharax*, and *Lates*.

Mammalian vertebrate fossils observed include *Elephas*, *Hipparion*, *Tragelaphus*, and *Kobus*. These fossils are mainly in the mudstone units. One hominid fossil, a partial cranium attributed to *Australopithecus afarensis* (KNM-ER 2602), has been found within fluvial channels (Feibel *et al.,* 1989). Other fossils include tree casts (Figure 19).

Feldspars from pumices found in the α-Tulu Bor Tuff in Area 207 yielded Ar^{40}/Ar^{39} dates of 3.438 ± 0.023 Ma, which is suggested as the maximum age of deposition of the Tulu Bor Tuff (McDougall and Brown, 2008). The pumice clast altered to chabazite that was collected from a channel east of the fining upward cycles in Area 117 yielded a K/Ar date of 3.06 ± 0.03 Ma (Feibel *et al.,* 1989). The Tulu Bor Member is the youngest member found in the study area, with the exception beds above the unconformity south of Il Aberegaiye, which is part of the upper Burgi Member (not examined in this study).

Feldspar separates from pumices found within the Ninikaa Tuff in Area 116 have been dated using the Ar^{40}/Ar^{39} method at 3.066 ± 0.017 Ma (McDougall and Brown, 2008). Sample MB08-28 must be younger than K80-187 and K80-213 because it incorporates glass shards of these tuffs, but it is likely older than the Ninikaa Tuff, because no shards of the composition of the Ninikaa Tuff were encountered during analysis.

5.4.2 Discussion

The Tulu Bor Member may have been deposited episodically, and may not be a continuous unit throughout the field area. In section A117.5 there is 3.2 m thick coarse-grained cross-bedded sandstone with a one cm thick pink sandy tuffaceous layer, which

Figure 19. Fossils within the Tulu Bor Member a) tree casts (Jacobs staff is 2 m long) Figure location: 4.0789 N 36.28265 E b) large fossil of mammalian metatarsus. Machete is 60 cm long.

contains glass shards of α-Tulu Bor. This cross-bedded sandstone is interpreted as a fluvial channel that has eroded into the underlying strata (see Figure 15). Sections A117.6 and A117.4 also show cross-bedded, medium grained sandstones, which are interpreted as fluvial channels.

The Tulu Bor Tuff is an extremely widespread volcanic tuff known from the Shungura and Nachukui Formations (Brown and Fuller, 2008; Haileab, 1995), and was deposited by a large, widespread river. Nonetheless, the presence of accretionary lapilli within some outcrops of the Tulu Bor Tuff suggests that there was air fall deposition in some locations in Area 117. It is possible that these are due to local rainstorms during primary deposition of the tuff.

Above the Tulu Bor Tuff are medium- to coarse-grained cross-bedded sandstones that fine upward to mudstones and siltstones. The siltstones and mudstones features root casts, calcite concretions and a rich vertebrate fossil assemblage. The compacted sandstones change lithology higher in section to incorporate more quartz and feldspar pebbles. In some cases these compacted sandstones rest on an erosional surface scoured into the underlying unit. These fining upward cycles indicate a large meandering river system within a lowland rich with abundant food for land-dwelling mammals.

5.5 Galana Boi Formation

"Galana Boi" is the Gabra name of Lake Turkana. The Galana Boi Formation, defined by Owen and Renaut (1986) is an Early Holocene lacustrine deposit that marks the shoreline of an ancient lake. This shoreline fluctuated with time with a maximum height of 95 m above modern Lake Turkana (Brown and Fuller, 2008).

5.5.1 Description

In Areas 117 and 137 the Galana Boi Formation is comprised of loosely compacted littoral sands typically containing mollusc and gastropod shells, loosely cemented sandstones that contain stromatolite, reworked volcanic tuffs of the Koobi Fora Formation which contains gastropod and mollusc shells as well as fossil vertebrate bones, and loosely compacted laminated diatomite beds. Each outcrop of reworked volcanic tuff is at an elevation of 440 m, which is the highest elevation Galana Boi bed noted in the study area. This member is exposed in multiple localities and little effort was made to map the extent of the Galana Boi Formation because in many cases it was difficult to distinguish the Galana Boi Formation from the surrounding alluvial cover. Mapped units include reworked volcanic tuffs, stromatolite beds and buttress unconformities (Appendix A and Figure 20).

Fossils found within the Galana Boi Formation include shells of *Melanoides* sp., *Cleopatra* sp., *Gabbiella* sp., *Caelatura* sp., *Cameronia* sp., *Mutela* sp., *Etheria* sp., and *Corbicula* sp. Reworked tuffs contain many of these shells as well as vertebrae of Nile Perch. Some extensive beds of stromatolite beds were also noted (near Mt. Buchanan).

The radiocarbon age of the beginning of the Galana Boi Formation is 9,880 ± 670 years BP (Owen and Renaut, 1986) and deposition ended around 3,000 years BP (Owen *et al.*, 1982).

5.5.2 Diatoms

Frustules of diatoms, as well as microscleres of sponges (Penney and Racek, 1968) and volcanic glass were found in some diatomite beds of the Galana Boi

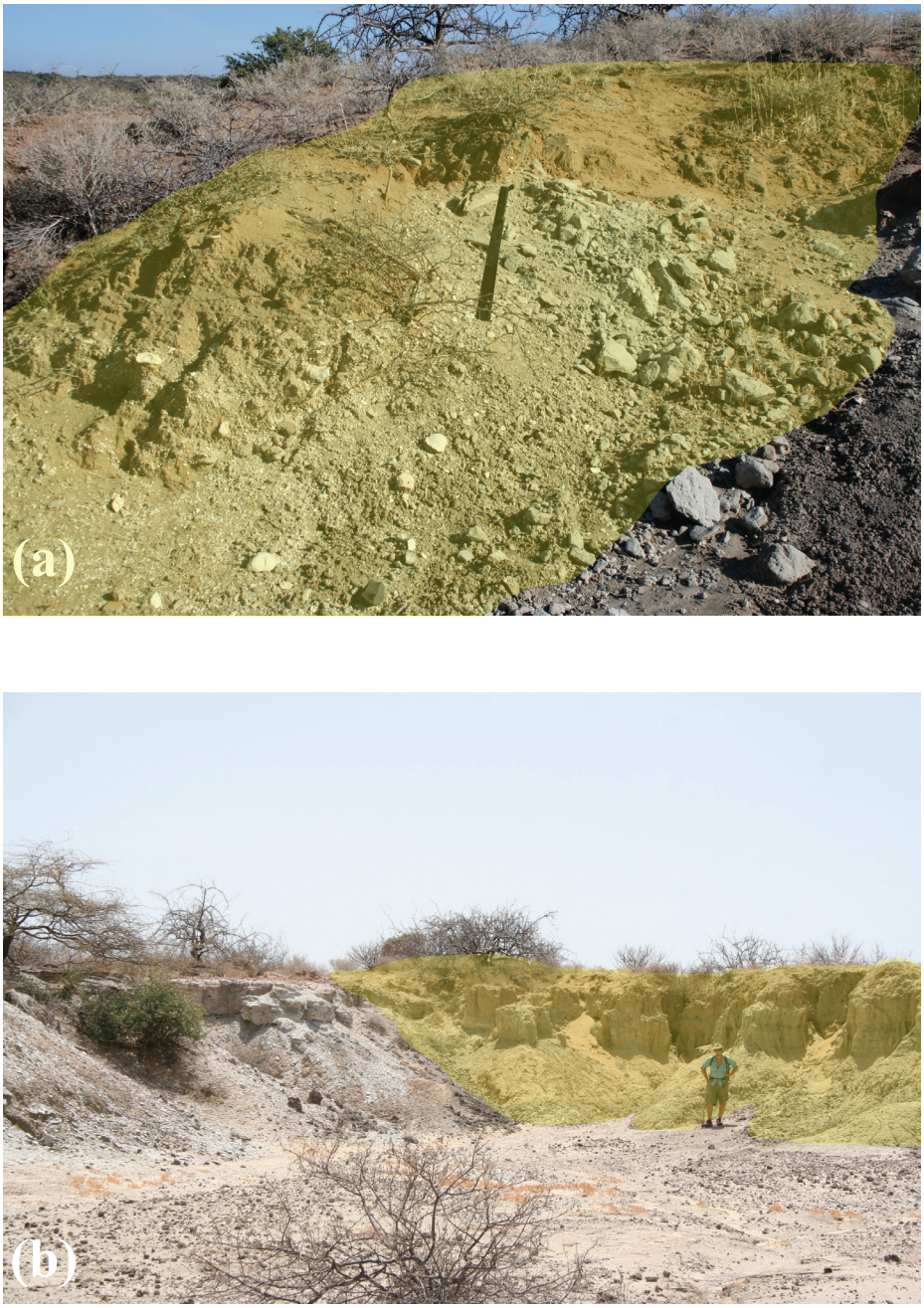

Figure 20. Buttress unconformity between Koobi Fora Formation against Galana Boi Formation (yellow). a) Naibar Tuff (right). Image location 4.0993 N 36.2819 E looking north-west. b) Tulu Bor Tuff (left). Orion Rogers for scale (1.93 m). Image location 4.0722 N 36.2763 E looking east by southeast

Formation. These diatomite beds share the same elevation, approximately 440 m, throughout the region. Nine taxa of diatoms were identified by electron microscopy.

Rhopalodia vermicularis is the most abundant species in the Galana Boi Member diatomites from Areas 117 and 137 (Figures 21 and 22). This was also noted by Cerling (1977). *R. vermicularis* was identified by the strong bilateral symmetry about the apical plan, the linear valve construction and the concave striae (Round *et al.,*1990). *R. vermicularis* grows in fresh to hyperalkaline lakes (see Table 5).

Synedra ulna (Figure 21) was identified on the basis of the thickness of the frustule (5μm), the capitate ending of the valves and the number of striae in 10μm (10). *S. ulna* lives in fresh to alkaline lakes (see Table 5) (Gasse, 1986).

Achnanthes engelbrechtii (Figure 21) shows an asymmetrical rapheless P- valve and has an asymmetrical central valve due to shortened central striae. There are 16 striae along the 10 μm length of the diatom. The frustule is approximately 2–5 μm wide. The apices are apiculate to subrostrate. *A. engelbrechtii* is considered a brackish water diatom (see Table 5) (Cholnoky, 1955; Gasse,1986).

Cymbella turgida (Figure 21) shows an arcuate shape, asymmetric valves about the apical plane, raphe parallel to the ventral margin with the central terminations showing expanded pores which are deflected towards the dorsal margin and terminal fissures being hooked towards the ventral margin. There is no central stigma. The striae contains elongate poriods which are on a nonpunctate surface, and a single row of well spaced striae (7 in 10 μm on the dorsal side, 8 in 10 μm on ventral side). *C. turgida* grows in lakes with slightly alkaline waters (see Table 5) (Owen, 1981; Gasse, 1986).

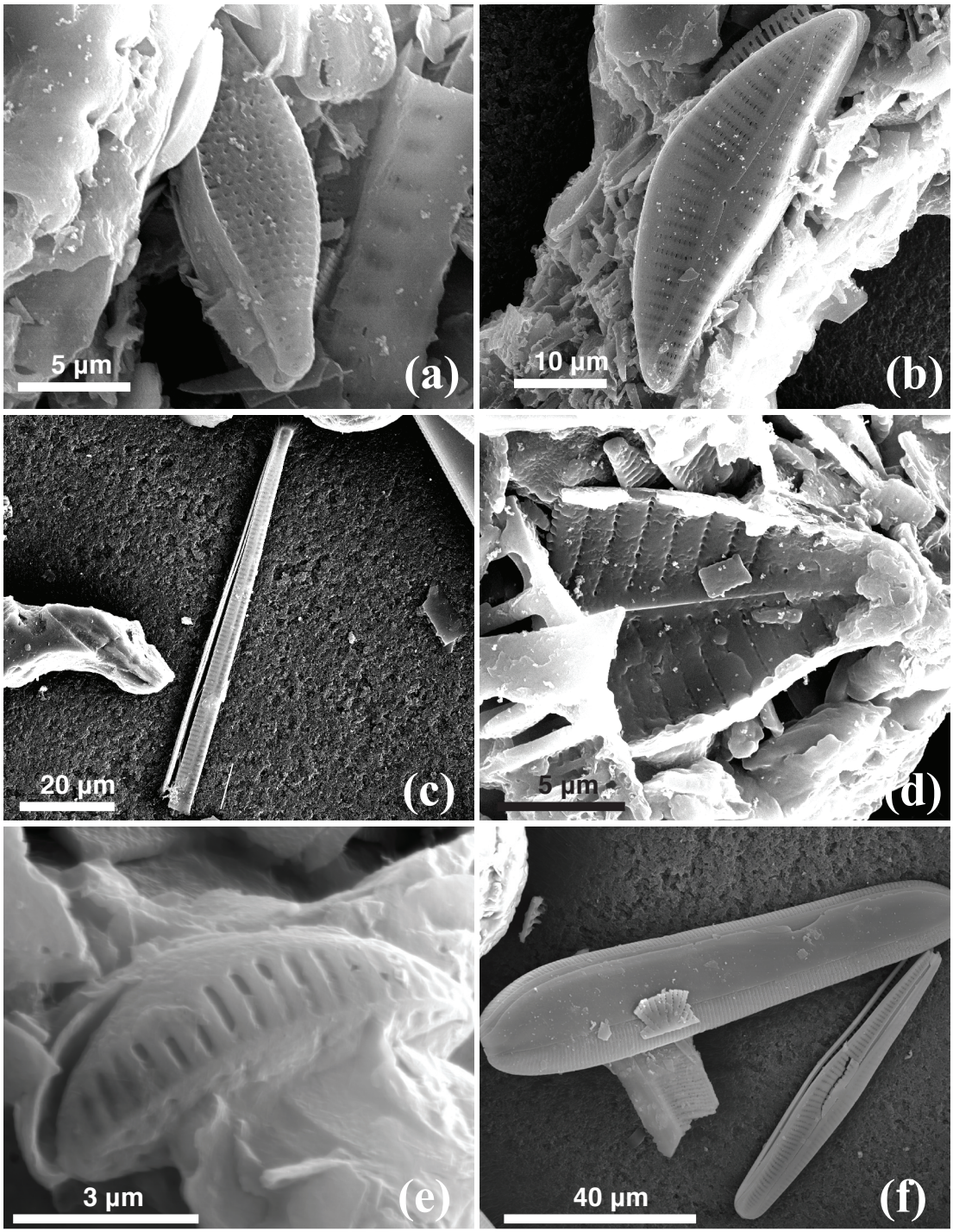

Figure 21. Diatom frustules from diatomite beds of the Galana Boi Formation. a) *Fragilaria* sp. b) *Cymbella turgida* c) *Synedra ulna* d) *Navicula gastrom* e)*Achnanthes Engelbrechtii* P- (rapheless) valve. f) *Rhopalodia vermiclaris* (top), *Navicula radiosa* (bottom)

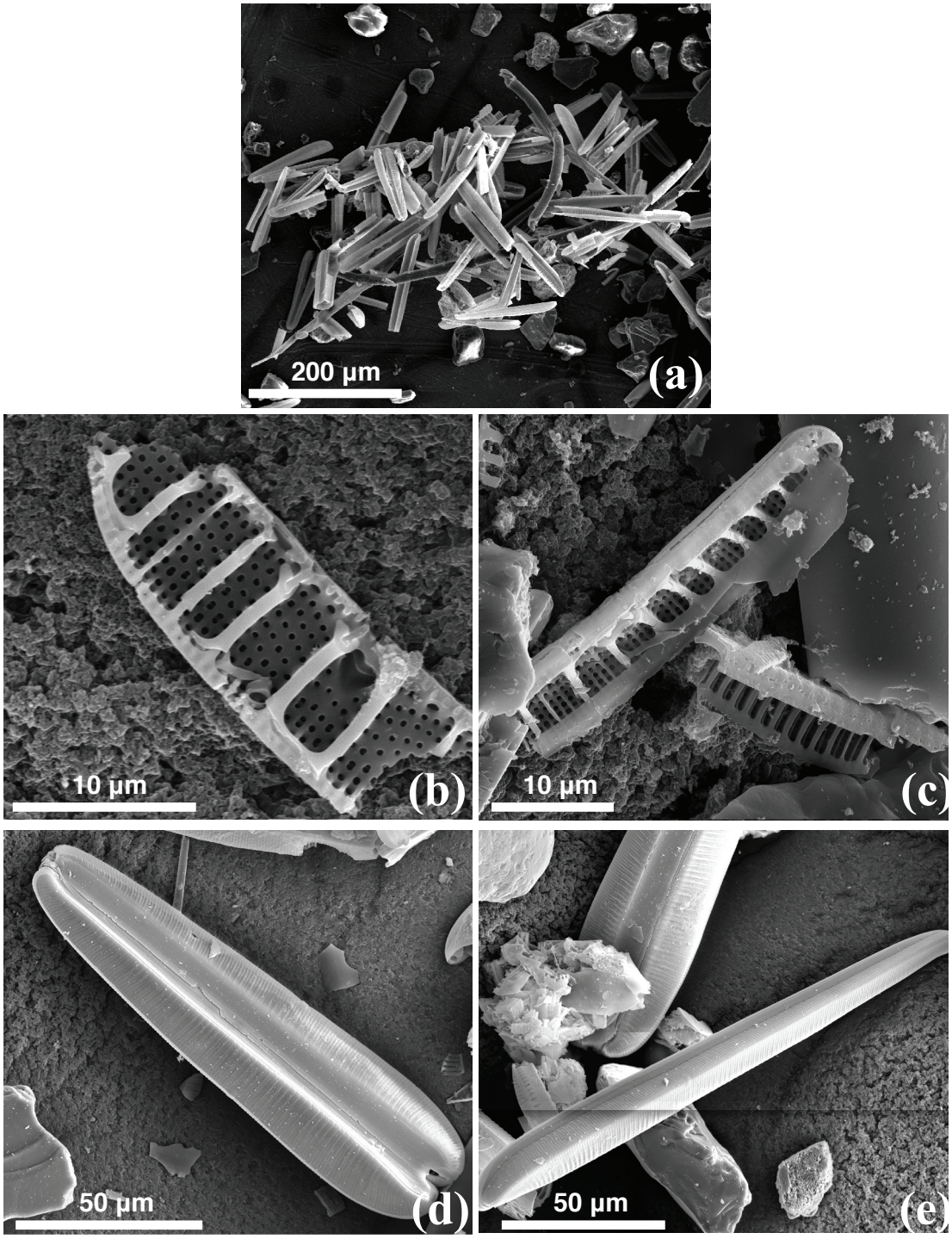

Figure 22. Diatomite from the Galana Boi Formation a) Diatomite showing a large proportion of *Rhopalodia vermicularis* and microscleres of *Spongilla* Sp. b) *Epithema zebra* c) *Epithema zebra* arrow shows raphe d) *Rhopalodia vermicularis* e) *R. vermicularis* valve view (top) girdle view (bottom).

Table 5. Modern environment of the diatoms found in diatomite beds of the Galana Boi Formation.

Taxon	pH	Temperature (℃)	Conductivity ($\mu S \cdot cm^{-1}$)	Alkalinity (meq^{-1})	Anion/Cation Pairs
Rhopalodia vermicularis	7-9.5	21-27	300-10,000	10-100	Na^{+} - HCO_3^{-} or (Ca^{+2} + Mg^{+2})-HCO_3
Syendra ulna	6-8.5	10-27	300-1,000	2-100	HCO_3^{-}-CO_3^{2-} or (Ca^{+2} + Mg^{+2}) - HCO_3^{-}
Achnanthes engelbrechtii	6-7	10-21	<300	-	-
Cymbella turgida	6-9.5	10-35	300-3,000	2-50	-
Epithemia zebra	7-9.5	10-27	300-1,000	2-50	Na^{+} - HCO_3^{-} or (Ca^{+2} + Mg^{+2})-HCO_3
Navicula radiosa	>7.0	21-27	300-1,000	10-50	Na^{+} - HCO_3^{-} or (Ca^{+2} + Mg^{+2})-HCO_3
Navicula gastrum	6-8.5	10-27	300-1,000	~50	Na^{+} - HCO_3^{-} or (Ca^{+2} + Mg^{+2})-HCO_3

(Müller, 1897; Cholnoky, 1955; Owen, 1981; Gasse, 1986)

Epithemia zebra (Figure 21) has short raphe slits near the pole, which lie on the side of the ventral mantle and are curved strongly toward the face. The ventral margin is slightly concave, the valve apex rounded to slightly rostrate, and the frustules are ~8 µm thick and ~35 µm long. There are three to four slightly radial costae per 10 µm, and three to six areola rows between the each costae. *E. zebra* is found in littoral areas of low alkalinity lakes (see Table 5) (Owen, 1981; Gasse, 1986).

Navicula radiosa (Figure 21) is bilaterally symmetrical about the apical plane. The central striae have no stigmata above them. The raphe is parallel to the ventral margin with the central terminations showing expanded pores and terminal fissures that are hooked towards the ventral margin. The valve is lanceolate with sharply rounded apices. The striae are radial at the center and slightly convergent at the apices. There are 10 striae in 10 µm. This frustule is approximately 70 µm long and 10 µm wide. *N. radiosa* is found in littoral areas of lakes and is pH and cationic indifferent (see Table 5) (Owen, 1981; Gasse, 1986).

Navicula gastrum (Figure 21) is naviculoid in shape, has a blunt apex, a flat valve face, spherical poroids, and aligned striae that give the appearance of curving longitudinal striations (most likely radial). There is a central linear raphe, but the central and terminal endings cannot be observed. *N. gastrum* is approximately 10 µm wide and is estimated to be 20 - 40 µm long. There are 8 - 10 striae in 10 µm. *N. gastrum* is found in lakes with low mineral content (see Table 5) (Owen, 1981; Gasse, 1986).

Fragilaria sp. (Figure 21) is 8 µm long, has 19 striae in 10 µm, shows no raphe, and has small rounded spines along striae.

Gasse (1986) studied the ecology of modern diatoms in East African Lakes. Table 5 shows a summary of his findings for diatoms found in the Galana Boi Formation during this study.

5.5.3 Discussion

The highest elevation bed of Galana Boi diatoms is 440 m. The diatoms reflect a littoral setting, which corresponds to the interpretation of Owen and Reanut (1986).

Cerling (1977) suggests that the Galana Boi Lake was either not fresh or that outlet was close to a major inflow and the lake was only fresh in a small area between the inflow (the Omo River) and outflow (the Nile River). The diatoms identifiable to the species level in Area 117 and 137 indicates the Galana Boi Lake may have had temperatures of approximately 21°C, with a conductivity of approximately 300–1000 μS cm^{-1} with a pH around 7. The majority of the modern examples of diatoms grow in slightly to moderate alkaline lakes.

CHAPTER 6

STRUCTURES

The field area is near the current divergent axis of the northern Kenyan Rift (currently under Lake Turkana) and all structures within the field area are associated with this rift. There are three types of recognized structures within the field area: normal faults, fault bend folds, and anticlines. These structures can be attributed to normal faulting and are controlled by the eastern bounding faults of the northern Kenyan Rift extension as described by Morley *et al.* (1992) and Ebinger *et al.* (2000).

6.1 Faults

Some normal faults in the field area are obvious whereas other are inferred. The major difficulty in mapping normal faults is the lack of topographic relief and the extensive Holocene and Recent cover. There are seven ways to recognize faults within the field area: 1) Offset of contacts between rock units; 2) two rock units of differing age being near each other; 3) change in attitude of bedding near the end of a contact (drag folding); 4) repetition of stratigraphic sequences; 5) blocks of "floating" rock units that are foreign or in strange orientations compared to the underlying strata (Compton, 1962); 6) general trend in the change of laga orientation; and 7) small scale synclines and anticlines.

6.1.1 Minor Normal Faults

Minor normal faults have very little offset. Most minor normal faults occur between cuestas capped with the Tulu Bor Tuff. These west dipping normal faults were recognized by the repetition of strata, the 10–15° dip change of the cuestas on the west side of the contact between sedimentary strata and the Holocene cover, and the presence of north-south trending calcite-filled joints on the east side of many contacts. These faults have a maximum displacement of 11 m (Figure 23).

Minor normal faults occur in the Kokoi Highlands, near K. Nyasaga Uguosaga Uġuo Gaġwea, that offset the sedimentary strata of the Lonyumun Member. These minor normal faults have offsets of approximately 8 m (down to the east) and are within a few m of an intrusion of Gombe Group basalts (Figure 15). This normal faulting can be attributed to the intrusion of the Gombe basalt into the Lonyumun Member.

6.1.2 Large-scale Normal Faults

Large-scale normal faults are faults that have a large enough offset to bring two separate members in contact with each other. Evidence for these faults includes large fault bend folds, repetition of strata, small scale rollover syn- and anticlines, two rock units of differing ages within the same proximity, and, in some cases, an abrupt change in the direction of channels of ephemeral streams. Because of the extensive tracts of alluvial cover, the locations of many faults are inferred, but, this notwithstanding, there is overwhelming evidence for the existence of these structures. There are four major normal faults one of which bifurcates into several splays that deviate from the main trend of the fault. The succeeding description of these faults is from east to west. The

Figure 23. Minor faults near cuestas topped with Tulu Bor Tuff: a) general dip changes from approximately 3˚ to 12˚. The feature is interpreted as a drag-fold caused by a small fault. Tuff is 2m thick. Image location: 4.1090 N 36.3037 E looking southeast. b) minor fault zone with approximately 1 m of offset on the Tulu Bor Tuff. Tuff is 1.8 m thick. Image location: 4.0917 N 36.3128 E looking west.

easternmost large-scale fault has its southern terminus beneath the Burgi unconformity south of Il Aberegaiye (see Appendix A). Several small, north-south trending normal faults associated with this fault occur between the eastern and western contact of the Moiti Member (which contains the Aberegaiye Tuff of the Moiti Member) south of Il Aberegaiye. In this area Il Aberegaiye makes a 90° turn, flowing from the west to the north and immediately makes a hairpin turn flowing to the south and then turns again flowing to the west towards Lake Turkana. Comparing the Google Earth images with aerial photos shows that the channel along this hairpin turn has moved about 270 m northward since 1970. The Kaado Tuff (which lies below the Tulu Bor Tuff northwest of Lake Turkana) outcrops immediately west of this abrupt change in stream direction. All this is taken as evidence for a northeast trending normal fault, which separates the Moiti Member to the southeast from the Tulu Bor Member to the northwest.

The next normal fault to the west bifurcates into fault splays. The southern terminus of these fault splays is near Il Aberegaiye. The south-eastern of these splays separates the Lokochot/Moiti Member (to the west) from the Tulu Bor Member (to the east), and the south-western splay separates the upper Tulu Bor Member (where sample K80-176 was found) from the Lokochot/Moiti Member. The south-western splay can be observed in a cut bank of Il Aberegaiye (Figure 24). These two splays join somewhere in the vicinity of Kolom Mardule Imi Kijieskà, east of a prominent cuesta capped by the α-Tulu Bor Tuff. The fault bifurcates again, the northwestern splay separating the lower Tulu Bor Member from the upper Lokochot Member. The fault can be clearly seen by the contact between the β-Tulu Bor tuff with a mudstone of the Moiti/Lokochot Member (Figure 25). No slickenlines or fault breccias were observed on any fault in the field area,

Figure 24. Fault exposed in Il. Aberegaiye. Machete is 60 cm. Top strata are those of the Galana Boi Formation. Image location: 4.0653 N 36.3037 E looking southwest.

Figure 25. Fault zones with two different lithologic units in contact: a) β-Tulu Bor Tuff (left) in contact with a mudstone (right) of the Moiti/Lokochot Member; machete (60 cm) is in the fault zone. Image location: 4.1158 N 36.3191 E looking north. b) Tulu Bor-α tuff (left arrow) striking against a mudstone of the Lonyumun Member (right arrow) along trend of fault from (a). Note Galana Boi Formation buttress unconformity in the middle. Image location: 4.1168 N 36.3193 E looking north.

which is attributed to the poorly compacted, sometimes loose, nature of the rocks. The western splay is responsible for many of the dip changes in the strata in the area, and separates the top of the Moiti/Lokochot Member from a lower portion of the same member. This splay bifurcates to the west and is responsible for separating the Tulu Bor Member from the Moiti/Lokochot Member. This normal fault exits the study area to the northeast and might be the cause of a fault bend anticline in a bed of Tulu Bor Tuff observed in Area 131 (east of the Kokoi Highland).

The next fault to the west shows very clear evidence for its motion. The southern terminus of this fault could not be determined, but it may continue well into Area 136. The first signs of faulting are two well-defined faults within 150 m of each other. The western fault is east-dipping and produced drag folds within the sedimentary strata the west of the fault plane (Figure 26). The eastern fault is west-dipping (Figure 26). These two faults create a small graben that makes it impossible to assign the strata within the graben to a specific member. The western fault is observed again approximately two kilometers to the northeast, where it separates sands and muds of the Moiti/Lokochot Member (Figure 27). The fault continues to the northeast and terminates at the Kokoi Highland. Near the termination of this fault is the β-Tulu Bor Tuff, which has been folded into a synform with an axial trace of 045°. The maximum dip of the limbs of the folds are 9°, and the limbs strike at acute angles to the axial trace suggesting that the synform is moderately plunging to the north. This syncline is either caused by the tip of an upward propagating normal fault (Hardy and Ford, 1997), or by a higher angle ramp along the plane of the normal fault (Twiss and Moores, 1992).

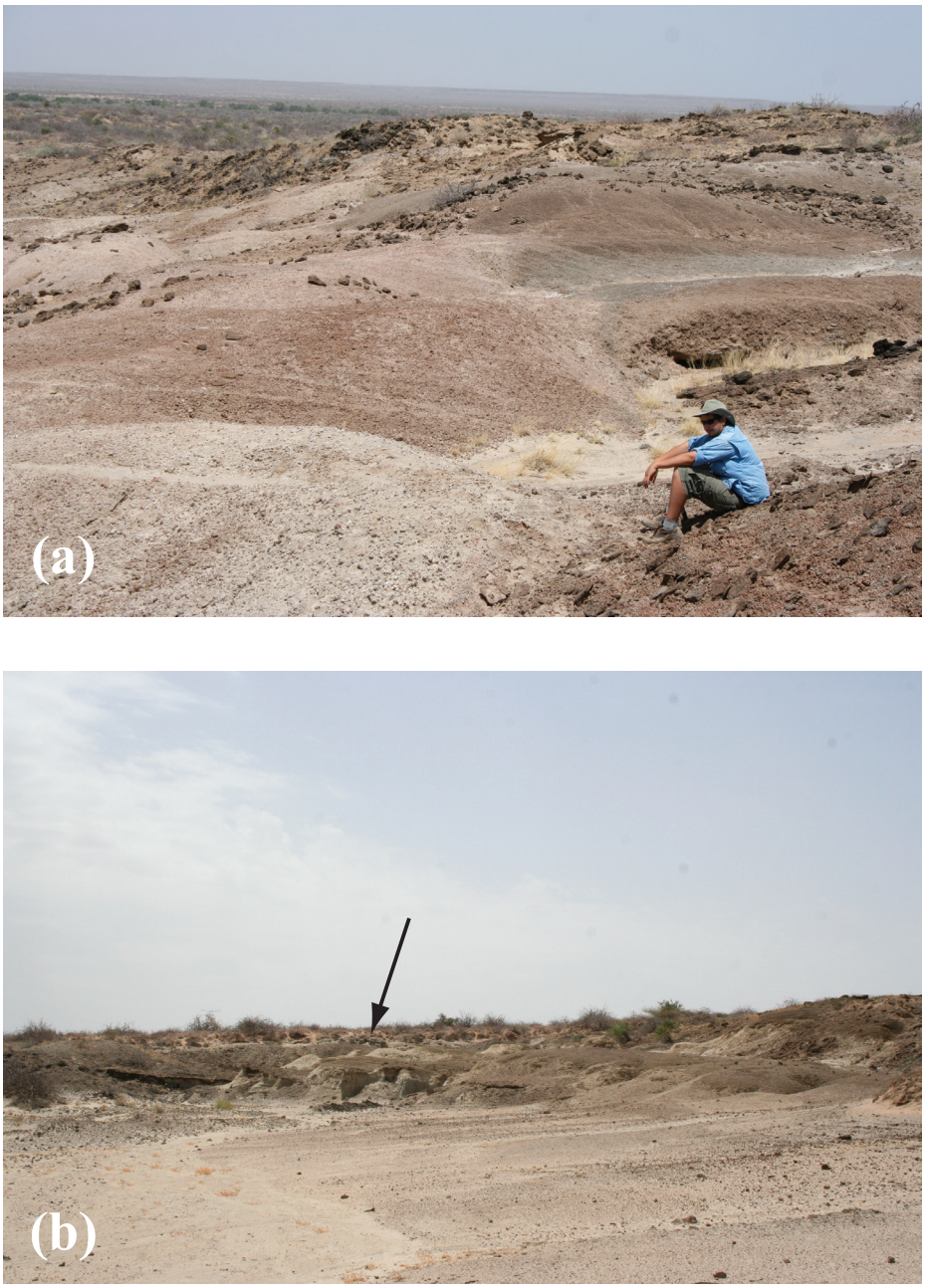

Figure 26. Bounding faults of mini graben: a) west dipping fault with the upper Tulu Bor fluvial upward-fining sequences on the right (east) and undifferentiated Koobi Fora Formation on the left (west). Image location: 4.0711 N 36.2829 E looking north. b) drag folds on the western bounding fault. Drag fold indicates an east dipping fault. Arrow indicates Tulu Bor Tuff. Image location: 4.0687 N 36.2810 E looking north.

Figure 27. Fault separating Lokochot Member sandstone unit (to the right) and mudstone unit (to the left). Orion Rogers (1.93 m) and machete (60 cm) for scale. Image location: 4.0915 N 36.3903 E looking north.

One more large-scale normal fault is observed on the western edge of outcrops in Area 117 north-northwest of Kulau. Evidence for a fault is the large number of north-south trending calcite filled joints in the area, an anticline nicely outlined by the Lokochot Tuff, and numerous small scale normal faults (Figure 28). The antiform has an axial trace of 320°. The western limb has an attitude of S50E/04° and the eastern limb has an attitude of N55E/08° suggesting that the antiform is moderately plunging and the limbs are moderately inclined to the west. The difficulty in inferring a large-scale fault is the absence of exposures to the west.

6.2 The Structure of the Kokoi Highland

The question of the existence and placement of the Kokoi highland through time has changed dramatically from the first studies. In the geologic map produced by Bowen (1974) the Kokoi Highland is called the Kokoi Horst and is shown as being bounded to the east and west by normal faults. Findlater (1976), in his structural elements map, shows an anticline with an axial trace going northeast/southwest in the middle of the Kokoi. Findlater referred to the Kokoi as an uplift and part of the volcanic basement, which caused the sediments around the Kokoi to be deformed (Findlater, Figure 8:1, 1976). Recent studies made by Haileab *et al.* (2004) shows that the basalts that make up the Kokoi Highland, the Gombe Group basalts, are younger than the oldest surrounding sedimentary strata. The Kokoi dips slightly to the southeast and the presence of an anticline is doubtful.

On the western edge of the Kokoi Highland the dips of strata in the Lonyumun through Tulu Bor Members change dramatically, increasing from 3˚ to 30˚ in just a few

Figure 28. Evidence for faulting on the western edge of Area 117: a) strata a Lonyumun Member sandstone abutting against mudstone. Image location: 4.0687 N 36.2660 E looking south. b) anticline outlined by Lokochot Tuff. Tuff is 2.1 m thick. Image location: 4.0699 N 36.26597 E looking north by northwest.

tens of m, which may be explained by a normal fault along its margin. Gathogo (2003) inferred a fault west of the Kokoi Highland (herein called the Kokoi normal fault) and mapped it into Area 41, some 25 km northwest of where the fault emerges from Lake Turkana. Morley (1999b) noted a fault under Lake Turkana using seismic reflection data and mapped it 1/3 of the way into Lake Turkana, approximately 25 km, to the southwest of where the fault would pass into the lake. If these faults are the same that would indicate the fault is at least 50 km long. This fault brings the Lonyumun Member in contact with the Silbo Tuff of the Chari Member (dated at 0.74 Ma), which would represent a minimum of 450 m of displacement in that area (Gathogo, 2003; Haileab *et al.*, 2004). This fault is also responsible for dip changes in all members of the Koobi Fora Formation east of the Kokoi Highland.

6.3 Discussion

The Kokoi Highland represents a large upfaulted block. This is the largest structural feature in the area. As the Kokoi Highland began to uplift, stresses would be applied to the relatively weak sedimentary strata of the hanging wall south of the Kokoi Highland manifest in footwall deformation structures. These footwall deformation structures are principally west-dipping normal faults that parallel the main Kokoi fault. Displacement on this series of faults is larger closer to the Kokoi normal fault, which would be expected, and is responsible for lowering the areas to the south, called the Il Naibar Lowlands by Brown and Feibel (1991), in comparison to the Kokoi Highland. The faulting and uplifting of the Kokoi Highland would also cause the magnitude of dips of sedimentary strata on or within the Kokoi to change.

During the movement along this fault a south-southwest trending normal fault developed in the Nabalware Valley and caused the sediments of the Lower Koobi Fora Member to be down dropped into the valley, causing repetition of strata seen in sections A137.1 and A137.2. The movement along this fault is approximately 15–20 m.

The major southwest trending normal faults in Area 117 could not followed south of Il Aberegaiye. It is doubtful that the faults continue into the upper Burgi Member, thus the faulting along the Kokoi Highland must have occurred during the 1.0 Ma depositional hiatus between the upper Tulu Bor Member and the upper Burgi Member.

CHAPTER 7

DISCUSSION

The axial center of the Turkana Basin currently lies below Lake Turkana and has been there since at least 5 Ma (Haileab *et al.*, 2004). By this time the minimum horizontal stress within the Kenya Rift had rotated counter-clockwise to its present position of northwest/southeast (Bosworth and Strecker, 1997).

Around 4.5 Ma the ancestral Omo River was captured by the Turkana Basin creating the Lonyumun Lake, which is estimated to have been three times larger than Lake Turkana (Brown and Feibel, 1991). The basal units of the Lonyumun Member are pelagic in nature and suggest that this area was below wave base during deposition of these sediments. Minor pebble conglomerates and sandstones higher in the section indicate that the level of the Lonyumun Lake was falling, allowing streams to extend farther into the basin.

During this lacustrine stage basalts of the Gombe Group intruded into sedimentary strata deposited in the Lonyumun Lake. The intrusion of hot basaltic magma into the cool sedimentary rocks caused the outer walls of these intrusions to form pillow structures and glassy selvages along the chilled margins. The centers of these intrusive dikes cooled slowly enough so that hexagonal columns formed. Glass selvages formed on these wavy columnar basalts may be attributed to water percolating into the cooling

intrusive body. By 4.0 Ma the lake started to drain as indicated by the higher ratios of coarse to fine grained material higher in section. The volcanic event that created the Kanyeris Tuff had happened and had deposited an ash layer by this time. Another volcanic eruption created the tephra that would become the Naibar Tuff. A fluvial system brought the Naibar tephra to the shores of the receding Lonyumun Lake, in the process incorporating some volcanic glass shards from the previously deposited Kanyeris Tuff. The volcanic material was reworked along the shores of the lake. Some plants began to take root, but were short lived because a second pulse of fluvial activity brought down another layer of Naibar tuff atop the plants. In some places small hills of Naibar Tuff outcrop next to an intrusive dike of Gombe Group Basalts. These outcrops show no deformation, show no effects of heating at the margin, and have a dip consistent with other outcrops of Naibar Tuff indicating that the Gombe Group basalts did not intrude to the level of the Naibar Tuff and the Gombe Basalts outcropped as small hills as far back as 4 Ma.

Temporal resolution is poor in Area 117 from 3.9 to 3.6 Ma. Brown and Feibel (1991) report a fluvial phase during this time interval. The Moiti Tuff (3.97 Ma) is completely missing in the field area and the Lokochot Tuff (3.60 Ma) is nearly absent. This is also true for areas to the north as far as Ileret (Gathogo, 2003).

Around 3.6 Ma a lake began to form again and Area 117 was a vast lowland. This region was occupied by a delta front of the ancestral Omo River that shed sediments into the newly formed lake. The western portion of the Il Naibar lowlands has higher amounts of muds and clays, whereas the eastern portions are richer in sand. Crocodiles,

turtles, fish and algae are amongst the many animals that made this lowland lake environment their home at this time.

At Kataboi, three precessional cycles (60,000 years each) are recorded in the diatomites of the Lokochot lake, thus, the total time that the lake existed is probably <100,000 years (deMenocal and Brown 1999). A large river, dubbed the Turkana River by Feibel (1988), flowed through the Il Naibar lowlands. The tephra that makes up the Tulu Bor Tuff was erupted at this time. The deposition of α-Tulu Bor began suddenly. A large channel that incised into the stratigraphically lower Moiti/Lokochot Member is filled by a sandstone that contains approximately 80% glass shards in the 0.250 mm-0.125 mm fractions, but is mainly a coarse-grained quartz sandstone which contains significantly less glass shards and a high proportion of biotite. This first fluvial channel preceded an even larger widespread fluvial channel filled with a sandstone that contains mostly volcanic glass shards of α-Tulu Bor composition. A paleosol developed above this tuffaceous layer before the tuffaceous fluvial channel filled with the β-Tulu Bor Tuff was deposited. Following this, at least eight upward-fining sequences were laid down in the region, and this must have continued until some time after 3.06 Ma, the date on a pumice (sample K80-176) from one of the basal fluvial channels near the top of this sequence.

During this time movement along the Kokoi normal fault commenced which created the hanging wall faults seen in Area 117 as evidenced by the dip changes due to faulting in the foothills east of the Kokoi Highland.

Lying unconformably above this is the upper Burgi Member of Area 116, which is also present in areas north of the Kokoi Highland and northeast of Area 117, towards

the Karari Escarpment. The KBS Member also crops out to the northeast in Areas 130, 131 and north of the Kokoi Highland in the Ileret region. The Okote and the Chari Members are also represented in areas north of the Kokoi Highland (Gathogo, 2003). The upper members of the Koobi Fora Formation may have been deposited within the study area, and have been eroded away subsequently, leaving no trace of their former existence in the region.

The Silbo Tuff was deposited 0.74Ma. The Kokoi normal fault brought this tuff in contact with the Lonyumun Member, which indicates 450 m of movement within the past 740,000 years (Gathogo, 2003).

The Holocene Galana Boi Lake was deposited approximately 10,000 years BP (Owen and Renaut, 1986). The highstand of the lake is seen in Area 117 by strand lines in the Kokoi Highland and by littoral facies diatom beds and reworked tuffs at an elevation of 440 m, which is 80 m above present day Lake Turkana. The Galana Boi Lake lasted until approximately 3,000 years BP. Between 3,000 years BP and today much of the Holocene Galana Boi Formation has been removed from Area 117 by erosion.

CHAPTER 8

CONCLUSION

This study used various geologic techniques to map and identify the lithologic units of Area 117, Area 137, and a small part of Area 116. This study was able to constrain the ages of sedimentary strata within the field area to the lower part of the Koobi Fora Formation with a temporal range between 4.20 Ma and ~3.06 Ma. This is contrary to past studies that described deposits of the KBS Tuff in Area 117.

Nine volcanic tuffs were identified in the study area: the Naibar Tuff, the Aberegaiye Tuff, the Loruth Tuff, the Lokochot Tuff, the Kaado Tuff, the α-Tulu Bor-Tuff, the β-Tulu Bor Tuff, and an unnamed tuff of the Tulu Bor Member (sample MB08-28). One further tuff, sample MB08-40/41 was recognized in the fluvial sequences of the Tulu Bor Member, but it is so altered that no glass separate could be obtained. These tuffs, and their relationship to other strata of the Koobi Fora Formation in the study area was established within the study area.

Sedimentary strata of the Holocene Galana Boi Formation are present, and diatoms from these beds were identified and found to be related to the littoral zone of the Galana Boi Lake highstand, which was slightly alkaline in the study area. The study also identified major structural elements, showed that these structures are related to the uplift

of the Kokoi Highland, began after the deposition of the upper Tulu Bor Member, and have been active at least until 740,000 years ago. This study suggests why no strata above the Lonyumun Member have been identified on the Kokoi Highland, yet there are younger strata within valleys of the Kokoi Highland.

Finally, this study presented a geologic history of the study area, and surrounding areas to the north and south, based on stratigraphic, structural and microfossil evidence.

8.1 Stratigraphy

The Lonyumun, Lokochot, the Moiti and the Tulu Bor members of the Koobi Fora Formation are present in the study area. Thirteen stratigraphic sections measured in the study area were correlated to each other, which provided clues to the depositional environments and the structural history of the study area.

This study was able to elucidate the relationship between the Gombe Group basalts and the Lonyumun Member. This contact shows a chilled margin and proves that some Gombe Group basalts intruded into the sediments at the bottom of the Lonyumun Lake. The Gombe Group basalts did not intrude up to the level of the Naibar Tuff and must predate deposition of that tuff. Reworked tuffs and diatomite beds of Galana Boi age reflect a littoral lacustrine environment.

Using aerial photos taken in 1970 and comparing them to Google Earth images dated from 2005, it was shown that the seemingly dry ephemeral sand streams have been very active and some main channels have shifted by up to 273 m in the past 35 years.

8.2 Structures

The structural components of the study area were identified and mapped. The key structures are believed to be controlled by the large-scale Kokoi normal fault, movement on which was determined by Gathogo (2003). Using data from Gathogo (2003) as well as Haileab *et al.* (2004), Morley (1999b) and this study, the nature and timing of the Kokoi Highland was determined. The fault must have been initiated after deposition of the upper Tulu Bor Member, but before the deposition of the upper Burgi Member. This makes sense in that no strata between 2.5 and 2.0 Ma old are known anywhere in the Koobi Fora region, so that it is reasonable that these faults were part of other structural adjustments that elevated the eastern part of the basin during this interval. Movement along the Kokoi normal fault continued to at least after deposition of the 0.74 Ma old Silbo Tuff, which is in contact with the Lonyumun Member north of the Kokoi Highland.

Small scale faults that formed during the time interval between the upper Tulu Bor Member and the upper Burgi Member are believed to be associated with the Kokoi normal fault.

The structural nature of the Kokoi Highland also explains why the Lonyumun Member is topographically higher than the Moiti, Lokochot and Tulu Bor Members within the Kokoi. The Kokoi Highland may not have been a topographic high during deposition of the Lonyumun Member, but small local hills must have been present so that the Naibar Tuff could be deposited proximate to the Gombe Group Basalts. The Moiti, Lokochot and Tulu Bor Members were free to be deposited over what is now the Kokoi highland and within small hills and valleys that the basalts made. After movement along

the fault, the Kokoi highland began to be uplifted, which prohibited deposition of strata of the upper Koobi Fora Formation on top of the Kokoi Highland.

8.3 Future Work

Future work within the field area could focus within the Kokoi Highland to investigate the numerous dikes and faults, search for tuffs of Moiti, Lokochot and Tulu Bor Members, as well as investigate the nature of the Lonyumun Member.

Investigation of the faults and sedimentary strata east of the field area may yield important clues to the deposition of strata between Area 117 and the Karari ridge. These investigations could also further define the timing of motion on the Kokoi normal fault.

One curious aspect of Area 117 is the central drainage basin between Il Naibar and Il Aberegaiye. Streams draining into Il Naibar form a central drainage basin approximately twice as big as that of Il Aberegaiye. There is a slight northward dip to Area 117 and there is a slight trough at the base of the Kokoi highland and a detailed DEM analysis and field work could be instructive in deciphering the origin of these features.

A season in the field in Area 116 and 136 could yield important information on the nature of deposition of the Koobi Fora Formation in those areas. This might tie previous studies together and provide a history of deposition and structural geology for the area between Ileret and the Koobi Fora spit.

APPENDIX A

GEOLOGIC MAP

Geologic Map of Area 117 and Vicinities, Lake Turkana Kenya

Michael J Buchanan

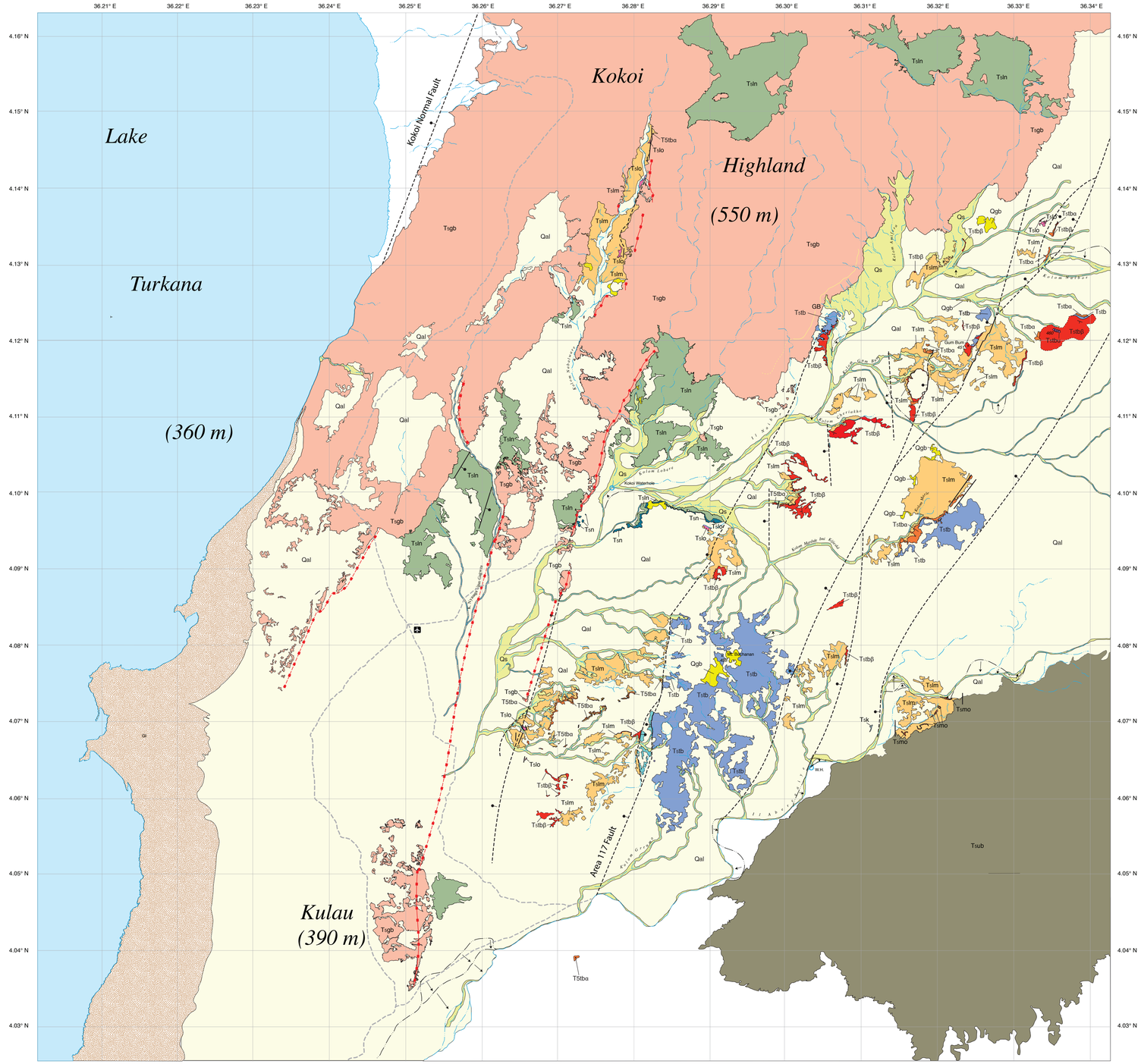

Explanation

Tsn / Tsln — **Geologic contact with map-unit label. Solid where identity, existence and location is certain. Dashed where identity and existence is certain, location inferred.**

Normal fault. Barb and ball on downthrown block. Solid where identity, existence and location is certain. Dashed where identity and existence is certain, location inferred.

Basalt dike. Solid where identity, existence and location is certain. Dashed where identity and existence is certain, location inferred.

Four-wheel-drive or unimproved roadway.

Ephemeral sand streams (laga in Gabra). Large streams are called Il and small streams are call Kolom in the Dhasanaac language.

Shifted ephemeral stream channel. Black dashed line indicates previous location of channel from HSL KEN 70 aerial photos to modern location of channel. Arrow indicates direction of shift.

GB — **Galana Boi Lake level strandline.**

/ 05 — **Attitude of bedding. Barb indicating dip, number indicating dip angle.**

Horizontal bedding.

Airstrip

Location of major water holes

References

Bowen, B. (1974). The geology of the Upper Cenozoic sediments in the East Rudolf embayment of the Lake Rudolf basin, Kenya.

Brown, F., & Cerling, T. (1982). Stratigraphical significance of the Tulu Bor Tuff of the Koobi Fora Formation. Nature, 299 (5880), 212–215.

Brown, F., & Feibel, C. (1986). Revision of lithostratigraphic nomenclature in the Koobi Fora region, Kenya. Journal of the Geological Society , 143 (2), 297–310.

Feibel, C., Harris, J., & Brown, F. (1991). Paleoenvironmental Context for the Late Neogene of the Turkana Basin. Koobi Fora Research Project, Vol. 3, 3, 321–346.

Haileab, B., Brown, F., Mcdougall, I., & Gathogo, P. (2004). Gombe Group basalts and initiation of Pliocene deposition in the Turkana depression, northern Kenya and southern Ethiopia. Geological Magazine, 141 (1), 41–53.

Federal Geographic Data Committee (prepared for the Federal Geographic Data Committee by the U.S. Geological Survey), 2006, FGDC Digital Cartographic Standard for Geologic Map Symbolization: Reston, VA., Federal Geographic Data Committee Document Number FGDC-STD-013-2006, 290 p., 2 plates.

Holocene

Unstudied – *Areas that were not studied in detail enough to map.*

Qal — **Cover (Holocene) –** *Deposits of mainly fine- to coarse-grained sand, and eroded surficial Gombe Group basalts.*

Qs — **Stream Deposits (Holocene) –** *Deposits of ephemeral sand streams, mainly quartz sand and eroded surficial Gombe Group basalt.*

Qi — **Lacustrine (Holocene) –** *Sands deposited by Lake Turkana at the modern shore line.*

Qgb — **Galana Boi (Holocene) –** *Galana Boi lake beds, includes littoral sands with bivalve and gastropod shells, stromatolite beds in a cemented sandstone matrix, and reworked volcanic tuffs. Not extensively mapped.*

Pliocene

T5kf — **Undifferentiated Koobi Fora Formation (Pliocene – Pleistocene –** *Sedimentary strata of the Koobi Fora Formation including sands (compacted and cemented), muds, tuffs, and diatomites.*

Burgi Member

T5ub — **Upper Burgi (~2Ma) –** *Tan ferruginized medium-grained sandstone with abundant fish vertebrae. Thickness: approximately 10 cm.*

Tulu Bor Member

T5tbu — **Unnamed tuff above Tulu Bor (Pliocene) –** *Unnamed tuff stratigraphically above the β-Tulu Bor Tuff only found in the northeast corner of Area 117.*

T5tb — **Tulu Bor Member (Pliocene) –** *All sedimentary strata between the top of the Tulu Bor-beta Tuff and the base of the Burgi Tuff (not observed in Area 117). Includes upward fining upward cycles of sandstone (compacted and cemented) and mudstones. Macro fossils include Elephas, turtle shells, hippo, hominids Type Locality: Area 202 and Area 204. Type Thickness: 86.2 m.*

T5tbβ — **beta-Tulu Bor Tuff (Pliocene, 3.380 Ma) –** *Blue to white coarse-grained tuff with >90% glass tephra; between 1.45 m to 3.9 m thick. Along with α-Tulu Bor, this unit forms large cliffs resistant to erosion. Type Locality: Area 202 and Area 204.*

T5tbα — **alpha-Tulu Bor (Pliocene, 3.438 ± 0.023 Ma) –** *White to yellow, medium- to coarse-grained tuff containing flat and bubble junction glass shards; commonly crossbedded. Tuff ranges in thickness from 0.90 m to 2.85 m. This unit is commonly (but not always) associated with the β-Tulu Bor Tuff. Type Locality: Area 192*

Lokochot Member

T5k — **Kaado Tuff (Pliocene) -** *Blue-grey fine-medium grained tuff. Tuff is approx. one meter thick and outcrops west of Il Aberegaiye. Type Locality: Loruth Kaado (northwest Lake Turkana). Type thickness: 10 m*

T5lm — **Combined Moiti/Lokochot Members (Pliocene) –** *Due to the of erosion at the base of the overlying Tulu Bor Member fluvial deposits, it is unclear whether the deposits directly below the Tulu Bor tuff are Moiti or Lokochot Member. Lacustrine and deltaic deposits with fossils of crocodiles and turtles. Moiti Tuff is not observed in the field area. Moiti Tuff Age: 3.969 Ma Lokochot Tuff Age:3.596 Ma*

T5lt — **Lokochot Tuff (Pliocene, 3.596 ± 0.05 Ma) –** *Blue laminated tuff containg >80% glass asphia with a maximum thickness of 1.10 m. Shards are flat or blocky. A 3 cm thick accretionary lapilli layer is present around 20 cm from the base of the tuff. Type Locality: Area 250. Type Thickness: 34.4 m.*

Moiti Member

T5lo — **Loruth Tuff (Pliocene) –** *Type Locality: Loruth Kaado, also occurs in Area 250.*

T5mo — **Aberegaiye Tuff (Pliocene) –** *White fine-grained wavy laminated rhyolitic tuff. Outcrops south of Il Aberegaiye. Type Locality: Area 116. Type thickness: 1.5m*

T5gb — **Gombe Group Basalts (Pliocene –4.2 - 4.0 Ma) –** *Black to light purple medium grained basalt intrusions and/or flows. Occurs in two locales, the Kokoi Highlands and Kulau Hill. Intrusion surfaces show 2-4cm glassy selvages. Type Locality: ? Type Thickness: <100 m.*

Lonyumun Member

T5n — **Naibar Tuff (Pliocene, ~4.01 Ma) –** *Light grey coarse to medium-grained volcanic tuff with >80% glass shards (mainly bubble junction and flat). 3.55 m thick. Marks the top of the Lonyumun Member in Area 117. Type Locality: Area 117. Type Thickness: 3.55 m.*

T5ln — **Lonyumun Member (Pliocene, ~4.2 - 4.01 Ma) –** *All sedimentary strata lying below the Naibar Tuff. Mudstone, highly gypsiferous claystones, compacted and cemeted sandstones, massive and laminated diatomites. Basal contact is not observed. Intruded by Gombe Group basalts near the Kokoi Highlands and Kulau Hill. Composite thickness of 106.25 m. Type Locality: Area 260. Type Thickness: 36.8m.*

SCALE 1:31 680

1 1/2 0 1 MILE

1 0.5 0 1 KILOMETER

13° TRUE NORTH MAGNETIC NORTH

Derived from Google Earth Images obtained in 2008. Photoinspected from imagery taken in 1970 by the Hunting Survey (series HSL KEN 70). Some major drainage and culture changes noted, but not mapped.

World Geodetic System of 1984 (WGS84).

APPENDIX B

SAMPLE LOCATIONS

Table 6. Locations of samples pertinent to this study.

Sample	Type	Member	Latitude	Longitude
75-117A	Rhyolitic Tuff	Naibar	-	-
75-117B	Rhyolitic Tuff	Lokochot Tuff	-	-
75-117C	Rhyolitic Tuff	Tulu Bor-β	-	-
ANU 83-1	Pumice	Moiti Tuff	-	-
ANU 83-2	Pumice	Moiti Tuff	-	-
IL03-008	Rhyolitic Tuff	Kanyeris Tuff	4.2412	36.32050
IL03-012	Rhyolitic Tuff	Kanyeris Tuff	4.2219	36.31020
K77-27	Rhyolitic Tuff	Loruth	-	-
K80-176	Pumice	Tulu Bor Member	4.07630	36.29770
K80-187	Rhyolitic Tuff	Tulu Bor Member		
K80-213	Rhyolitic Tuff	Tulu Bor Member	4.1966	36.40750
K81- 586	Rhyolitic Tuff	Moiti Member	3.7020	36.3903
K81-586	Rhyolitic Tuff	Moiti Member	3.6877	36.4184
K81-650	Rhyolitic Tuff	Tulu Bor Member	-	-
K82- 870	Rhyolitic Tuff	Naibar	4.0972	36.2906
K82-746	Rhyolitic Tuff	Tulu Bor-α	-	-
K82-860	Rhyolitic Tuff	Tulu Bor Member	4.1222	36.3360
K82-875	Rhyolitic Tuff	Naibar	4.0979	36.28900
K82-876	Rhyolitic Tuff	Naibar	4.0963	36.2906
K82-1363	Rhyolitic Tuff	Naibar	3.6814	36.37590
K82-1364	Rhyolitic Tuff	Lonyumun	3.6814	36.37590
K82-1367	Rhyolitic Tuff	Moiti Tuff	3.6814	36.37590
K82-1369	Rhyolitic Tuff	Moiti Tuff	3.6814	36.37590
K83-1721	Rhyolitic Tuff	Lokochot	4.1357	36.33440
K84-1815	Basalt	Gombe Group	~3.46	~36.31
K98-3743	Rhyolitic Tuff	Topernawi	3.8592	35.73400
K09-573	Basalt	Gombe Group	4.0433	36.2461
MB08-01	Rhyolitic Tuff	Tulu Bor-β	4.0136	36.2415
MB08-02	Rhyolitic Tuff	Tulu Bor-β	4.0135	36.2415
MB08-03	Rhyolitic Tuff	Naibar	4.0966	36.2795
MB08-05	Rhyolitic Tuff	Naibar	4.0969	36.2732
MB08-06A	Pumice	Naibar	4.0973	36.2904
MB08-06B	Pumice	Naibar	4.0973	36.2904
MB08-07	Rhyolitic Tuff	Naibar	4.0973	36.2904
MB08-08	Rhyolitic Tuff	Lokochot	4.0971	36.2903
MB08-09	Rhyolitic Tuff	Tulu Bor-β	4.0577	36.2702
MB08-10	Rhyolitic Tuff	Tulu Bor-β	4.0577	36.2702
MB08-10a	Pumice	Tulu Bor-β	6.0577	38.2702
MB08-11	Rhyolitic Tuff	Tulu Bor-β	4.0633	36.2700

Table 6. continued.

Sample	Type	Member	Latitude	Longitude
MB08-12	Rhyolitic Tuff	Lokochot	4.0660	36.2661
MB08-13	Rhyolitic Tuff	Lokochot	4.0699	36.2960
MB08-14	Rhyolitic Tuff	Tulu Bor-α	4.0681	36.2665
MB08-15	Rhyolitic Tuff	Tulu Bor-α	4.0692	36.2693
MB08-16	Rhyolitic Tuff	Tulu Bor-α	4.0741	36.2809
MB08-17	Rhyolitic Tuff	Tulu Bor-α	4.0761	36.2839
MB08-18	Rhyolitic Tuff	Tulu Bor-β	4.0903	36.2912
MB08-19	Rhyolitic Tuff	Naibar	4.1070	36.2785
MB08-20	Rhyolitic Tuff	Tulu Bor-β	4.1178	36.3058
MB08-21	Rhyolitic Tuff	Tulu Bor-β	4.1202	36.3054
MB08-22	Rhyolitic Tuff	Tulu Bor-β	4.1295	36.3174
MB08-23	Diatomite	Unknown	4.1362	36.3263
MB08-24	Diatomite	Unknown	4.1355	36.3274
MB08-25	Rhyolitic Tuff	Lokochot	4.1362	36.3337
MB08-26	Rhyolitic Tuff	Lokochot	4.1356	36.3335
MB08-27	Rhyolitic Tuff	Tulu Bor-β	4.1238	36.3374
MB08-28	Rhyolitic Tuff	Tulu Bor Member	4.1218	36.3354
MB08-29	Rhyolitic Tuff	Tulu Bor-β	4.1188	36.3320
MB08-30	Rhyolitic Tuff	Lokochot	4.1228	36.3278
MB08-32	Rhyolitic Tuff	Tulu Bor-β	4.0991	36.2988
MB08-33	Rhyolitic Tuff	Tulu Bor-β	4.1051	36.3027
MB08-34	Rhyolitic Tuff	Tulu Bor-β	4.1025	36.3056
MB08-35	Rhyolitic Tuff	Tulu Bor-β	4.1067	36.3061
MB08-36	Rhyolitic Tuff	Tulu Bor-α	4.1103	36.3094
MB08-37	Rhyolitic Tuff	Tulu Bor-α	4.1124	36.3167
MB08-38	Rhyolitic Tuff	Tulu Bor-β	4.1152	36.3164
MB08-38p	Pumice	Tulu Bor-β	4.1152	36.3164
MB08-39	Rhyolitic Tuff	Tulu Bor-β	4.1215	36.3261
MB08-40	Rhyolitic Tuff	Tulu Bor Member	4.0770	36.29296
MB08-41	Rhyolitic Tuff	Tulu Bor Member	4.0770	36.29296
MB08-42	Rhyolitic Tuff	Tulu Bor-β	4.0859	36.3077
MB08-43	Rhyolitic Tuff	Tulu Bor-β	4.0868	36.3078
MB08-44	Rhyolitic Tuff	Tulu Bor-α	4.0983	36.3214
MB08-45	Rhyolitic Tuff	Moiti Member	4.0736	36.3215
MB08-46	Rhyolitic Tuff	Tulu Bor-β	4.0799	36.3085
MB08-47	Rhyolitic Tuff	Tulu Bor-α	4.0989	36.2996
MB08-48	Rhyolitic Tuff	Tulu Bor-α	4.0989	36.2996
MB08-49	Rhyolitic Tuff	Tulu Bor-β	4.1044	36.3003
MB08-50	Rhyolitic Tuff	Tulu Bor-β	4.1049	36.3028

Table 6. continued.

Sample	Type	Member	Latitude	Longitude
MB08-51	Rhyolitic Tuff	Tulu Bor-β	4.1049	36.3028
MB08-52	Rhyolitic Tuff	Tulu Bor-β	4.1101	36.3124
MB08-53	Rhyolitic Tuff	Tulu Bor-α	4.1189	36.3192
MB08-54	Rhyolitic Tuff	Tulu Bor-α	4.0698	36.3019
MB08-55	Rhyolitic Tuff	Tulu Bor-β	4.0853	36.3056
MB08-56	Rhyolitic Tuff	Tulu Bor-α	4.0723	36.2669
MB08-58	Rhyolitic Tuff	Naibar	4.1483	36.2826
MB08-59	Rhyolitic Tuff	Lokochot	4.1477	36.2823
MB08-60	Rhyolitic Tuff	Tulu Bor-β	4.1476	36.2825
MB08-61	Rhyolitic Tuff	Tulu Bor-β	4.1475	36.2828
MB08-62	Rhyolitic Tuff	Tulu Bor-α	4.0991	36.2609
MB08-63	Rhyolitic Tuff	Lokochot	4.1000	36.2730
MB08-65	Rhyolitic Tuff	Tulu Bor-β	4.0689	36.2810
MB08-66	Rhyolitic Tuff	Tulu Bor-β	4.0687	36.2810
MB08-67	Rhyolitic Tuff	Tulu Bor-β	4.1339	36.3236
MB08-68	Pumice	Lokochot	4.1353	36.3290
MB08-69	Pumice	Lokochot	4.1365	36.3337
MB08-70	Rhyolitic Tuff	Tulu Bor-α	4.1356	36.3357
MB08-71	Rhyolitic Tuff	Tulu Bor-β	4.1356	36.3357
MB08-73	Rhyolitic Tuff	Tulu Bor-α	4.0991	36.3016
MB08-74	Rhyolitic Tuff	Tulu Bor-α	4.0991	36.3016
MB08-75	Rhyolitic Tuff	Tulu Bor-α	4.1122	36.3079
MB08-77	Rhyolitic Tuff	Moiti Member	4.0724	36.3204
MB08-78	Rhyolitic Tuff	Naibar	4.0980	36.2817
MB08-79	Rhyolitic Tuff	Naibar	4.0980	36.2817
MB08-80	Rhyolitic Tuff	Lokochot	4.0960	36.2904
MB08-81	Rhyolitic Tuff	Lokochot	4.0959	36.2904
MB08-82	Rhyolitic Tuff	Tulu Bor-β	4.0905	36.2922
MB08-83	Rhyolitic Tuff	Tulu Bor-β	4.1103	36.3165
MB08-84	Rhyolitic Tuff	Tulu Bor-β	4.1195	36.3338
MB08-85	Rhyolitic Tuff	Tulu Bor-α	4.1208	36.3333
MB08-86	Rhyolitic Tuff	Tulu Bor-α	4.1240	36.3399
MB08-87	Rhyolitic Tuff	Tulu Bor-β	4.1233	36.3397
MB08-88	Rhyolitic Tuff	Galana Boi	4.1258	36.3239
MB08-89	Rhyolitic Tuff	Tulu Bor-α	4.0674	36.2714
MB08-90	Rhyolitic Tuff	Naibar	4.0985	36.2619
MB08-91	Rhyolitic Tuff	Lokochot	4.1321	36.2785
MB08-92	Diatomite	Lonyumun	4.1302	36.2741
MB08-93	Rhyolitic Tuff	Tulu Bor-β	4.1056	36.3017

APPENDIX C

STANDARDS

Table 7. Standards used for Electron Microprobe Analysis.

Standard	Chemical Composition	Element	Crystals	Count Time (sec.)
MM3 (Obsidian)	See APPENDIX D	O,Al,K,Si	PC1,TAP,PET	20, 15, 15, 15
Fluorite	CaF_2	F	PC1	20
Albite	$NaAlSi_3O_8$	Na	TAP	4
Diopside	$CaMgSi_2O_6$	Mg,Ca	TAP, PET	20, 20
Zircon	$ZrSiO_4$	Zr	TAP	20
Tugtopite	$Na_4AlBeSi_4O_{12}Cl$	Cl	PET	20
Barite	$BaSO_4$	Ba	PET	20
Rhodochrosite	$MnCO_3$	Mn	LIF	25
Rutile	TiO_2	Ti	LIF	25
Hematite	Fe_2O_3	Fe	LIF	25

APPENDIX D

MAJOR ELEMENT COMPOSITION OF MM3 STANDARD

Table 8. Major Elements in MM3 standard.

Element	Wt%	Error (±)
O	49.35	0.36
Si	35.71	0.31
Al	6.50	0.06
K	4.35	0.07
Na	2.62	0.02
Fe	0.51	0.06
Ca	0.39	0.05
F	0.13	0.05
Ti	0.08	0.02
Cl	0.07	0.01
Mg	0.04	0.02
Mn	0.04	0.02
Ba	0.01	0.01
Total	99.8	0.53

APPENDIX E

DETAILED DESCRIPTIONS OF STRATIGRAPHIC COLUMNS MEASURED IN THE STUDY AREA

Detailed descriptions of stratigraphic columns of the Koobi Fora Formation measured in Areas 117, 137 and 116. Unless otherwise noted all units are well compacted. Descriptions begin with the lowest unit in each section.

Section A137.1

Starts at 4.14771 N, 36.28230 E with an attitude of N15E/15

Unit I. 90 cm thick, mudstone, medium-brown, massive. Contains calcite concretions and gypsum rosettes/needles on fracture surfaces.

Unit II. 180 cm thick, sandy mudstone coarsening upward to clayey sandstone. Contains small rounded rip-up clasts near the center.

Unit III. 110cm thick, vitric tuff (Lokochot), medium-grained, bluish-grey, thinly laminated. Contains a 3 cm thick accretionary lapilli (diameter is 3 mm) layer 24 cm from the base of the unit. Sample MB08-59 (Lokochot Tuff).

Unit IV. 145 cm thick, clayey-sandstone, sub-rounded, fine-grained, light brown, massive. Contains iron-manganese oxide films on fracture surfaces.

Unit V. 45 cm thick, claystone, massive, contains iron-manganese oxide films on fractures surfaces. Interbedded 10 cm sandstone, fine-grained, white, with angular rip-up clasts of claystone.

Unit VI. 1150 cm, claystone, medium-brown, massive. Contains fine-grained, angular quartz sand grains and subrounded clasts of yellowish-grey tuff.

Unit VII. 150 cm, tuffaceous sandstone with ostracod (mm scale). Sample MB08-60 (β-Tulu Bor Tuff).

Terminated by a fault (4.14759 N, 36.28249 E). Total thickness is 18.6 m.

Section A137.2

Lies atop section A137.1 (4.14759 N, 36.28249 E) with an attitude of N15E/15

Unit I. 165 cm thick, sandstone, medium-grained, tan, massive, well compacted. Contains quartz, potassium feldspar, basalt clasts and calcite concretions at the base.

Unit II. 130 cm thick, mudstone, tan to light brown, laminated. Contains broken small bivalve shells at the base and 3-5 cm diameter calcite concretions ~ 40 cm from the base.

Unit III. 165 cm thick, sandstone, subrounded, coarse-grained, tan to orange, cm-scale crossbeds. Contains quartz grains and some basalt clasts. Bottom few centimeters are a calcite concreted medium-grained sandstone, thinly bedded and contains quartz and biotite.

Unit IV. 785 cm thick, mudstone, light brown, massive. Contains gypsum rosettes on fracture surfaces. Surface weathers to a popcorn texture.

Unit V. 225 cm thick tuff, altered, pale yellow, massive, lots of clay.

Unit VI. 90 cm thick tuff, very pale grey, laminated. Sample MB08-61 (β-Tulu Bor Tuff).

Terminated by a fault (4.14748 N, 36.28283 E) with a trend of S20W. Total thickness is 15.6 m.

Section A117.1

Starts at 4.07212 N, 36.26761 E with a bedding attitude of S30E/03 and a column attitude normal to the bedding attitude.

Unit I. 460 cm thick, mudstone, light brown. Contains iron-manganese oxides on fracture surfaces and weather popcorn surfaces. Contains numerous vertebrate fossils including turtle shells, fish vertebrae, and crocodile scutes.

Unit II. 85 cm thick. Bottom 80 cm: sandstone, subrounded, medium-grained, light brown. Quartz, mica, iron-oxide minerals present. Mudstone rip-up casts are present near the top. Top 5cm: well cemented sandstone same as below.

Unit III. 600 cm thick, covered exposure.

Sectioned moved to 4.07212 N, 36.26902 E.

Unit IV. 45 cm thick, sandstone, subangular, medium grained cross-bedded. Contains gastropod shells, mainly *Cleopatra*.

Unit V. 395 cm thick, claystone, medium brown, massive. Iron-manganese films on fractures surfaces. Contains 3-10 cm thick sandstone lenses, medium grained.

Section moved to 4.07347 N, 36.26987 E.

Unit VI. 415 cm thick, clay-rich sandstone, fine-grained, light brown, cross-bedded (mm scale). Contains quartz, and biotite.

Unit VII. 660 cm thick, claystone, medium brown, massive. Iron-manganese films on fractures surfaces. Contains 3–10 cm thick sandstone lenses, medium grained.

Unit VIII. 90 cm thick, clay-rich sandstone, fine-grained, light brown, cross-bedded (mm scale). Contains quartz, and biotite.

Unit IX. 240 cm thick, claystone, medium brown, massive. Iron-manganese oxide films on fracture surfaces. Contains 3-10 cm thick sandstone lenses, medium grained.

Unit X. 295 cm thick, tuff, medium grained, pale yellow, thinly bedded. Sample MB08-15 and -16 (α-Tulu Bor Tuff).

Section ends at 4.07345 N, 36.27037 E with a thickness of 32.85 m.

Section A117.2

Starts at 4.07363 N, 36.32165 E.

Unit I. 325 cm thick, sandstone, angular, coarse-grained, light brown, thinly bedded (mm scale). Contains quartz and feldspar.

Unit II. 160 cm thick, tuff, very fine grained, white, thinly bedded. Sample number MB08-45 and -77 (Aberegaiye Tuff). Capped by sandstone, concreted, containing rhizoliths.

Section moved to 4.07093 N, 36.31990 E.

Unit III. 530 cm thick, sandstone, angular, medium-grained, light brown, thinly bedded. Contains quartz, feldspar, and biotite. Top 20 cm is calcite concreted and limonite stained.

Unit IV. 480 cm thick, mudstone, light brown, massive. Contains biotite, iron-manganese films on fracture surfaces and fossils (fish vertebrae, turtle plastron and carapace fragments and disarticulated mammalian fossils.

Unit V. 10 cm thick, pebble conglomerate, coarse-grained matrix, calcite cemented. Contains bivalves and molluscs, subrounded sandstone and mudstone clasts, angular quartz pebbles.

Unit VI. 235 cm thick, sandstone, angular, coarse-grained, light brown, thinly bedded (mm scale). Contains quartz and feldspar.

Unit VII. 10cm thick, sandstone, subrounded, coarse-grained, medium brown, cross-bedded, calcite cemented. Contains fish vertebrae, feldspar and mudstones clasts.

Unit VIII. 8 cm thick, sandstone, medium grained, tan, ferruginized. This unit is the upper Burgi Member and rests unconformably on all lower units.

Section ends at 4.07027 N, 36.32033 E and is 17.58 m thick.

Section A117.3

Starts at 4.13638 N, 36.33399 E. Section is covered by pebble- to cobble-sized clasts of Gombe Group basalts.

Unit I. 360 cm thick. Bottom: tuff, fine-grained, white. Sample MB08-25 (Loruth Tuff). Middle: tuff, medium-grained, blue. Sample K83-1721 (Lokochot Tuff). Top: 10 cm thick, sandstone, calcite concreted, white, containing rhizoliths. Unit is mainly unexposed due to cover by recent alluvium; thickness was obtained by pacing.

Unit II. 475 cm thick, claystone, medium brown, massive. Contains cm-scale calcite nodules, iron-manganese oxides and gypsum rosettes on fracture surfaces. This unit coarsens upward to clayey sandstone, fine-grained, light-brown. Top: 175 cm, sandstone, subangular, medium-grained, massive, calcite concreted.

There is a fault between Unit II and Unit III.

Unit III. 300 cm thick, sandstone, medium grained, tan. Poorly exposed, covered by basalt clasts.

Unit IV. 195 cm thick, clay-rich sandstone, fine-grained, medium brown. Poorly exposed, covered by basalt clasts.

Unit V. 90 cm thick, tuff, coarse-grained, pale yellow, cross-bedded. Sample MB08-71 (α-Tulu Bor Tuff). Attitude is N10E/04

Unit VI. 170 cm thick, tuff, medium-grained, massive. Sample MB08-71 (β-Tulu Bor Tuff). Attitude same as Unit V.

Unit VII. 920 cm thick. Base: mudstone, grey. Middle: sandstone, subangular, tan. Top: pebble conglomerate, calcite concreted. Unit is covered by clasts of Gombe Group basalt and lithologies were determined by digging and following insect burrow tailing piles.

Section ends at 4.13537 N, 36.33628 E and is 25.00 m thick.

Section A117.4

Starts at 4.09933 N, 36.30107 E with a bedding attitude of S20W/04 and a column attitude normal to the bedding attitude.

Unit I. 70 cm thick. Sandstone, angular, medium- to coarse-grained, light brown, massive, calcite concreted. Contains rounded mudstone clasts, quartz and feldspar.

Unit II. 55 cm thick. Sandstone, subangular, medium-grained, light brown, cross-bedded. May contain minor soft-sediment deformation.

Unit III. 170 cm thick. Clay-rich sandstone, fine-grained, tan, massive. Fines upward to mainly claystone with some sand.

Unit IV. 120 cm thick. Sandstone, subangular, medium-grained, light brown, cross-bedded, soft-sediment deformation. Limonite mottling. Top 10 cm is burnt orange, and coarse-grained.

Unit V. 145 cm thick. Claystone with coarse-grained, sub-angular sand grains. Contains gypsum rosettes along fracture surfaces and montmorillonite "popcorn" surface.

Unit VI. 115 cm thick. Sandstone, subangular, medium-grained, light grey, thinly laminated. Contains quartz and feldspar.

Unit VII. 435 cm thick. Mudstone, very fine-grained, light brown, massive.

Unit VIII. 145 cm thick. Tuff (α-Tulu Bor), medium- to coarse-grained, yellow, cross-bedded. Contains coarse-grained quartz grains. Top 10 cm: tuff (β-Tulu Bor), medium-grained, beautiful volcanic glass.

Section ends at 4.09903 N, 36.30125 E and is 12.55 m thick.

Section A117.5

Starts at 4.09908 N, 36.30164 E with a bedding attitude of S20W/04 and a column attitude normal to the bedding attitude.

Unit I. 155 cm thick. Mudstone, medium-brown, with iron-manganese oxide films on fracture surfaces.

Unit II. 95 cm thick. Tuffaceous sandstone, angular, coarse-grained, cross-bedded (mm scale). Contains a thin calcite concreted rhizolith layer and a 10 cm thick interbedded claystone layer 30 cm from the base of the unit..

Unit III. 320 cm thick. Tuffaceous sandstone, coarse-grained, highly compacted, grey, cross-bedded (cm-m scale). Contains a 1 cm thick pink layer, coarse-grained with much volcanic glass (sample MB08-73, α-Tulu Bor). This is a large obvious channel that incises into the underlying section (Figure 16)

Unit IV. 85 cm thick. Mudstone, fine-grained, medium-brown.

Unit V. 150 cm thick. Tuff (α-Tulu Bor), medium-grained, yellow. Sample MB08-74.

Unit VI. 35 cm thick. Tuff (β-Tulu Bor), very clean, white.

Section ends at 4.0990 N, 36.3015 E and is 8.40 m thick.

Section A117.6

Starts at 4.0949 N, 36.31556 E with a bedding attitude of N45E/04 and a column attitude normal to the bedding attitude.

Unit I. 10 cm thick. Mudstone, massive bedding.

Unit II. 355 cm thick. Sandstone, angular, medium- grained, light brown, massive. Fines upward to sandstone, subrounded, fine-grained.

Unit III. 365 cm thick. Bottom 10 cm: Sandstone, subangular, medium-grained, massive, cemented. Top 355 cm: Sandstone, subangular, coarse-grained, cross-bedded.

Unit IV. 155 cm thick. Claystone, medium-brown, thinly bedded.

Unit V. 270 cm thick. Base: Sandstone, angular, coarse-grained. Fines upward to: clay-rich sandstone, rounded, very fine-grained.

Unit VI. 300 cm thick. Claystone, medium-brown, thinly bedded. Top few cm is black.

Unit VII. 175 cm thick. Tuff (α-Tulu Bor), medium-grained, coarse glass shards, cross-bedded. Sample MB08-44

Section moved to 4.0976 N 36.32100 E. Section is flat and had to be walked.

Unit VIII. 465 cm thick. Sandstone, rounded, fine-grained.

Unit IX. 190 cm thick. Clay-rich mudstone, ferruginized. Capped by 10 cm thick sandstone, angular, coarse-grained, cemented.

Unit X. 480 cm thick. Sandstone, subangular, medium-grained, grey, massive. May contain shell fragments. Capped by 25 cm thick cemented sandstone, fine-grained.

Unit XI. 250 cm thick. Sandstone, subangular, medium-grained, massive. Topped by 10 cm thick sandstone, fine-grained, angular.

Unit XII. 325 cm thick. Sandstone, angular, coarse-grained, tan. Fines upward to: clay-rich sandstone. Capped by a 25 cm thick sandstone, medium-grained, cross-bedded.

Unit XIII. 15 cm thick. Sandstone, sub-rounded, coarse-grained, poorly-sorted, cross-bedded.

Section ends at 4.0971 N, 36.3229 E and is 33.55 m thick.

Section A117.7

Starts at 4.1145 N, 36.2807 E.

Unit I. 440 cm thick. Claystone, light brown, thin bedded. Contains gypsum rosettes on fracture surfaces.

Unit II. 320 cm thick. Diatomite, pale yellow.

Unit III. 490 cm thick. Claystone, light-brown. Contains replaced fish fossils, and gypsum rosettes on fracture surfaces.

Unit IV. 25 cm thick. Mudstone, light-brown with coarse-grained, angular quartz clasts.

Unit V. 30 cm thick. Claystone, light grey. Contains iron-manganese oxide films on fracture surfaces.

Unit VI. 280 cm thick. Mudstone, medium-brown. Contains gypsum rosettes.

Unit VII. 40 cm thick. Pebble conglomerate, coarse- to pebble-sized grains. Cross-bedded.

There is 375 cm of unexposed section here.

Unit VIII. 160 cm thick. Claystone, medium-brown, laminated.

Unit IX. 40 cm thick. Diatomite, white.

Unit X. 135 cm thick. Mudstone, medium-brown, thinly laminated. Contains gypsum rosettes on fracture surfaces.

Unit XI. 100 cm thick. Clay-rich sandstone, fine-grained, light-brown.

Unit XII. 2000 cm thick. Claystone. Contains large gypsum plates and green replaced fish bones. Poorly exposed. 180 cm thick. Diatomite, eggshell white.

Unit XIII. 510 cm thick. Diatomite, eggshell white.

Unit XIV. Claystone, medium- to dark-brown. Contains gypsum rosettes on fracture surfaces.

Unit XV. 20 cm thick. Pebble conglomerate, very-fine grain sandstone matrix. Contains subangular quartz pebbles.

Section is covered by Holocene lithologic units. Continues at 4.1053 N 36.2828 E.

Unit XVI. 50 cm thick. Sandstone, medium-grained, angular. Capped by a 5 cm thick well cemented, limonitized, cross-bedded sandstone with inner molds of gastropod shells.

Unit XVII. 105 cm thick. Claystone, light grey. Contains iron-manganese oxide films on fracture surfaces.

Unit XVIII. 315 cm thick. Mudstone, light- to medium-grey. Contains montmorillonite "popcorn" surfaces, orange coprolites, and iron-manganese oxide films on fracture surfaces.

Unit XIX. 355 cm thick. Tuff (Naibar Tuff). Bottom 65 cm: Pale-green tuff, coarse-grained, small (mm) scale pumices, cross-bedded. Sample MB08-78. Middle 20 cm: Calcite concreted layer containing rhizoliths (paleosol?). Top 250 cm: Tuff, dark grey, cross-bedded. Sample MB08-79.

Unit XX. 225 cm thick. Bottom 10 cm: Mollusc-packed sandstone, fine-grained. Middle 205 cm: Mudstone, light brown, parallel laminated. Top 10 cm: Broken up calcite concreted bed containing rhizoliths.

Unit XXI. 50 cm thick. Tuff (Lokochot), yellowish-blue, large glass shards. Sample MB08-08

Section ends at 4.0791 N 36.2903 E and is 106.25 m thick.

Section A117.8

Starts at 4.1239 N, 36.3399 E.

Unit I. 410 cm thick. Clay-rich sandstone, fine-grained.

Unit II. 20 cm thick. Sandstone, subangular, medium-grained.

Unit III. 160 cm thick. Tuff (α-Tulu Bor), yellow, cross-bedded. Sample MB08-86.

Unit IV. 75 cm thick. Sandstone, grey, fine-grained.

Unit V. 220 cm thick. Sandstone, coarse-grained, subangular, massive.

Unit VI. 280 cm thick. Sandstone, coarse-grained, subangular, massive. Very loosely compacted.

Unit VII. 260 cm thick. Tuff (β-Tulu Bor), white, large glasses, small pumice rich layer (mm in diameter) near the top. Sample MB08-87.

Section moved to 4.1221 N 36.3368 E.

Unit VIII. 300 cm thick. Mudstone, brown, poorly exposed.

Unit IX. 15 cm thick. Sandstone, tan, coarse-grained, subangular.

Unit X. 135 cm thick. Mudstone, light brown, thinly laminated (mm-scale),

Unit XI. 10 cm thick. Sandstone, angular, medium-grained, cross-bedded.

Unit XII. 620 cm thick. Mudstone, medium-brown, halite on fracture surfaces.

Unit XIII. 20 cm thick. Sandstone, subrounded, coarse-grained, thickly bedded, colorful quartz. Sample K80-861.

Unit XIV. 365 cm thick. Sandstone, medium-grained, subrounded.

Unit XV. 300 cm thick. Tuff (unnamed tuff of the Tulu Bor Member), white, abundant glass shards, parallel laminated. Makes a prominent hill. Sample MB08-28.

Section ends at 4.12178 N 36.3363 E and is 31.90 m thick.

Section A117.9

Starts at 4.11913 N 36.32474 E.

Unit I. 245 cm thick. Mudstone, medium-brown. Contains gypsum on fracture surfaces. Fines upward to claystone, dark-brown containing gypsum rosettes.

Unit II. 175 cm thick. Claystone, medium-brown. Contains iron-manganese oxide films and gypsum rosettes on fracture surfaces. Top centimeter is a thin calcite concreted bed.

Unit III. 285 cm thick. Tuff (α-Tulu Bor), medium-grained, yellow, cross-bedded.

Unit IV. 160 cm thick. Tuff (β-Tulu Bor), medium-grained, white.

Section ends at 4.1191 N, 36.3243 E and is 10.45 m thick.

Section A117.10

Starts at 4.1154 N, 36.3156 E.

Unit I. 175 cm thick. Mudstone, medium-brown, massive bedding. Contains coarse-grained quartz grains.

Unit II. 130 cm thick. Sandstone, angular, fine-grained, light brown, parallel laminated. Top 25 cm is a concreted sandstone, sub-angular, coarse-grained.

Unit III. 90 cm thick. Mollusc-packed sandstone, medium-grained, tan, angular. Possible fossil wood.

325 cm is unexposed.

Unit IV. 155 cm thick. Clay-rich sandstone, angular, fine-grained, light-brown, parallel laminated (10 cm scale and thinning upward).

Unit V. 145 cm thick. Mudstone, medium-brown. Contains coarse-grained quartz sand.

Unit VI. 230 cm thick. Sandstone, subangular, coarse-grained. Contains calcite nodules.

Unit VII. 285 cm thick. Claystone, tan. Contains gypsum rosettes on fracture surfaces.

Unit VIII. 250 cm thick. Tuff (α-Tulu Bor), medium-grained, yellow, cross-bedded. Sample MB08-37.

Unit IX. 490 cm thick. Tuff (β-Tulu Bor), medium-grained, white. Sample MB08-38.

Section ends at 4.1152 N 36.3167 E. Total thickness is 23.65m.

Section A117.11

Section starts at 4.0626 N 36.2862 E. This section was measured by F.H. Brown and R. L. Bruhn.

Unit I. 30 cm thick. Sandstone, cross-bedded, cemented.

Unit II. 380 cm thick. Mudstone, medium-brown. Top of cycle not exposed, eroded by Unit III.

Unit III. 300 cm thick. Sandstone, fine-grained, bottom 30 cm is cemented.

Unit IV. 500 cm thick. Siltstone, medium to pale-green. Contains root casts.

Unit V. 250 cm thick. Mudstone.

Unit VI. 130 cm thick. Sandstone, poorly cemented.

Unit VII. 50 cm thick. Sandstone, well-cemented. Basal 30 cm contains cross-beds.

Unit VIII. 580 cm thick. Sandstone, medium- to fine-grained. Cross-bedded (10 cm sets).

Unit IX. 280 cm thick. Mudstone, pale-brown, montmorillonite “popcorn surfaces”. Contains a calcite layer 130cm from the top.

Unit X. 240 cm thick. Silt-pebble-conglomerate.

Section ends at 4.0597 N 36.2861 E and is 27.40 m thick.

APPENDIX F

SAMPLE K80-176

Preparation

Sample K80-176 is a pumice found in a fluvial channel in the upper Tulu Bor Member. Feldspar separates from this pumice yield a K/Ar date of 3.06 ± 0.03 Ma (Feibel et al., 1989). Most of the glass within the pumice has been altered to chabazite and the pumice has a high proportion of calcite, which made locating and separating glass shards from the pumice difficult. The method used to separate glass shards from this sample is as follows.

The pumice was crushed with a placed in a 10% nitric acid bath over night. The calcite reacted with the nitric acid. The residue was washed with deionized water and dried. The sample was then crushed and sieved and all material <0.250 mm was retained. This fraction was treated with 5% hydrofluoric acid (HF) to remove clay and zeolite. The HF was decanted from the sample, and the sample was rinsed three times in deionized water and placed in an oven set at 80 °C. Once dried, magnetic and non-magnetic separates were obtained using a Frantz Isodynamic Separator.

Two 50 mL centrifuge tubes were filled with approximately 40 mL of lithium metatungstate (LM), with a density set to approximately 2.65 g/cc. The tubes were then filled with five mL of laboratory grade acetone which has a specific gravity of approximately 0.8. The magnetic and non-magnetic separates were placed in the acetone layer of the centrifuge tubes and the tubes were placed in a centrifuge. The centrifuge was turned on for 30 seconds causing dense materials to sink to the bottom of the centrifuge tubes while any material which <2.65 g/cc remained along the LM/acetone interface. The LM was then flash frozen using liquid nitrogen and the less dense materials were decanted into a Büchner flask fitted with a funnel that had filter paper in

it. Residual heavy liquid and acetone was washed from the sample under a vacuum. The sample was dried and paced in a methyl methacrylate polymer microprobe mounts and cemented using a two-part epoxy resin. Seven glass shards were separated from the pumice and analyses using the electron microprobe.

Discussion

Results from electron microprobe analysis are presented in Table 9. The sample has two principal modes, five shards have about 0.50 – 0.95 % Fe_2O_3, and two shards have about 5.50 % Fe_2O_3. The second mode corresponds to analyses from K80-650 and PNG00-WT08, which are both reported to be just below the Ninikaa Tuff, which is consistent, within error, with the K/Ar date of 3.06 Ma (Feibel *et al.* 1989).

Table 9. Electron microprobe analyses of glass shards from pumice K80-176.

Sample #	SiO_2	TiO_2	Al_2O_3	Fe_2O_3[a]	MnO	MgO	CaO	Na_2O	K_2O	F	Cl	Less Cl, F for O	H_2O[b]	Total
K80-176, Pumice, Low Iron														
K80-176	73.58	0.12	12.61	0.45	0.10	0.02	0.48	3.65	4.42	0.01	0.07	0.02	5.54	101.05
K80-176	73.68	0.04	12.65	0.49	0.11	0.05	0.50	3.68	4.26	0.03	0.07	0.03	5.81	101.38
K80-176	72.65	0.07	12.43	0.56	0.05	0.05	0.48	3.55	4.48	-0.01	0.06	0.01	6.07	100.57
K80-176	72.43	0.06	12.63	0.61	0.11	0.01	0.49	3.64	4.34	0.04	0.07	0.03	6.04	100.45
K80-176	69.87	0.12	13.17	0.94	0.06	0.13	0.76	2.72	4.72	-0.01	0.15	0.03	8.84	101.48
K80-176, Pumice, High Iron														
K80-176	71.15	0.35	9.51	5.51	0.27	0.09	0.19	1.78	2.23	0.27	0.20	0.16	9.24	100.96
K80-176	71.87	0.32	9.73	5.56	0.24	0.12	0.19	2.73	3.48	0.35	0.21	0.20	7.71	102.59
K81-650	69.83	0.39	10.01	5.93	0.32	0.16	0.20	4.38	4.27	0.12	0.17	0.09	5.10	100.99
PNG00-WT-08	73.71	0.32	9.56	5.20	0.23	0.09	0.18	1.02	1.39	0.05	0.24	0.13	7.03	99.15
PNG00-WT-08	73.87	0.29	9.66	5.20	0.28	0.09	0.19	0.20	0.51	0.22	0.24	0.20	8.86	99.82
PNG00-WT-08	73.27	0.28	9.36	5.21	0.29	0.08	0.19	0.88	1.38	0.14	0.26	0.17	7.75	99.32
PNG00-WT-08	73.68	0.28	9.46	5.30	0.26	0.07	0.18	1.29	1.75	0.14	0.26	0.17	6.95	99.83

a) All iron expressed as Fe_2O_3

b) Water calculated as explained in Nash (1992)

REFERENCES

Bainbridge, R. B., 1976, Stratigraphy of the Lower Member, Koobi Fora Formation, northern Karari Escarpment, East Turkana Basin, Kenya: Unpublished M.S. Thesis, Iowa State University, Ames, Iowa, 133 p.

Behrensmeyer, A. K., 1970, Preliminary geologic interpretation of a new hominid site in the Lake Rudolf Basin: Nature, v. 226, p. 225–226.

Boschetto, H. B., 1988, Geology of the Lothidok Range, northern Kenya. Unpublished M.S. Thesis, University of Utah, Salt Lake City, 203 p.

Boschetto, H. B., F.H. Brown, and I. McDougall, 1992, Stratigraphy of the Lothidok Range, northern Kenya, and K/Ar ages of its Miocene primates: Journal of Human Evolution, v. 22, p. 47–71.

Bosworth, W., and M. Strecker, 1997, Stress field changes in the Afro-Arabian rift system during the Miocene to Recent period: Tectonophysics, v. 278, p. 46–62.

Bowen, B. E., 1974, The geology of the Upper Cenozoic sediments in the East Rudolf embayment of the Lake Rudolf basin, Kenya: Unpublished Ph.D. Dissertation, Iowa State University, Ames, Iowa, 164 p.

Bowen, B. E., and C. F. Vondra, 1973, Stratigraphical Relationships of the Plio-Pleistocene Deposits, East Rudolf, Kenya: Nature, v., 242, p. 391–393.

Brown, F. H., 1972, Radiometric dating of sedimentary formations in the lower Omo Valley, Ethiopia, *in* W. W. Bishop, and J. A. Miller, eds., Calibration of hominoid evolution: Edinburgh, Scottish Academic Press, p. 273–287.

Brown, F. H., 1994, Development of Pliocene and Pleistocene chronology of the Turkana Basin, East Africa, and its relation to other sites, *in* R. Ciochon, and R. Corriuccini, Integrative Paths to the Past, Englewood Cliffs, New Jersey, Prentice Hall, p. 285–312.

Brown, F. H., and T. E. Cerling, 1982, Stratigraphical significance of the Tulu Bor Tuff of the Koobi Fora Formation: Nature, v. 299, p. 212–215.Brown, F. H., and C. S. Feibel, 1986, Revision of lithostratigraphic nomenclature in the Koobi Fora region, Kenya: Journal of the Geological Society, London, v. 143, p. 297–310

Brown, F. H., and C. S. Feibel, 1991, Stratigraphy, depositional environments, and palaeogeography of the Koobi Fora Formation, *in* J. M. Harris, ed., Koobi Fora Research Project, Volume 3, The Fossil Ungulates: Geology, Fossil Artiodactyls, and Palaeoenvironments, Oxford, Clarendon Press, p. 1–30.

Brown, F. H., and C. Fuller, 2008, Stratigraphy and tephra of the Kibish Formation, southwestern Ethiopia: Journal of Human Evolution, v. 55, p. 366–403.

Brown, F. H., A. M. Sarna-Wojcicki, C. E. Meyer, and B. Haileab, 1992, Correlation of Pliocene and Quaternary tephra layers between the Turkana Basin of East Africa and the Gulf of Aden: Quaternary International, v. 13/14, p. 55–67.

Brown, F. H., R. T. Shuey, and M. K. Croes, 1978, Magnetostratigraphy of the Shungura and Usno Formations, southwestern Ethiopia: new data and comprehensive reanalysis: Geophysical Journal of the Royal Astronomical Society, v. 54, p. 519–538.

Burggraf, D. R., Jr., 1976, Stratigraphy of the Upper Member, Koobi Fora Formation, southern Karari Escarpment,East Turkana Basin, Kenya: Unpublished M. S. Thesis. Iowa State University, Ames, Iowa, 116 p.

Cerling, T. E., 1977, Paleochemistry of Plio-Pleistocene Lake Turkana and diagenesis of its sediments: Unpublished Ph.D. Dissertation, University of California, Berkeley, California, 185 p.

Cerling, T. E., and D. W. Powers, 1977, Paleorifting between the Gregory and Ethiopian Rifts: Geology v. 5, p. 441–444.

Cholnoky, B. J., 1955, Diatomeen aus salzhaltigen Binnengewässern der westlichen Kaap-Provinz in Südafrika: Berichte der Deutschen Botanishen Gesellschaft, v. 68, p. 11–23.

Cohen, A. S., 1982, Ecological and paleoecological aspects of the Rift Valley lakes of East Africa: Unpublished Ph.D. Dissertation, University of California, Davis, California, 314 p.

Compton, R. R., 1962, Manual of Field Geology: New York, Wiley and Sons, 378 p.

deMenocal, P. B., and F. H. Brown, 1999, Pliocene tephra correlations between East African hominid localities, the Gulf of Aden, and the Arabian Sea, *in* J. Agusti, L. Rook, and P. Andrews, eds., Hominid Evolution and Climatic Change in Europe: The Evolution of Neogene Terrestrial Ecosystems in Europe: Cambridge, Cambridge University Press, p. 23–54.

Dunkelman, T. J., J. A. Karson, and B. R. Rosendahl, 1988, Structural style of the Turkana Rift, Kenya: Geology, v. 16, p. 258–261.

Ebinger, C. J., T. Yemane, D. J. Harding, S. Tesfaye, S. Kelley, and D. C. Rex, 2000, Rift deflection, migration, and propagation: Linkage of the Ethiopian and Eastern Rifts, Africa: Geological Society of America Bulletin, v. 112, p. 163–176.

Federal Geographic Data Committee (prepared for the Federal Geographic Data Committee by the U.S.Geological Survey), 2006, FGDC Digital Cartographic Standard for Geologic Map Symbolization: Reston, Va., Federal Geographic Data Committee Document Number FGDC-STD-013-2006, 290 p., 2 plates.

Feibel, C. S., 1983, Stratigraphy and paleoenvironments of the Koobi Fora Formation along the western Koobi Fora Ridge, East Turkana, Kenya: Unpublished M. S. Thesis, Iowa State University, Ames, Iowa, 104 p.

Feibel, C. S., 1988, Paleoenvironments from the Koobi Fora Formation, Turkana Basin, northern Kenya: Unpublished Ph. D. Dissertation, University of Utah, Salt Lake City, 330 pp.

Feibel, C. S., 2003, Stratigraphy and depositional history of the Lothagam Sequence. *in* M. G. Leakey and J. M. Harris, eds., Lothagam: The dawn of humanity in eastern Africa: New York, Columbia University Press, p. 17–29.

Feibel, C. S., F. H. Brown, and I. McDougall, 1989, Stratigraphic context of fossil hominids from the Omo Group deposits, northern Turkana Basin, Kenya and Ethiopia: American Journal of Physical Anthropology, v. 78, p. 595–622.

Feibel, C. S., J. M. Harris, and F. H. Brown, 1991, Palaeoenvironmental Context for the Late Neogene of the Turkana Basin, *in* J. M. Harris, ed., Koobi Fora Research Project, Volume 3, The Fossil Ungulates: Geology, Fossil Artiodactyls, and Palaeoenvironments, Oxford, Clarendon Press, p. 321–370.

Findlater, I. C., 1976, Stratigraphic analysis and palaeoenvironmental interpretation of a Plio/Pleistocene sedimentary basin east of Lake Turkana: Unpublished Ph.D. Dissertation, Birkbeck College, University of London, London. 252 p.

Frank, H. 1976, Stratigraphy of the Upper Member, Koobi Fora Formation, northern Karari Escarpment, East Turkana Basin, Kenya: Unpublished M.S. Thesis, Iowa State University, Ames, Iowa, 118 p.

Gasse, F., 1986, East African Diatoms, Taxonomy, ecological distribution: Berlin, Germany, Gebrüder Borntraeger, 201 p., 44 plates.

Gathogo, P. N., 2003, Stratigraphy and paleoenvironments of the Koobi Fora Formation of the Ileret Area, Northern Kenya: Unpublished M.S. Thesis, University of Utah, Salt Lake City, Utah, 160 p.

Gathogo, P. N., and F. H. Brown, 2007, Stratigraphy of the Koobi Fora Formation (Pliocene and Pleistocene) in the Ileret region of northern Kenya: Journal of African Earth Sciences, v. 45, p. 369–390.

Goldstein, J., D. Newbury, D. Joy, C. Lyman, P. Echlin, E. Lifshin, L. Sawyer, and J. Michael, 2003, Scanning Electron Microscopy and X-Ray Microanalysis: New York, Springer Science, 689 p.

Haileab, B, 1988, Characterization of tephra from the Shungura Formation, southwestern Ethiopia: Unpublished M.S. Thesis, University of Utah, Salt Lake City, 130 p.

Haileab, B., 1995, Geochemistry, geochronology and tephrostratigraphy of tephra from the Turkana Basin, southern Ethiopia and Northern Kenya, Unpublished Ph.D. Dissertation, University of Utah, Salt Lake City, 369 p.

Haileab, B., F. H. Brown, I. McDougall, and P. N. Gathogo, 2004, Gombe Group basalts and initiation of Pliocene deposition in the Turkana depression, northern Kenya and southern Ethiopia: Geological Magazine, v. 141, p. 41–53.

Hardy, S., and M. Ford, 1997, Numerical modeling of trishear fault propagation folding: Tectonics, v. 16, p. 841–854.

Harris, J. M., 1978, Palaeontology, *in* M. G. Leakey, and R. E. Leakey, eds., Koobi Fora Research Project, Volume 1. The fossil hominids and an introduction to their context, Oxford, Clarendon Press, p. 32–63.

Harris, J. M. and T. D. White, 1979, Evolution of Plio-Pleistocene African suidae: Transactions of the American Philosophical Society, v. 62, no. 2, p. 1–128.

Harris, J. M., M. G. Leaky, and F. H. Brown, 2006, A brief history of research at Koobi Fora, Northern Kenya: Ethnohistory, v. 53, p. 35–69.

Harris, J. M., F. H. Brown, M. G. Leakey, A. Walker, and R. E. Leakey, 1988, Pliocene and Pleistocene hominid-bearing sites from west of Lake Turkana, Kenya: Science, v. 239, p. 27–33.

Jackson, J. A., ed., 1997, Glossary of Geology, 4th Edition: Alexandria, Virgina, Amerian Geological Institute, 769 p.

Key, R. M. and R. T. Watkins, 1988, Geology of the Sabarei area: Report of the Mines and Geology Department, Kenya, no. 111, 57 p.

Lahee, F. H., 1961, Field Geology: New York, McGraw Hill Company, 926 p.

Leakey, M. G., and R. E. Leakey, eds., 1978, Koobi Fora Research Project, Volume 1, The fossil hominids and an introduction to their context, Oxford, Clarendon Press, 191 p.

Leakey, R. E., 1970, New hominid remains and early artefacts from northern Kenya: Nature, v. 226, p. 223–226.

Levin, N. E., 2008, Isotopic records of Plio-Pleistocene climate and environments in Eastern Africa: Unpublished Ph.D. Dissertation, University of Utah, Salt Lake City, Utah, 381 p.

Martz, A. M., 1976, Petrology and chemistry of tuffs from the Shungura Formation, southwest Ethiopia: Unpublished M.S. Thesis, University of Utah, Salt Lake City, Utah, 82 p.

Martz, A. M., and F. H. Brown, 1981, Chemistry and mineralogy of some Plio-Pleistocene tuffs from the Shungura Formation, southwest Ethiopia: Quaternary Research, v. 16, p. 240–257.

McDougall, I., and F. H. Brown, 2008, Geochronology of the pre-KBS Tuff sequence, Omo Group, Turkana Basin: Journal of the Geological Society, v. 165, p. 549–562.

McDougall, I., and F. H. Brown, 2009, Timing of volcanism and evolution of the northern Kenyan Rift: Geological Magazine, v. 146, p. 34–47.

Morley, C. K., ed., 1999a, *Geoscience of Rift Systems – Evolution of East Africa*: American Association of Petroleum Geologists Studies in Geology, no. 44, 242 p.

Morley, C. K., 1999b, Basin Evolution Trends in East Africa, *in* C. K. Morley ed., Geoscience of Rift Systems – Evolution of East Africa: American Association of Petroleum Geologists Studies in Geology, no. 44, p. 131–150.

Morley, C. K., D. K. Ngenoh, and J. K. Ego, 1999a, Introduction to the East African Rift System, *in* C. K. Morley ed., Geoscience of Rift Systems – Evolution of East Africa: American Association of Petroleum Geologists Studies in Geology, no. 44, p. 1–18.

Morley, C. K., D. K. Ngenoh, and J. K. Ego, 1999b, Geology and Geophysics of the Western Turkana Basins, Kenya, *in* C. K. Morley ed., Geoscience of Rift Systems – Evolution of East Africa: American Association of Petroleum Geologists Studies in Geology, no. 44, p. 19–54.

Morley, C, K., W. A. Wescott, D. M. Stone, R. M. Harper, S. T. Wigger, and F. M. Karanja, 1992, Tectonic evolution of the northern Kenya Rift: Journal of the Geological Society of London, v. 149, p. 333–348.

Müller, O., 1897, Rhopalodia ein neus Genus der Bacillariaceen: Botanische Jahrbücher fur Systematik, Pflanzengeschichte und Pflanzengeographie, v. 22, n. 54–71.

Nash, W. P., 1992, Analysis of oxygen with the electron microprobe: Applications to hydrated glass and minerals: American Mineralogist, v. 77, p. 453–457.

Owen, R. B., 1981, Quaternary diatomaceous sediments and the geological evolution of Lakes Turkana, Baringo and Bogoria, Kenya Rift Valley: Unpublished Ph.D. Dissertation, University of London, London, England, 465 p.

Owen, R. B. and R. W. Renaut, 1986, Sedimentology, stratigraphy and paleoenvironments of the Holocene Galana Boi Formation, NE Lake Turkana, Kenya. *in* L. E. Frostick, R. W. Renaut, I. Reid, and J. J. Tiercelin, eds., Sedimentation in the African rifts: Geological Society Special Publication 25, Oxford, Blackwell, p. 311–322.

Owen, R. B., J. W. Barthelme, R. W. Renaut, and A. Vincens, 1982, Paleoclimatology and archaeology of Holocene deposits northeast of Lake Turkana, Kenya: Nature, v. 298, p. 523–529.

Penney, J. T. and A. A. Racek, 1968, Comprehensive revision of a worldwide collection of freshwater sponges *Porifera Spongillidae*: Smithsonian Institution, United States National Museum Bulletin, v. 272, 184 p.

Pouchou, J. L., and F. Pichoir, 1991, Quantitative analysis of homogeneous or stratified microvolumes applying the model "PAP", *in* Heinrich, K. F. J., and D. E. Newbury, eds., Electron probe quantization: New York, Plenum Press, p. 31–75.

Rogers, R. J. and F. H. Brown, 1979, Authigenic mitridatite from the Shungura Formation, southwestern Ethiopia: American Mineralogist, v. 64, p. 169–171.

Rosendahl, B. R., 1987, Architecture of continental rifts with special reference to East Africa: Annual Reviews of Earth and Planetary Science, v. 15, p. 445–503.

Round, F. E., R. M. Crawford, D. G. Mann, 1990, The Diatoms: Biology & Morphology of the Genera: Cambridge, Cambridge University Press, 747 p.

Sarna-Wojcicki, A. M., C. E. Meyer, P. E. Roth, and F. H. Brown, 1985, Ages of tuff beds at East African early hominid sites and sediments in the Gulf of Aden: Nature, v. 313, p. 306–308.

Tindall, K. W., 1985, Stratigraphy and sedimentology of the Koobi Fora Formation, eastern Koobi Fora Ridge, East Turkana, Kenya: Unpublished M.S. Thesis, Iowa State University, Ames, Iowa, 125 pp.

Twiss, R. J. and E. M. Moores, 1992, Structural Geology: New York, W. H, Freeman, 736 p.

von Höhnel, L., 1894, Count Teleki and the discovery of Lakes Rudolf and Stefanie: London, Longmans, Green and Company, 435 p.

Vondra, C. F. and B. E. Bowen, 1978, Stratigraphy, sedimentary facies and paleoenvironments, East Lake Turkana, Kenya, *in* W. W. Bishop, ed., Geological background to fossil man: Edinburgh, Scottish Academic Press, p. 395–414.

Vondra, C. F., G. D. Johnson, B. E. Bowen, and A. K. Behrensmeyer, 1971, Preliminary stratigraphical studies of the East Rudolf basin, Kenya: Nature, v. 231, p. 245–248.

Walker, J.D., and J. W. Geissman, compilers, 2009, Geologic Time Scale: Geological Society of America.

Watkins, R. T., 1986, Volcano-tectonic control on sedimentation in the Koobi Fora sedimentary basin, Lake Turkana. *in* L. E. Frostick, R. W. Renaut, I. Reid, and J. J. Tiercelin, eds., Sedimentation in the African rifts: Geological Society Special Publication 25, Oxford, Blackwell, p. 85–95.

White, H. J., 1976, Stratigraphy of the Lower Member, Koobi Fora Formation, southern Karari Escarpment, East Turkana Basin, Kenya: Unpublished M. S. Thesis, Iowa State University, Ames, Iowa, 134 p.

White, T. D., and J. M. Harris, 1977, Suid Evolution and Correlation of African Hominid Localities: Science, v. 198, p. 13–21.